Modeling the *in vitro* aggregation of 4R tau isoforms for a comparative study of FTDP-17 mutants



By FNU Yamini

Submitted to the graduate degree program in Department of Molecular Biosciences and the Graduate Faculty of the University of Kansas in partial fulfillment of the requirements for the degree of Doctor of Philosophy.

_____

Chair: Dr. T Chris Gamblin

_____

Dr. Brian Ackley

_____

Dr. Kristi Neufeld

_____

Dr. Liang Xu

_____

Dr. Prajna Dhar

Date Defended: 14 December 2017

The dissertation committee for Fnu Yamini certifies that this is the approved version of the following dissertation:

Modeling the *in vitro* aggregation of 4R tau isoforms for a comparative study of FTDP-17 mutants

Chair: Dr. T Chris Gamblin

Date Approved: 15 December 2017

## Abstract

Tau is a microtubule binding protein typically found in neuronal axons. In an adult human brain, six isoforms of tau are generated by alternate mRNA splicing. These isoforms of tau differ from each other either based on the number of N-terminal inserts and/or the number of microtubule binding repeats. Tau is also closely related to a group of progressive neurodegenerative disorders together known as tauopathies. In these disorders, tau gets misfolded and its ability to stabilize microtubules gets compromised. Monomers of tau then begin to polymerize to form pathologic aggregates. These aggregates of tau get deposited in the patient's brain and are closely related to neuronal dysfunction and death of neurons. Although the aggregation of tau is a central event for the majority of these tauopathies, the precise neuropathologic and clinical presentation differs between these diseases. The age of onset, area of brain affected, morphology of tau aggregates and the isoform of tau deposited as aggregates are a few of the distinguishing features between these tauopathies. The underlying mechanism of tau aggregation as well the mechanisms leading to these differences are not well understood. Before effective therapies can be devised to stop the process of tau aggregation, the mechanisms influencing this process need to be understood. One of the ways employed to gain a mechanistic understanding of this process is by using an *in vitro* aggregation model. In this model, an inducer molecule is used to generate aggregates of recombinantly produced tau and various mechanisms influencing the process of aggregation can be studied. This method has been successfully used to model aggregation of the longest isoform of tau called the 2N4R isoform, however the applicability of this methodology to isoforms missing one or more of the N-terminal inserts has proven to be challenging. In this study, we optimized the process of *in vitro* aggregation for these isoforms. We discovered that the major differences between the isoelectric points of the N-terminal region of these tau isoforms leads to

behavioral changes between these isoforms. This observation favors the notion that the isoforms of tau might also get disproportionately influenced by disease related mechanisms leading to their differential deposition as aggregates in certain tauopathies. On the contrary, the isoforms of tau have often been used interchangeably for the design of many studies. Using the optimized aggregation conditions, we investigated the effects of one such disease related changes in tau on various isoforms of tau. We performed a comparative study of autosomal dominant mutations in tau selected from three different regions and investigated their effects on the aggregation propensity and microtubule stabilizing properties of tau. We found subtle but significant differences in the effect of these mutations on various tau isoforms for all three selected mutants. Overall, these findings have opened up new avenues for the study of aggregation of various tau isoforms. They also helped us understand the differences between tau isoforms as well as how disease related changes could potentially influence the tau isoforms differentially.

## Acknowledgements

First, I would like express my gratitude towards my mentor Dr. Chris Gamblin for his tremendous guidance. He has been a great source of encouragement and support throughout my journey towards getting a doctoral degree. It would have been impossible to accomplish the goals achieved during my graduate career without his advice and insight. The environment that he has created in his laboratory, his enthusiasm for science and his mentorship style has not just helped me in graduate school but, I believe, that it would greatly encourage me to achieve many more goals in my forthcoming scientific career. I am grateful for the opportunity to work under his guidance.

I would also like to thank all present and past Gamblin lab members for their help, support and friendship. I am thankful to Dr. Benjamin Combs who trained me on a great majority of lab techniques that I learned in Gamblin lab during my first year of graduate school. He was always available to answer my questions and point me in the right direction. Dr. Mythili Yenjerla brought in a new perspective to the lab and helped me develop a new skillset. I am also thankful to Dr. Smita Paranjape, Bryce Blankenfeld, Adam Miltner, Maggie Hornick, Corinna Lemke and David Ingham for their friendship, support and assistance in conducting the experiments.

I would like to thank my committee members, Dr. Brian Ackley, Dr. Kristi Neufeld, Dr. Liang Xu and Dr. Prajna Dhar for their valuable suggestions. They all brought in perspectives from different fields related to biology during my committee presentations. Their individual insights and comments made me more inquisitive and encouraged me to learn about tau from a different point of view.

I would also like to thank my parents and my brother for their unwavering trust in me. Their teachings, love and support has guided me throughout my life and their pride in me has inspired me to work hard. Finally, I would like to thank my husband for his immense support, love and friendship. He has always boosted my morale and helped me get through any difficulties that ever came my way. His own passion for science has also kept me interested in science and helped me reach to this point.

# TABLE OF CONTENTS

# CHAPTER 1: Introduction

# Chapter I: Introduction

## 1.1 Tau Overview

The protein tau was first discovered in 1975 by Weingarten et al. and was noted as an important mediator of neuronal tubulin polymerization and stabilization of microtubules (1). Tau is predominantly expressed in neurons but can also be detected in glia and other non-neuronal cell types (2). Early research in the field of tau biology was focused on uncovering the relationship of tau with microtubules (3). About ten years from its initial discovery, in 1986, tau gained additional importance in the field of neurodegenerative disorders when several groups reported tau to be a component of the pathological intracellular neurofibrillary tangles (NFTs) or paired helical filaments (PHFs) found in Alzheimer's disease (AD) (4-6). Further research involving the determination of the primary structure of the PHF core conclusively proved tau to the major constituent of PHFs (7). Since then, this neurofibrillary pathology composed by abnormal and aggregated tau protein is found to be closely associated with a group of dementias and movement disorders together termed as tauopathies (reviewed in (8)). This involvement of tau in numerous neurodegenerative diseases evoked interest in gaining a better understanding of the biochemical nature of tau, changes that may occur in tau during disease possibly leading up to its aggregation and how this aggregation could be toxic to the neurons. Despite the progress made, several questions pertaining to the cause of tau aggregation and the precise effects disease related mechanisms have on tau's aggregation and microtubule stabilization propensity must be answered before effective therapies can be devised.

## 1.2 Tau gene structure and isoforms

The human tau (MAPT) is a 134 kb gene located on chromosome 17 at position 17q21 and is made up of 16 exons (Figure 1) (9). The CNS forms of tau are generated by utilizing 11 of these exons (10). Exon 0 and 14 are transcribed but not translated. Exon 4a, 6 and 8 have only been reported in the peripheral tissue tau mRNA but not in the human brain. Exon 1, 4, 5, 7, 9, 11, 12 and 13 are constitutive exons. Exon 2, 3 and 10 are alternatively spliced to generate six different CNS isoforms of tau ranging from 352 to 441 amino acids in length (10). Exon 9 through 12 encode the highly conserved imperfect repeat sequences (denoted as R) responsible for tau's ability to stabilize microtubules and thus the alternative mRNA splicing of exon 10 alters the number of microtubule stabilizing sequences in tau (11,12). Isoforms containing exon 10 are noted as 4R isoforms and isoforms lacking exon 10 are noted as 3R. There are approximately equal amounts of 3R and 4R tau in a normal brain (13,14). Alternative mRNA splicing of exon 2 and 3 can alter the number of N-terminal inserts (denoted as N) present in tau. Inclusion of exon 3 is dependent on inclusion of exon 2 and isoforms containing exon 3 without exon 2 have not been reported (10). Thus, the alternative mRNA splicing of exon 2 and 3 results in isoforms containing either both exon 2 and 3 (+2+3 or 2N), isoforms containing exon 2 but lacking exon 3 (+2-3 or 1N) or isoforms lacking either of these inserts (-2-3 or 0N). 2N isoforms compose roughly 9%, 1N isoforms 54% and 0N isoforms 37% of cellular tau (13,15).

Overall, the six isoforms resulting from alternative mRNA splicing of tau are designated as 2N4R, 1N4R, 0N4R, 2N3R, 1N3R and 0N3R where the number preceding N corresponds to the number of N-terminal inserts and the number preceding R corresponds to the number of microtubule stabilizing repeats. Although, the relative expression levels of these isoforms are tightly regulated, the precise functional relevance of this regulation is not yet clear. The

expression of tau is also developmentally regulated. Fetal brain only expresses the 0N3R isoform of tau while all six isoforms are found in a normal adult human brain (16). Besides this, regional differences of tau expression and splicing within the brain have also been reported. For example, the granule cells of dentate gyrus only express 3R tau (17), the amount of 0N3R isoform was found to be lower in cerebellum (18) and the amount of 4R proteins was found to be higher in globus pallidus compared to other brain regions (19).

The most well-established function of tau is to bind and stabilize microtubules. Tau is known to affect various aspects of microtubule assembly. Tau is capable of promoting microtubule nucleation, growth and bundling as well as greatly reducing the dynamic instability of microtubules (20-22). Interaction of tau with microtubules is important for maintaining axonal transport and cell shape (23). Several cell culture models have also indicated tau's role in promoting neurite outgrowth and developing neuronal polarity (24-27). Tau is also known to influence the spacing of microtubules and thus control of the axonal diameter (28). This process of altering the microtubule spacing by tau is influenced by the size of the tau isoform (29). Bundling and spacing between microtubules can have great impact on transport of cargo and proteins along the microtubule tracks which in turn is particularly important for neurons due to their extended morphology.

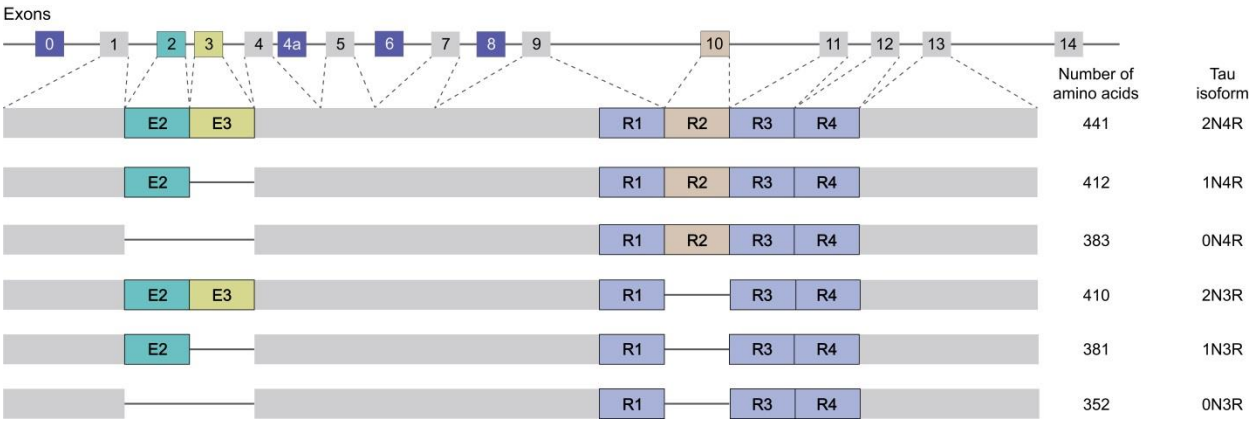


**Figure 1: Schematic representation of human tau gene and the six CNS isoforms generated by alternate mRNA splicing.** Human tau gene is located on chromosome 17 at position 17q21 and is made up of 16 exons. Exon 0 and 14 are transcribed but not translated. Exons 4a, 6 and 8 are not found in the CNS isoforms of tau. Alternative mRNA splicing of exons 2, 3 and 10 generates the six tau isoforms found in the brain. Inclusion or exclusion of exons 2 and 3 generates isoforms with either 2, 1 or no acidic N-terminal inserts. Exon 9 through 12 encode for the MT binding repeats. Alternative mRNA splicing of exon 10 determines the number of MT stabilizing sequences in tau. Overall, the resulting isoforms are noted as 2N4R, 1N4R, 0N4R, 2N3R, 1N3R and 0N3R. The numbers preceding N and R denote the number of N-terminal inserts and MT stabilizing repeats respectively. (Sizes of exons not drawn to scale)

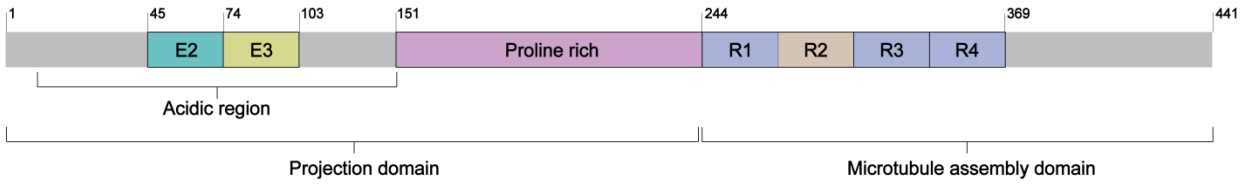


**Figure 2: Schematic representation for the longest 2N4R isoform of tau.** In the adult human brain, six isoforms of tau are generated by the alternate mRNA splicing of exon 2, 3 and 10 (represented as E2, E3 and R2 here). The N-terminal region of tau is rich in acidic residues followed by a proline rich region. The C-terminal half of tau contains the microtubule stabilizing pseudo-repeats encoded by exon 9 through 12 (represented as R1 through R4 here). The region preceding it projects off of the microtubules and is called the projection domain. The sequences important for aggregation are also contained within the repeat region and this region forms the core of the tau filament.

## 1.3 Tau function

In addition to tau's interaction with microtubules, increasing evidence has suggested tau's interaction with other cytoskeletal components. Tau has been found to be involved in remodeling of actin cytoskeleton (30-32). Tau also interacts with spectrin, plasma membrane and certain cellular components like mitochondria (33-35). These interactions have lead several to hypothesize that tau might be acting be as a mediator in establishing crosstalk between various cellular and cytoskeletal components. Further, Tau interacts with the SH3 domain of src-family non-receptor kinases such as fyn and fgr (36,37), phospholipase C-γ (PLC- γ) (38,39) and phosphatidylinositol bisphosphate (PIP2) (40) among several other cellular components that link tau as a signal transduction molecule with possible roles in maintenance of structural framework and neuronal polarity.

Besides this, several other less explored functions of tau have been suggested. Recent evidence suggests tau's possible role in neuronal activity, neurogenesis and synaptic plasticity (41-44). Tau has also been detected in the nucleus and nuclear tau seems to be playing a role in maintaining the integrity of DNA under normal and hyperthermic conditions (45,46).

## 1.4 Tau structure and domains

Tau has been classically described as a "natively unfolded" protein and biophysical studies have revealed very low secondary structure content (47,48). Consistent with the unfolded character of the protein, tau has an unusually high proportion of charged residues and a very low proportion of hydrophobic residues relative to other proteins, rendering tau to be an overall hydrophilic protein. The longest isoform of tau, 2N4R, contains 80 Serines or Threonines, 56 negatively charges residues, 58 positively charged residues and 8 aromatic residues. Tau is highly flexible,

resistant to heat or acid treatments and is very soluble in its native form (49). Although tau is overall a basic protein, the distribution of charges along the length of tau is another rather unique characteristic of tau. The first 120 residues are predominantly acidic followed by regions that have predominantly basic residues. This gives tau a dipole like characteristic. Further, there are several serine and threonine residues interspersed in between that can be phosphorylated to modulate charges along various regions of tau. The unfolded, flexible nature of tau along with the asymmetric distribution of charges are important properties that allow tau to bind to microtubules and several other partners.

Based on the distribution of amino acids as well as functional roles, tau molecules can be subdivided into two major domains: the C-terminal *microtubule binding domain* and the N-terminal *projection domain* (Figure 2). The microtubule binding domain contains 3 or 4 imperfect repeats (R1-R4), encoded by exon 9 through 12, responsible for tau's interaction with microtubules (11,12). Microtubule stabilization is achieved using an array of sites distributed within the 18 residue imperfect repeats (Figure 3) (50). These repeat regions are surrounded by 13 or 14 residue flanking regions which are also needed for tau's interaction with microtubules. 4R tau has an additional microtubule stabilizing repeat (encoded by exon 10) than the 3R tau. Further, the inter-repeat region between R1 and R2, particularly the peptide $^{274}$KVQIINKK$^{281}$, has been found to be the most potent in inducing microtubule assembly (11,22). This region is only present in the 4R isoforms. Because of these differences, 4R isoforms have a higher binding affinity than the 3R tau (51,52). Electrostatic interactions play an important role in mediating the interaction between tau and tubulin (53). The microtubule-binding repeat (MTBR) of tau has several positively charges lysines that are involved in tau's interaction with the acidic surface of

the microtubules (54). Charge altering post-translational modifications like phosphorylation within and around the repeat region are known to modulate tau's interaction with microtubules (55-57). While the MTBR region of tau engages in interactions with tubulin, the N-terminus of tau is known to project away from the surface of the microtubules and hence is called the projection domain (20). Although this region does not directly contribute in binding of tau with microtubules, it can influence microtubule organization and dynamics of tau's microtubule binding indirectly. One major impact of this region is affecting the spacing between microtubules (28,29). Alternative mRNA splicing in the N-terminal region can alter the number of N-terminal inserts and thus can generate tau with varying projection domain lengths which may alter the spacing between microtubules and axonal diameter. In line with this, peripheral neurons have a large axonal diameter. Peripheral neurons express an isoform of tau (also called "big tau") with an additional very long exon 4a (9,58). Apart from influencing the spacing, N-terminally truncated forms of tau also show altered microtubule interactions (59). Further, residue 2-18 of tau also called the PAD domain (Phosphatase-activating domain) is involved in a signaling cascade known to disrupt anterograde fast axonal transport in neurons (60). Other than the indirect influence of this region on tau's microtubule stabilization, the precise role for this region is not yet known. It has been proposed that tau's interaction with the plasma membrane is also mediated by its N-terminal region (34).

The region of projection domain preceding the microtubule stabilizing domain is rich in proline residues and is called the proline-rich region. This region of tau is involved in several signaling cascades. It has seven different PXXP motifs that provide recognition sites for several proteins like the Src family kinases like fyn and fgr (36). The interaction between tau and fyn has

proposed roles in mediating Aβ induced excitotoxicity (37). Additionally, the proline rich region and its phosphorylation state influences tau's interaction with microtubules (57,61).

Although tau is a natively unfolded protein with little to no secondary structure, recent biophysical data has revealed the existence of a global fold in tau in which various domains of tau engage in long-range interactions through its differently charged domains. This conformation of tau is called the "hairpin" or "paperclip" conformation in which both the N-terminal and C-terminal regions of tau fold over to interact with each other as well as the microtubule stabilizing region of tau and thus bringing the termini closer to each other (Figure 4) (62). This structure of tau has been proposed to be affected by both physiological mechanisms like MT binding and pathological changes like hyperphosphorylation and point mutations in tau (63,64).

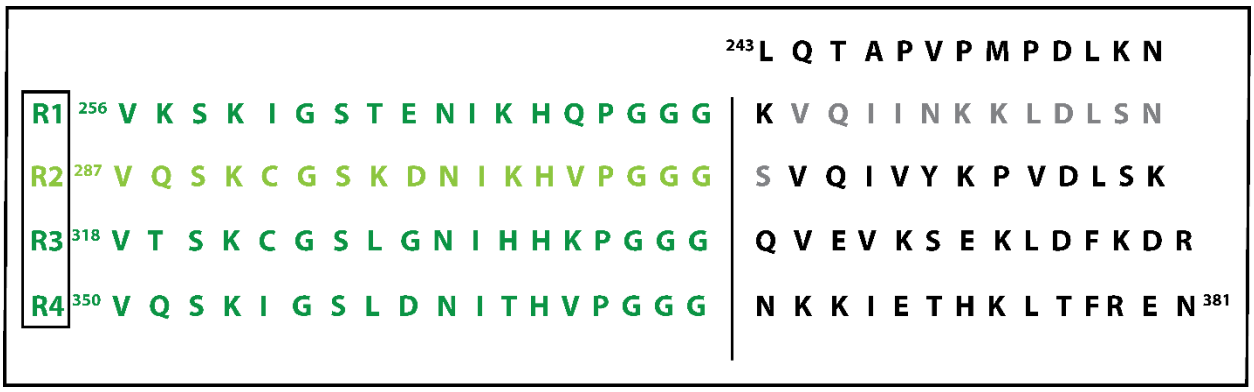


**Figure 3: Microtubule binding repeat region of tau.** The residues in green form the pseudo-repeat region with MT binding sequences. The residues on the right side of the vertical line represent the residues before and after the MT binding regions as well as the residues from the inter-repeat regions. Repeat R2 and the inter-repeat region preceding it are only present in the 4R isoforms of tau.

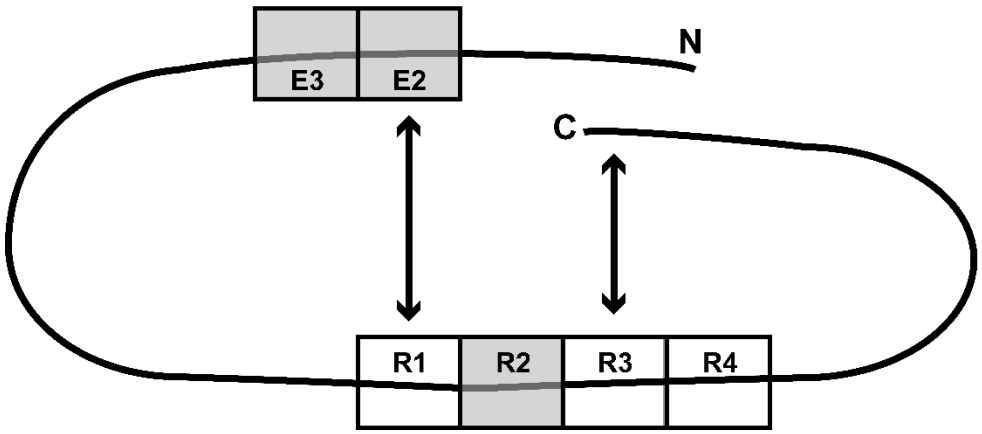


**Figure 4: The global hairpin structure of tau.** In the global hairpin also known as the "paperclip" conformation of tau, the N and C termini fold over to interact with the each other as well the interior of the protein through long range interactions.

## 1.5 Tau in pathology

Tau is involved in pathogenesis of a wide spectrum of neurodegenerative disorders collectively termed as tauopathies. A common feature of these tauopathies is the accumulation of intracellular filamentous aggregates of hyperphosphorylated tau. Despite intense investigation, the precise mechanism of tau mediated toxicity in these diseases remains elusive. In these disorders, due to possible alterations in tau like abnormal post-translational modifications or mechanisms promoting conformational changes in tau, tau loses its ability to effectively stabilize microtubules (65). Tau's inability to stabilize microtubules can lead to destabilization of microtubule network and cytoskeletal changes. The resulting unbound tau can then associate with each other to form insoluble and potentially toxic aggregates. Therefore, both loss of function and toxic gain of function have been implicated. Besides this, other mechanisms like tau mis-localization or direct toxicity of misfolded monomer tau are also being investigated.

There are arguments both supporting and opposing the loss of function hypothesis. Tau knockout mice only display minor cytoskeletal changes and lack any major abnormalities (28). However, recent evidence suggests behavioral alterations and brain atrophy in tau knockout mice even though tau's microtubule stabilizing function can partly be compensated by other microtubule associated proteins (MAPs) (66). A better understanding of the loss of function mechanism will be achieved as novel possible roles of tau in processes like neurogenesis, synaptic plasticity, neuronal activity get investigated.

Several arguments can be made in support of toxic gain of function hypothesis. The regional distribution of tau aggregates correlates with the severity of cognitive impairment in Alzheimer's disease (67,68). A five to ten-fold overexpression of tau in transgenic mice leads to formation of

intracellular inclusions of tau and the presence of these aggregates correlates with axonal degeneration (69). Another strong argument in support of this hypothesis is the discovery of autosomal dominant mutations in tau several of which have been found to be pro-aggregation and are known to cause tauopathies (14,70,71). Some of these mutations are found in exon 10 of tau which is only present in the 4R isoforms of tau, and thus would only affect 20-25% of the tau molecules expressed with 75-80% of tau being normal, raising a strong possibility for a toxic gain of function rather than a loss of function. In order to understand the nature of the underlying cause and toxicity of tau aggregation, the biochemical nature of aggregation and mechanisms affecting aggregation need to be understood.

## 1.6 Tau aggregation

Aggregation of tau is a characteristic feature of several neurodegenerative disorders. The presence of aggregates of tau in almost all of the tauopathies strongly suggests that aggregates of tau might exert toxicity but very little is known about what causes tau to aggregate and how this aggregation could be toxic. Given the soluble and unfolded nature of native tau, its aggregation into an ordered filamentous structure seems counterintuitive. Biochemically, the paired helical filaments of tau (PHFs) have a highly ordered β-sheet rich core (72,73). There are two short hexapeptide motifs in the beginning of the second and third microtubule binding repeats of tau, called PHF6 and PHF6* respectively, that have a propensity to change into β-sheets and are thought to be the drivers of tau aggregation (74,75). The first of these sequences, PHF6, $^{275}$VQIINK$^{280}$, is located in the second microtubule binding repeat which is only present in the 4R isoforms of tau. The second hexapeptide motif, $^{306}$VQIVYK$^{311}$, is present in the third microtubule binding repeat and is therefore present in all six isoforms of tau. These regions of tau are made of a stretch of alternate polar and apolar amino acids known to favor beta sheet

formation in proteins. In-between are also present amino acids like prolines that break this pattern and are known to disfavor β-sheet formation (76). Mutations in these regions that favor β-sheet formation, like P301L, are known to be pro-aggregation (77,78). Conversely, *in vitro* designed substitutions of two prolines for isoleucines , I277P and I308P, residing within the PHF6 and PHF6* motifs make tau incapable of assembling into aggregates (79).

In-vitro studies have demonstrated that the aggregation of tau proceeds by a nucleation-elongation mechanism (80). Initially, tau monomers join to form oligomeric structures. These oligomeric structures have been observed in cases of Alzheimer's disease and other tauopathies and just by themselves are proposed to be toxic. The oligomeric structures provide a nucleus for recruitment of more tau monomers and the smaller oligomeric aggregate elongates to form a large filamentous cross-beta structure (81). In the cross-beta structures, the beta sheet rich monomers of tau are stacked on top of each other through intermolecular interactions and the orientation of beta sheets is perpendicular to the longer axis of the filament. The core of these filaments is formed by the repeat region of tau and the unstructured N and C terminal portions of tau protrude out from the core and form a "fuzzy coat", named so because of its fuzzy appearance next to the highly ordered core region of the filament (82). These filamentous aggregates often take the form of paired helical filaments (PHFs) that have a periodicity of about 80 nm in AD (83). Apart from PHFs, tau aggregates in the form of straight filaments lacking periodicity have also been found in Alzheimer's disease brains (84). As these fibrillar structures grow and continue to accumulate, they form larger inclusions which, in the case of AD, are called neurofibrillary tangles (NFTs). The exact morphology of aggregates and appearance of inclusions is dependent on the tauopathy and will be discussed in later sections.

Although nucleation-elongation seems to be the path followed in formation of pathological tau aggregates, several questions remained unanswered. It is not clear what triggers the aggregation of highly soluble tau in the first place. *In vitro*, tau aggregation can be triggered using polyanionic compounds possibly through a conformational change in tau (85). Induction of tau aggregation has also been reported by two proteins, FKBP4 and FKBP52, through possible conformational changes induced in tau by these proteins (86). But, neither the nature of the inducer *in vivo* or the nature of conformational change is precisely known. Since tau recovered from NFTs is known to be highly phosphorylated, initial research in the field has focused on examining the effects of post-translational modifications of tau in order to identify possible differences between soluble and insoluble forms of tau.

## 1.7 Tau phosphorylation

Phosphorylation is the most widely studied post-translational modification of tau due to its role in both physiology of tau as well as the suspected role in pathology. It is also the most commonly occurring tau post-translational modification. Phosphorylation of tau is widely accepted to be a mechanism for modulating tau's interaction with microtubules under normal conditions (55). Phosphorylation of tau is tightly controlled by a balance of protein kinases and phosphatases. Kinases like glycogen synthase kinase 3 (GSK3), Cdk5, protein kinase A (PKA) (87-89) and phosphatases like phosphoprotein phosphatase 2A (PP2A) and PP-1 (90,91) are among the key players in modulating tau's phosphorylation state. There are 85 different putative phosphorylation sites in tau. In terms of pathology, it is not clear whether hyperphosphorylation of tau plays a causative role or is just a by-product of the pathological changes occurring in the cells. Nonetheless, aggregated tau from patients and in transgenic mice is found to be hyperphosphorylated. In normal brain, there is approximately 2 to 3 mole of phosphate found

per mole of tau but for tau extracted from AD brains, there can has as much as 5 to 9 mole of phosphate per mole of tau (92). Out of 85 potential phosphorylation sites, 28 are only found to be phosphorylated in AD brains compared to normal brain (reviewed in (93)). Abnormal tau phosphorylation is known to reduce microtubule binding. The impact of phosphorylation on aggregation of tau has been a matter of debate. Phosphorylation of tau precedes tau aggregation (94) though it is neither necessary nor sufficient on its own to drive tau aggregation *in vitro* . The effect of phosphorylation on tau aggregation has been difficult to understand partly due to the sheer number and combination of phosphorylation sites possible. To study the effect of phosphorylation *in vitro* in a more systematic manner, pseudo-phosphorylation has been utilized. Under this technique, serine and threonine residue are mutated to aspartate and glutamate using site-directed mutagenesis. These point mutations are made to mimic the size and charge of phosphorylated serine or threonine residues. Using this technique, it was found that pseudo-phosphorylation reduces the mobility of tau on SDS-PAGE indicating a possible change a conformation of tau (95). Pseudo-phosphorylation was also found to have an impact on tau's aggregation propensity in a manner dependent on the tau isoform. Even though phosphorylation of tau might be inducing a conformational change, its link with tau aggregation remains complex and is still a matter under investigation.

## 1.8 Other post-translational modifications of tau

Tau is known to undergo several other post-translational modifications like acetylation, nitration, glycosylation and oxidation among others (reviewed in (93)). The effect of these modifications of tau on its biochemical properties is not well understood. Acetylation is another tau modification that has gained attention in recent years. Lysine 280 has been recognized as a major site for tau acetylation.  A Drosophila transgenic model mimicking tau acetylation at site K280

exacerbated the toxicity observed in this model due to tau overexpression (96). Further, acetylation of tau seems to alter the phosphorylation state of tau in this model. Acetylation of tau is also suspected to have an impact on synaptic function and memory (97). Abnormal nitration of tau has also been detected in AD and other tauopathies. Nitration of tau reduces tau's ability to bind microtubules as well as have an impact on aggregation of tau (98). The major effect of glycosylation on tau seems to be enhancing phosphorylation of tau by suppressing its dephosphorylation and thus glycosylation can augment the potential toxic effects of hyperphosphorylation of tau (99). Finally, oxidation of tau at C322 has also been detected in tau from AD brain. C322 is present in the third microtubule binding region and can affect the conformation and aggregation of tau (100).

## 1.9 Tauopathies

Although the mechanisms inducing conformational changes in tau or triggering its aggregation remain under investigation, dysfunction and aggregation of tau is unequivocally linked to a wide spectrum of progressive neurodegenerative disorders together known as tauopathies. These disorders are characterized by intracellular aggregates of tau, progressive degeneration and death of neurons. Despite these commonalities, these group of diseases are rather heterogenous. These diseases differ from each other in terms of area of brain affected, age of onset, morphology of tau aggregates observed in these, isoforms of tau affected and presence of other proteins in the aggregates (reviewed in (8)). A brief overview of few of these: Alzheimer's disease (AD), Progressive Supranuclear Palsy (PSP), Corticobasal degeneration (CDB), Pick's disease (PiD)

and Frontotemporal Dementia with Parkinsonism linked to Chromosome 17 (FTDP-17) will be provided in the following section.

### 1.9.1 Alzheimer's disease

Alzheimer's disease is the most prevalent and widely-studied form of tauopathy. AD alone is the 6$^{th}$ leading cause of death. Symptoms include but are not limited to memory loss and behavioral changes. The two major hallmarks of AD are intracellular neurofibrillary tangles composed by the tau protein and extracellular senile plaques primarily containing the β-amyloid (Aβ) peptide (101). The progression of the disease correlates well with the amount and spread of tau aggregation (68). The spread of pathology follows a consistent path and can be characterized by the sequential appearance of tau pathology in various brain regions: Braak stage I, tau pathology in transentorhinal/peripheral cortex; Braak stage II, CA1 region of the hippocampus; Braak stage III, limbic structures; Braak stage IV, amygdala, thalamus and claustrum; Braak stage V, isocortical areas; and lastly Braak stage VI, primary sensory, motor and visual regions.

The aggregated tau composing the neurofibrillary tangles in AD is polymerized predominantly into paired helical filaments. Although PHFs are more common in NFTs, straight filaments are also observed (102). Aggregates in AD contain all 6 isoforms of tau in roughly the same proportion as they are found in a normal brain (103). Other than tau, NFTs in AD also contain ubiquitin, RNA, GSK-3β, α-synuclein and apolipoprotein (104-108). Although no genetic polymorphisms are detected in tau in case of AD, 5% of the total AD cases are associated with genetic polymorphisms in other proteins, amyloid precursor protein (APP) or presenilins 1 and 2 (109). These cases are early onset compared to the sporadic AD cases. Aβ pathology is also most likely upstream of tau pathology. For these reasons, role of Aβ in AD took the primary focus.

While Aβ pathology may be upstream of tau, there are compelling arguments in favor of tau's role in AD. The location of NFTs correlates better with the regions of neurodegeneration and the observed clinical manifestations of the disease than the plaque pathology (67,110). In transgenic mice and cultured cells, Aβ requires the presence tau to exert any major toxic effects (63,111). On the other hand, toxic effects of tau can be seen independent of Aβ in cultured cells as well as in vivo models (112,113). The discovery of autosomal dominant mutations in tau in other tauopathies leading to tau aggregation and neurodegeneration supports tau's role in neurodegenerative process (70,71,114). Finally, neurodegeneration is observed in several other sporadic tauopathies without the presence of Aβ (115).

### 1.9.2 Progressive Supranuclear Palsy

Progressive Suprabuclear Palsy (PSP) is described as a late-onset atypical parkinsonism. PSP cases mainly display movement defects and personality changes (116). Although dementia is also observed at later stages of the disease (117). Neuropathologically, cases of PSP display neuron loss, gliosis and NFT formation primarily in subcortical regions particularly in subthalamic nucleus, basal ganglia and brainstem but not as much on the frontal cortex as in AD (118). Ultrastructural examination also points towards major differences between AD and PSP. Instead of paired helical filaments like AD, NFTs in PSP are composed primarily by straight filaments. Straight filaments are also observed in the glial cells (119,120) . PSP is primarily a 4R tauopathy, that is, tau filaments mainly contain 4R isoforms of tau, although variable amounts of 3R isoforms are also detected in some patients (121). Elevation in the levels of 4R isoforms mRNA is seen in the brainstem region of these patients and may contribute to the preferential deposition of 4R isoforms in PSP (122).

### 1.9.3 Corticobasal Degeneration

Corticobasal degeneration is a rare, sporadic, late onset and slow progressing neurodegenerative disorder. Some aspects of Corticobasal degeneration overlap with PSP (123). Like PSP, CBD is also a 4R tauopathy. However, it differs from PSP in terms of regions of brain affected. CBD pathology is observed in the cerebral cortex, substantia nigra and cerebellum (124). Ultrastructural analyses of CBD reveal both PHFs and straight filaments (125). Clinical symptoms include cognitive disturbances, difficulty with speech and motor dysfunction like rigidity and akinesia.

### 1.9.4 Pick's disease

Pick's disease is characterized by the presence of Pick bodies which are spherical inclusions containing both PHFs and straight filaments, however, filaments are wider than found in AD (126,127). Aggregates are composed of almost exclusively the 3R isoforms of tau. Clinical symptoms include mood disturbances and language difficulties leading to mutism. Pick bodies are predominantly found in the granule cells of dentate gyrus, hippocampus and cortical areas (128).

### 1.9.5 Frontotemporal Dementia with Parkinsonism Linked to Chromosome 17 (FTDP-17)

Frontotemporal Dementia with Parkinsonism linked to Chromosome 17 or FTDP-17 actually represents a group of clinically and pathologically heterogenous neurodegenerative disorders caused by autosomal dominant mutations in tau gene (129). The discovery of these mutations in late 1990's established the causative role of tau in neurodegeneration. To date, more than 50 different exonic and intronic mutations (Figure 5) have been identified to cause this early-onset

neurodegenerative tauopathy in approximately 150 different families across the globe (reviewed in (130)). Several of the mutations affect microtubule stabilizing propensity of tau or/and are pro-aggregation (77). Although, these mutations in themselves are rare, they have been widely used in the field of *in vitro* tau biology to understand the pathological changes that drive tau towards aggregation as well as the *in vivo* models to understand the neuropathology of tauopathies (131-133). Aggregation of tau is prevalent in cases of FTDP-17 but the clinical presentation and precise neuropathology can vary widely between families and sometimes within a same family (134-137). Age of onset can vary from the early 20s to late 70s with an average age of onset being 49 years (130). Symptoms often begin with psychiatric changes but progress to affect a wide range of brain functions. Some of the usual symptoms include behavioral changes, cognitive impairment, language difficulties, loss of executive functions and motor function. Due to the varied clinical symptoms and pathology, cases of FTDP-17 are often described by their similarities to other tauopathies like AD, Pick's disease, PSP and CBD. Several FTDP-17, particularly the ones near exon 10 or in the non-coding regions around exon 10, are known to affect the 3R to 4R tau isoform balance (138). 4R tau differs from the 3R tau in its ability to stabilize microtubules as well as its binding affinity for tubulin and may explain why the disruption of this ratio could be toxic. Further, biochemical analysis of aggregates from FTDP-17 cases reveal that some of the FTDP-17 mutations only cause certain isoforms of tau to be deposited in the brain, for example, in case of R5L and G389R, 4 of the six isoforms are found in the aggregates (139,140). Several FTDP-17, particularly the ones near exon 10 or in the non-coding regions around exon 10, are known to affect the 3R to 4R tau isoform balance (138). 4R tau differs from the 3R tau in its ability to stabilize microtubules as well as its binding affinity for tubulin and may explain why the disruption of this ratio could be toxic. Further, biochemical

analysis of aggregates from FTDP-17 cases reveal that some of the FTDP-17 mutations only cause certain isoforms of tau to be deposited in the brain, for example, in case of R5L and G389R, 4 of the six isoforms are found in the aggregates (139,140). Altered splicing patterns of the N-terminus of tau have also been detected for one of the mutations, E342V, causing a higher expression of tau isoforms missing the N-terminal inserts (141). Since the role of the N-terminal region is not clearly understood, the expression levels of these exons haven't been determined for several FTDP-17 cases and it is possible that these levels do get affected more than our current knowledge.

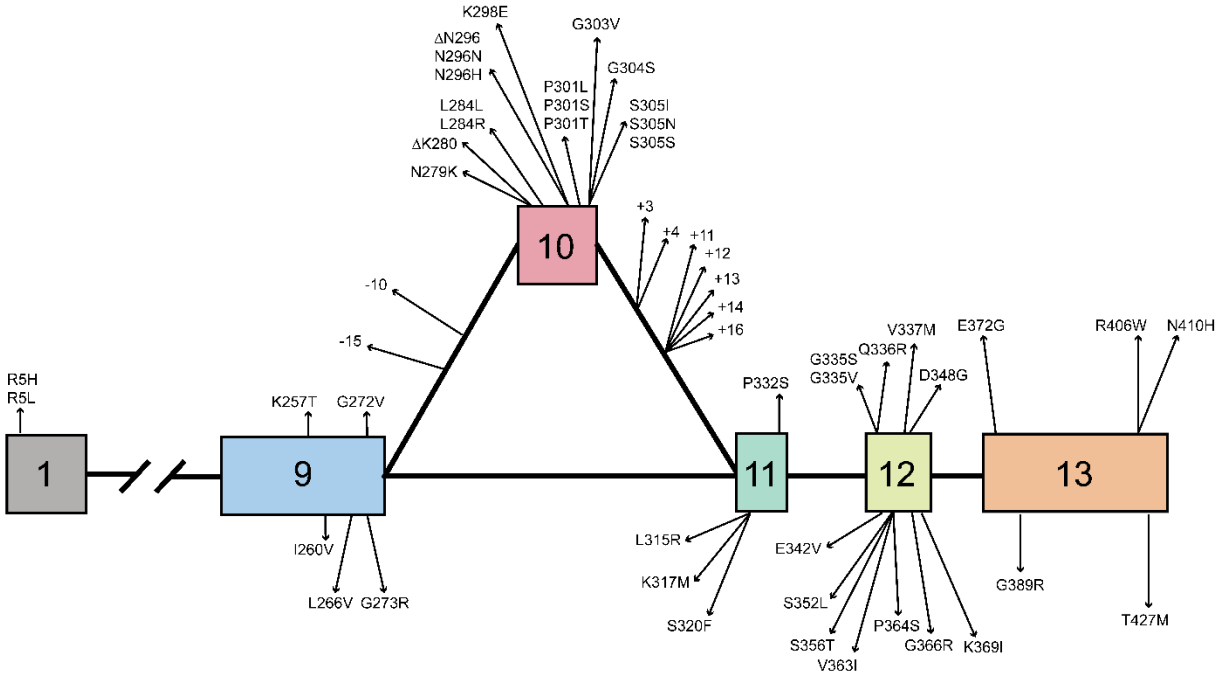


**Figure 5: The known FTDP-17 mutations and their location on the tau gene.** Intronic and exonic FTDP-17 mutations. Most of the mutations are present within and around the microtubule binding repeat region but mutations have also been discovered in the terminal exon 1 and 13.

(Adopted from B. Ghetti *et al.* **2015**)

## 1.10 In vitro induction of tau aggregation

In order to examine the effect of mechanisms influencing the process of tau aggregation or to find therapies that can impede the process of tau aggregation *in vitro*, aggregation of full length wild-type tau first needs to be achieved in a consistent manner. The highly soluble nature of native tau prevents it from aggregating on its own in a time-frame relevant for *in vitro* studies and requires the addition of an inducer molecule. Some of the common inducers of tau aggregation *in vitro* are polyanionic compounds like heparin, free fatty acids like arachidonic acid, planar aromatic dyes like congo red, and nucleic acids (74,142-144). Most of the inducer molecules known *in vitro* are negatively charged. The exact mechanism of aggregation induction by these molecules is not known but one of the suggested possibilities is that these negatively charged compounds mask the repulsive forces between the positively charged residues from the repeat regions of two tau monomers. Alternatively, some of the recent data suggests that these compounds cause PHF6 and PHF6* regions of tau to adopt an extended conformation which leads to loss of intramolecular interactions and favoring intermolecular interactions to initiate the fibrillization process (85).

Although it is not known what inducers, if any, trigger the aggregation of tau *in vivo*, a few of these like fatty acids and nucleic acids are within the realm of possibility. Arachidonic acid (ARA) induction of tau aggregation can be achieved in the laboratory using physiologically relevant concentrations of tau. The aggregates obtained using this method resemble the straight filaments seen in AD and other tauopathies (145). They also bind to the dyes like Thioflavin S often used to stain the cross-beta structured amyloidal aggregates. Finally, these aggregates are also recognized by antibodies that recognize the autopsy-derived PHFs.

The above-mentioned characteristics of aggregates obtained by the arachidonic acid induction have made this a routinely utilized method to induce tau aggregation. This methodology has been successfully used to conduct various studies, like looking at the effect of post-translation modifications, tau mutations and testing aggregation inhibitors among several others. However, A great majority of these studies have been conducted using the 2N4R isoform of tau, largely because of the difficulties associated with reliably using this method for other isoforms of tau (discussed in Chapter 2). The focus of the next chapter has been to first, identify some of these difficulties. Second, try to understand the reasons behind these difficulties in an effort towards understanding the fundamental differences between tau isoforms which can not only help overcome the challenges associated with *in vitro* aggregation of tau isoforms but can also further our understanding about tau isoforms. Once that goal was achieved, the modified *in vitro* aggregation conditions could then be used to understand the effect of FTDP-17 mutations on aggregation of various isoforms of tau (Chapter 3). In this chapter, a comparative study of three different FTDP-17 mutations was conducted to answer the question, whether the effect or the intensity of the effect of these mutations can differ between isoform. Further, to obtain a complete view of the effect of these mutations, along with aggregation, their effect on the normal functioning of tau (MT stabilization) was also examined.

# CHAPTER 2: Optimization of *in vitro* conditions to study the arachidonic acid induction of 4R isoforms of tau

# Chapter 2: Optimization of *in vitro* conditions to study the arachidonic acid induction of 4R isoforms of tau

## 2.1 Introduction

The accumulation of filamentous aggregates of microtubule associated protein tau is a pathological hallmark of several neurodegenerative disorders including Alzheimer's disease (AD) (4,146). In an adult human brain, six different isoforms of tau are generated by alternative splicing of exons 2, 3 and 10 from an mRNA encoded by a single gene (147,148). The C-terminal half of these proteins contains imperfect repeat sequences of amino acids encoded by exons 9 through 12 (149). The pseudo-repeats contain motifs responsible for tau's interaction with microtubules called microtubule-binding repeats (MTBR) (11,12). The second repeat (MTBR2) is encoded by exon 10 and thus its presence or absence categorizes tau into either four repeat (4R or $10^+$) or three repeat (3R or $10^-$) isoforms, respectively. Alternative mRNA splicing of N-terminal exons 2 and 3 can change the number of acidic N-terminal inserts present within tau and give rise to isoforms with either two N-terminal inserts (2N isoforms), one N-terminal insert encoded by exon 2 (1N isoforms), or isoforms without either N-terminal insert (0N isoforms). Therefore, the six tau isoforms are designated 2N4R, 1N4R, 0N4R, 2N3R, 1N3R, and 0N3R (148).

Expression of tau isoforms is both temporally and spatially regulated (16,150). Isoforms are also known to exist in a specific ratio in the brain and disruption of this balance is associated with tauopathies (70,122,151,152). The putative involvement of exon 10 in tau pathology has been extensively studied and its impact on tau pathology has been widely demonstrated (153,154). A number of studies have pointed out the differences between 3R and 4R tau and how a disruption of the 3R to 4R tau balance could impact pathology: 3R tau differs from 4R tau in its

stabilization of microtubules (155,156), its aggregation (95,157), and its seeding of the aggregation of monomeric tau (158). Disruption of the balance of the 3R to 4R tau isoform ratio has also been shown to affect anterograde vs retrograde transport of APP (159). However, the direct impact of exons 2 and 3 on tau pathology is less well understood. Recent evidence has established links between the inclusion or exclusion of the N-terminal inserts with increased pathology and disease (160-162), although the underlying mechanisms remain largely unclear. For example, the *MAPT* haplotype 2 resulting in higher levels of exon 3-containing transcripts of tau has been associated with reduced risk for tauopathies like progressive supranuclear palsy (PSP) and corticobasal degeneration (CBD) (163). A weak association between tau haplotype and increased risk for AD has been identified (164), as well as reports of altered tau isoform expression in some cases of AD (152). On a cellular level, the exogenous addition of Aβ42 peptide has been shown to favor the exclusion of exon 2 and 3 in tau transcripts *in vitro* (165). Furthermore, altered expression of N-terminal variants of tau or unexpected patterns of their inclusion in aggregates have been identified in specific cases of frontotemporal dementia with parkinsonism linked to chromosome 17 (FTDP-17) and PSP (135,139,141). It is likely that the N-terminal exons can play a significant role in the underlying mechanisms leading to tau-induced neurodegeneration and therefore warrants more in-depth investigation.

*In vitro* model systems utilizing negatively charged species as the inducer of tau aggregation have been pivotal in gaining insights into the mechanisms resulting in tau aggregation and possible factors influencing its aggregation (166-168). One such model is the use of the polyunsaturated fatty acid arachidonic acid (ARA) to induce the aggregation of tau *in vitro* (169). Fatty acid induction of tau aggregation may be of particular interest due to its potential biological role in the neurodegenerative process. For example, fatty acid metabolism is altered in

pathology (170,171). A rise in lipid peroxidation products and increased concentration of free cytosolic polyunsaturated fatty acids has also been linked to several neurodegenerative disorders (172,173). Fatty acids are also the prime components of cellular membranes and tau filaments have been observed to be either associated with or potentially growing out of membranes of neurons (174). ARA induced *in vitro* polymerization of tau is a widely established protocol and has successfully been used to model tau aggregation *in vitro* in a variety of studies, including the effects of phosphorylation, truncation, nitration, and FTDP-17 associated mutations in tau (77,175-177). However, the bulk of the ARA-induced aggregation studies of tau *in vitro* have focused on the 2N4R isoform. This could be due in part to the difficulties associated with *in vitro* ARA-induction of the 1N and 0N isoforms. For example, it has been reported that tau isoforms lacking exons 2 and 3 (the 0N isoforms of tau) fail to elongate into fibrils in the presence of ARA *in vitro* and only form short oligomeric aggregates of tau (178). To better understand the effect of disease related changes on 0N and 1N isoforms of tau, there is a need for a more robust *in vitro* aggregation model system for these isoforms.

We hypothesized that the change in the isoelectric points of the N-terminal projection domain (residues 1-243) that would result from the inclusion or exclusion of exons 2 and 3 was responsible for the differences previously observed in the *in vitro* ARA-induction of tau polymerization. We tested this hypothesis by altering the pH and ionic strength of both ARA-induced polymerization conditions and filament fixation conditions. We found that under normal *in vitro* polymerization conditions, the filaments formed by 1N4R and 0N4R isoforms have a tendency to aggregate into larger clusters of filaments. The degree of clustering was closely related to the overall charge of the N-terminal region. In conclusion, we show that by increasing the ionic strength of the *in vitro* ARA-induction of tau aggregation, robust and reliable amounts

of aggregation of all three 4R isoforms can be obtained, opening new avenues for tau aggregation studies that have previously been hampered by these differences in isoform isoelectric points.

## 2.2 Methods and Materials

### 2.2.1 Protein expression and purification

All wild-type 4R tau isoforms and corresponding pseudo-phosphorylated mutant proteins (7-phos) were expressed and purified as previously described (95,179). For the 7-phos proteins, mutations were introduced using the Quikchange site-directed mutagenesis kit (Agilent cat. 200523). The 7-phos proteins contained the following mutations (numbered according to the 2N4R isoform) S199E, S202E, T205E, T231E, S235D, S396E and S404E. DNA for all wild-type and mutant isoforms in the pT7C vector (with a 6X histidine tag on the N-terminus) were transformed into BL-21 cells. Proteins were expressed and purified using nickel affinity chromatography followed by size exclusion chromatography as described previously. Final elution of protein was in a 10 mM HEPES buffer pH 7.64. Protein concentrations were determined using the Pierce$^{TM}$ BCA protein assay kit (Thermo Scientific cat. 23225) following the manufacturer's protocol with BSA as a standard.

### 2.2.2 Tau polymerization with Arachidonic acid:

Proteins at the concentration of 2 µM were incubated with Arachidonic Acid (ARA) (Millipore cat. 181198-100MG) to a final concentration of 75 µM in the polymerization buffer containing NaCl, 10 mM HEPES pH 7.64, 0.1 mM EDTA, 5 mM DTT and 3.75% ethanol (vehicle for

ARA) for 24 hours at 25 °C. The standard final concentration of the NaCl in the tau polymerization reactions was 100 mM, but ranged from 100 mM to 250 mM dependent on the experiment (see Results). Control reactions (in absence of ARA) were treated the same way as polymerization reactions except ARA was replaced with ethanol carrier for these reactions.

### 2.2.3 Fixation of tau filaments and Electron Microscopy

Fixation: For experiments to determine the effect of pH (Fig 2, 4): Polymerization reactions performed at the standard conditions of salt (100 mM NaCl) and pH (7.64) were diluted 1:10 in a buffer of selected pH (dependent on the experiment) along with the fixative glutaraldehyde (Electron Microscopy Sciences cat. 16120) at a final concentration of 2%. Buffers used for dilution at specific pH were CAPS (pH 10), CHES (pH 8.7), HEPES (pH 7.64), MOPS (pH 6.8), MES (pH 6.1 or 6) and acetate (pH 5). All buffers were used at a 10 mM strength with 0.1 mM EDTA and 100 mM NaCl (same as polymerization conditions).

For experiments looking at the effect of pH at higher ionic strength (Fig 3): Polymerization reactions set up at the standard conditions of salt (100 mM NaCl) and pH (7.64) were diluted 1:10 in a fixation buffer that contained 200 mM NaCl instead of 100 mM at the pH values indicated in Fig 3.

For rest of the experiments (Fig 1, 5 and 7): Polymerization reactions were set up and diluted 1:10 for fixation in 10 mM HEPES buffer pH 7.64 with 0.1 mM EDTA. The concentration of NaCl in the fixation buffer was identical to the buffer utilized for polymerization.

After a 5-minute fixation at chosen conditions, samples were deposited on a formvar coated copper grid (Electron Microscopy Sciences cat. FCF-300CU) and stained with 2% uranyl acetate according to the previously published protocol (95). Briefly, 10 μL of diluted and fixed polymerization reactions are pipetted onto a piece of parafilm. EM grids are placed on top of the

drop where they float for 1 minute. The grid is then blotted on filter paper, placed on a drop of water, blotted with filter paper, placed on a drop of 2% uranyl acetate, and blotted dry. All drops are 10 µL pipetted onto parafilm. The grid is then placed on another drop of 2% uranyl acetate and floated for 1 minute, and blotted dry for a final time. To ensure consistency between grids, fixation times are not allowed to exceed 15 minutes. Care should be taken handling glutaraldehyde and uranyl acetate.

Electron Microscopy data collection: FEI TECNAI F20 XT field emission electron microscope (Hillsboro, OR) was used to examine the grids at a magnification of 3600x. Images were captured with the Gatan Digital Micrograph imaging system. Two different methods were employed to collect images: i) A *Random* selection method was utilized to minimize user bias. Under this method, five different areas of a grid were selected at random and images were captured. ii) A *Search* method was utilized to locate the less frequently encountered clusters of filaments. Here, the grid was searched until filament clusters were found and then images were captured. In general, five images are collected per grid.

### 2.2.4 Charge predictions

PROTEIN CALCULATOR v3.4 by Scripps Research Institute (http://protcalc.sourceforge.net/) was used to calculate the charges of N-terminal projection domain of 4R tau isoforms at several pH values.

### 2.2.5 Thioflavin S fluorescence

Thioflavin S (ThioS) (Sigma cat. T1892) was dissolved in MilliQ water at a concentration of 0.224 mg/ml followed by filtration through a 0.22 micron filter. The ThioS solution was protected from light, prepared and used the same day. 150 µL of polymerization reactions were

transferred to a 96 well, flat bottom, white plate. 6 µL of ThioS solution was added to each well. The plate was shaken for 30 seconds followed by an incubation in the dark for 20 minutes. An excitation wavelength of 440 nm and an emission wavelength of 520 nm was used to record the shift in fluorescence resulting from ThioS binding to tau aggregates (145) using a Cary Eclipse fluorescence spectrophotometer (Varian Analytical Instruments, Walnut Creek, CA). Control reactions were used to determine the background fluorescence readings, and these values were subtracted from experimental wells.

### 2.2.6 Right angle laser light scattering

Polymerized protein solutions were transferred to 5 mm X 5 mm optical glass fluorometer cuvettes (Starna Cells, Atascadero, CA) and illuminated with a 12 mW solid state laser with a wavelength of 532 nm and operating at 7.6 mW (B&W Tek, Inc., Newark, DE). An image of the amount of light scattered was captured at the angle perpendicular to the path of the laser using a SONY XC-ST270 digital camera at an aperture setting of f5.6-8. Precise conditions should be optimized for each specific laser and camera setup. The images were analyzed using the histogram function of Adobe Photoshop CS5 Version 12.0 x32 to obtain a mean intensity indicative of the amount of light scattered. A fixed area (150 px by 15 px) was selected from each image and the mean density was recorded to represent the amount of light scattered for each condition. For calculating the pixel intensity across an image of scattered light, the plot profile function of ImageJ was used for a 180 pixels wide line.

### 2.2.7 Kinetics of aggregation

Although data are not presented in this report, these methods can be used to follow the kinetics of tau polymerization. For right angle laser light scattering, reactions are prepared in a

microcentrifuge tube and transferred to 5 mm X 5 mm optical glass fluorometer cuvettes before the addition of ARA. The amount of background scattering without ARA is measured and is used for background subtraction. ARA is added, gently mixed, and the amount of scattering is immediately captured (time zero). Images of scattered light are generally taken at 5, 10, 15, 20, 25, and 30 minutes. Images are then taken at 45 and 60 minutes, followed by captures at 90, 120, 180, 240, 300, and 360 minutes. ARA-induced polymerization reactions generally have reached an apparent steady state after 6 hours of incubation. Similarly, the kinetics of polymerization reactions can be followed using electron microscopy, although this method is much more involved and time-consuming. For this approach, reactions are performed in microcentrifuge tubes and then samples are taken at various time points, fixed, and EM grids are prepared for viewing and quantitation. We often reduce the number of time-points taken using this approach. In general we do not use ThioS for measuring kinetics of reactions because we have found that the addition of ThioS at the beginning of an ARA-induction of tau polymerization enhances the rate and amount of aggregation.

## 2.3 Results

### 2.3.1 Problems associated with arachidonic acid induced in vitro aggregation of shorter human tau isoforms

ARA polymerization has been utilized in a number of studies targeted to investigate several aspects of tau aggregation *in vitro* (77,175-177). Using this technique, recombinantly expressed human tau isoforms are incubated in the presence of ARA in buffer containing 100 mM NaCl, 10 mM HEPES pH 7.64, 5mM DTT and 0.1 mM EDTA. Under these conditions, 2N4R and 1N4R isoforms polymerize to form filamentous aggregates of tau reminiscent of straight fibrils

associated with Alzheimer's disease and other tauopathies (Figure 6A). However, as previously reported, the 0N4R isoform fails to form straight filaments that are easily detectable by electron microscopy (Figure 6A). This result is confounded by the observation that ARA-induced 0N4R isoform polymerization reactions do have thioflavin S (ThioS) reactivity to an extent comparable with 2N4R and 1N4R isoforms (Figure 6B). There also seems to be an isoform-dependent difference in the appearance of laser light scattered by the filaments. The light scattered by the 0N4R isoform often has a speckled appearance, with density missing from certain regions and oversaturated foci of scattered light in other areas, in contrast to the light scattered by the 2N4R and 1N4R isoforms which has a smoother, more uniform appearance (Figure 6C).

The observed discrepancies between ThioS fluorescence and TEM data combined with the anomalous speckled appearance of the light scattered by the 0N4R isoform compared to the longer N-terminus variants, raised the possibility that the 0N4R tau filaments were conglomerating in solution. To investigate this possibility, we performed a thorough search of the microscopy grids for 0N4R isoform polymerization reactions rather than the standard operating procedure of randomly selecting areas of the grid for viewing to reduce observer bias in field selection. Large, amorphous structures with heavy stain accumulations and with what appeared to be filaments protruding from their edges were observed in 0N4R polymerization reactions using the search method (Figure 6D). Clusters of tau filaments were also occasionally detected with thorough searching of EM grids for 1N4R polymerization reactions (Figure 6D), but these clusters were smaller and accumulated less uranyl acetate stain than those observed with 0N4R isoforms. Clusters of 2N4R isoform filaments could not be found under these experimental conditions even with extensive searching (Figure 6D). It is clear from this data that

the filaments formed from N-terminal variants of 4R isoforms have distinct solution characteristics from one another under these conditions.

### 2.3.2 Differential electrostatics of the tau N-terminal projection domain and its role in filament clustering

One fundamental difference between these isoforms is in their primary structure. Exon 2 and exon 3 each contain 29 amino acids and both regions are acidic in nature (below).

| | | Net Charge |
|---|---|---|
| | - -- -- - - + - | |
| **Exon 2** | **E**SPLQTPT**ED**GS**EE**PGS**E**TS**D**A**K**STPTA**E** | -7 |
| | - -- + - - | |
| **Exon 3** | **D**VTAPLV**DE**GAPG**K**QAAAQPHT**E**IP**E**GTT | -4 |

At the standard working pH of 7.64, the N-terminal projection domain of the 2N4R (exon 2 and 3), 1N4R (exon 2 only), and 0N4R (neither exon) isoforms are predicted to have an overall charge of -5.6, -1.7, and +5.3, respectively (Table 1). The N-terminal projection domain remains largely disordered and protrudes from the filament core formed by the MTBR region of tau (7,168,180,181). We therefore hypothesized that the clustering of 1N and 0N filaments is an outcome of the lower acidity and the overall charge of the N-terminal projection domain extending from the filament core.

To test whether the decreasing acidity of the N-terminal projection domain leads to filament clustering through electrostatic interactions, we sought to counter this effect by either altering the pH or increasing the ionic strength of the solution containing tau filaments. Unlike what is predicted for the standard pH of 7.64, all three isoforms would have positively charged projection domains at a pH of 6.0, and all three isoforms would have negatively charged projection domains at a pH of 10.0 (Table 1).

We first investigated the effects of pH on tau filament clustering by varying pH at the time of fixation. Polymerization reactions were performed as previously described using standard conditions of 2 μM protein and 75 μM ARA in 10 mM HEPES buffer, pH 7.64, and 100 mM NaCl. After 16 hours of incubation, samples were prepared for electron microscopy. Samples were fixed with 2% glutaraldehyde in buffers with different pH values chosen to alter the overall charge of the N-terminal projection domain: all positively charged (pH 6); standard conditions with different charges (pH 7.64); and all negatively charged (pH 10) (see Table 1). As predicted, buffer conditions for positively charged N-terminal projection domains (pH 6) results in filament clusters for all three 4R tau isoforms that could be located on EM grids with searching (Figure 7A, 7G, 7M). Under these conditions, most EM fields of view selected at random had few filaments with only small particles of tau visible (Figure 7B, 7H, 7N). Fixation buffer conditions for negatively charged N-terminal projection domains (pH 10) resulted in even distributions of single strands of tau filaments on the electron microscopy grid for all three 4R isoforms, even with extensive searching (Figure 7E, 7F, 7K, 7L, 7Q, 7R). The 0N4R isoform, previously thought to only make small oligomeric aggregates with ARA (178), also showed filamentous tau aggregates when fixed at pH 10 (Figure 7Q, 7R), suggesting the possibility that the increase in pH causes clusters of filaments to dissociate during the fixation process.

The modulation of filament clustering by changes in pH is consistent with the hypothesis that this phenomenon is mediated through electrostatic interactions. To further test this model, we sought to determine whether filament clustering observed under standard polymerization conditions could be disrupted with increased ionic strength. Tau aggregation reactions were again performed under standard conditions of pH 7.64 and 100 mM NaCl. Tau filaments were subsequently diluted in buffers containing higher amount of salt (200 mM) before glutaraldehyde

fixation in buffers with the same low (6), standard (7.64), and high (10) pH values examined above. Increased ionic strength of fixation buffers drastically decreased filament clustering (Figure 8). For example, the clustering of 0N4R filaments was essentially eliminated when the filaments were fixed at pH 7.64 and 200 mM NaCl (compare Figure 7O-P and 8O-P). The increased ionic strength also drastically reduced the amount of 2N4R isoform filament clustering observed at pH 6 (compare Figure 7A-B and 8A-B). Therefore, increased ionic strength reduced the degree of filament clustering in a manner that correlates with the degree of negative charges in the N-terminal projection domains.

### 2.3.3 Change in the acidity of the projection domain of tau through pseudo-phosphorylation impacts filament clustering

The previous results indicate that the clustering of filaments is due to electrostatic interactions involving the N-terminal projection domain, and more negatively charged amino acids in this region reduce clustering of tau filaments. We tested this directly by comparing non-modified protein with "pseudo-phosphorylated" versions. Pseudo-phosphorylation involves the mutation of serines and threonines to aspartic or glutamic acids. We used proteins called 7-phos because they have 7 different phosphorylation-mimicking mutations. Five of these residues (S199E, S202E, T205E, T231E, and S235D) are located in the N-terminal projection domain and the other two (S396E and S404E) are in the C-terminal region.

Due to the presence of additional acidic residues, the pH at which the projection domains of pseudo-phosphorylated proteins would become positively charged and thus potentially result in filament clustering are expected to be lower than their wild-type counterparts (Table 2). We compared all three 4R isoforms wild-type proteins with their pseudo-phosphorylated forms using ARA and standard buffer conditions of 100 mM NaCl and pH 7.64. The fixation conditions were

chosen on an isoform-specific basis for high pH (both negatively charged), intermediate pH (different charges for N-terminal projection domains), and low pH (both positively charged) (Table 2).

The filaments formed by all three pseudo-phosphorylated 4R isoforms required a lower pH than their corresponding wild-type proteins for clustering (Figure 9A-C). For example, an even distribution of filaments was observed for the 7-phos 1N4R protein at pH 6.8 (negatively charged), while the wild-type 1N4R filaments (positively charge at this pH) were completely clustered (Figure 9B). An even distribution of filaments was observed at pH 10 (both negatively charged) for both these proteins, while filaments of both wild-type and pseudo-phosphorylated proteins clustered at pH 6 (positively charged). These results indicate that the pseudo-phosphorylation did not change the overall pattern of response of filament-filament interaction to changing pH, but rather changed the pH at which filaments clustered. Conditions that result in a positively charged N-terminal projection domain resulted in filament clustering, and conditions that result in a negatively charged N-terminal projection domain reduced filament clustering as demonstrated by even distributions of filaments on the EM grid.

### 2.3.4 Effect of polymerization buffer salt concentration on total amount of aggregation of tau isoforms

Because increasing the ionic strength of the fixation buffer or increasing its pH to 10 prevented the clustering of 1N4R and 0N4R filaments, we sought to determine whether employing these conditions during the polymerization reaction itself would have similar results.

Increasing the pH for our tau polymerization reaction to pH 10 inhibited tau aggregation completely (data not shown). There could be several explanations for this outcome. One reason

could be that rise in pH could change the micellar state of ARA which in turn can alter its ability to cause tau aggregation. Another possible reason could be that a rise in pH may alter the conformation of tau and render it incapable of aggregation.

We sought to determine whether increasing the ionic strength during polymerization would eliminate the clustering without compromising the total amount of aggregation of 4R tau isoforms. ARA-induced polymerization reactions were performed using pH 7.64 and 200 mM NaCl instead of 100 mM NaCl. Under these conditions, the filaments for all three isoforms were evenly distributed on the grid when fields were selected randomly. Clusters of filaments were not detected for any of the three isoforms even with extensive searching (Figure 10A). Furthermore, laser light scattered by the filaments assembled at 200 mM NaCl for 0N4R tau also had a smooth appearance (Figure 10B) unlike the speckled appearance observed at 100 mM NaCl (compare Figure 6C with Figure 10B).

To compare the overall levels of tau polymerization with increasing ionic strength, 2 μM protein was incubated with 75 μM ARA for 24 hours at pH 7.64 and NaCl ranging from 100 mM to 250 mM. At the end of the incubation period, the extent of polymerization was measured by two different techniques, a laser light scattering assay (Figure 11A) and a ThioS fluorescence assay (Figure 11B). None of these salt concentrations had any significant impact on the total amount of polymerization of any of the 4R isoforms of tau to a level detectable within the error of the techniques employed.

Overall, increasing the ionic strength of the polymerization buffer or fixation buffer improved the utility of electron microscopy data for shorter tau isoforms, possibly by overcoming the

electrostatic interactions causing filament clustering (Figure 7,10) without inhibiting the process of tau aggregation to any significant extent (Figure 11).

### 2.3.5 Utility of new aggregation conditions for in vitro aggregation studies of mixed tau isoforms

Efforts to co-aggregate different 4R tau isoforms have proven to be difficult. Using the physiological ratio of 2N:1N:0N 4R isoforms of 9:54:37 (13,15), a final, total protein concentration of 2 µM was induced with 75 µM ARA at 100 mM NaCl (pH 7.64). These conditions resulted in clusters of aggregates that can be encountered frequently on the electron microscopy grid (Figure 12A). Increasing the ionic strength of polymerization reactions to 200 mM NaCl eliminates the clustering of tau filaments completely (Figure 12A) without impacting the overall levels of polymerization when measured using laser light scattering (Figure 12B) or ThioS fluorescence (Figure 12C).

It is not entirely known if various N-terminal variants of 4R tau isoforms can co-polymerize or seed the aggregation of other tau N-terminal variants. Unreliable polymerization of 0N4R tau isoform has previously hampered such studies. Here we present a model of co-polymerization of N-terminal variants of tau that can be employed to answer such questions in the future (Figure 12).

## 2.4 Discussion and Conclusions

Aggregation of tau is a central event in the course of numerous neurodegenerative disorders (115). An *in vitro* model employing arachidonic acid as an inducer of tau aggregation has helped gain insight into the pathological mechanisms and factors influencing this event (77,166). While

this is true for the 2N4R isoform of tau, a reliable interpretation of data for the 1N4R and 0N4R isoforms of tau has been a challenging task (Figure 6) (178). In this study we have identified filament clustering of shorter isoforms of tau as a reason behind some of these complexities. Our data suggests that the electrostatic interactions involving the unstructured N-terminal projection domain of tau protruding from the filament core influences this clustering behavior.

Specifically, we observed an inverse relationship between the acidity of tau N-terminal projection domain and the propensity of tau filaments to cluster. First, exclusion of the acidic N-terminal inserts rendered the filaments formed by 0N and 1N isoforms of tau more sensitive to fluctuations in pH and salt and caused them to form clusters of filaments. Modulating the pH, and thus altering the overall charge carried by the N-terminal projection domain, indicated that a positively charged N-terminal projection domain results in filament clustering while this clustering behavior can be overcome by making the N-terminal projection domain negatively charged (Table 1 and Figure 7). Second, this hypothesis could be corroborated by utilizing mutations that raise the acidity of N-terminal projection domain (pseudo-phosphorylation). Pseudo-phosphorylated 4R tau isoforms require a lower pH to form clusters of filaments (Figure 9).

Interestingly, Wegmann *et. al.* observed that the adhesive properties of the "fuzzy coat", formed by the unstructured regions of tau protruding from the filament core, change with pH and ionic strength of the environment surrounding tau filaments (181). Moreover, they observed that lowering the pH and thus making the fuzzy-coat overall positively charged enhanced adhesion to negatively charged particles. The reason behind a positively N-terminal projection domain leading to a tau filament clustering observed in our study is not yet clear but negatively charged species such as the fatty acid arachidonic acid (also present in the solution) could play a role in

facilitating the interactions between tau filaments, although more work would be needed to decipher their exact role. Nonetheless, this study sheds light into some of the processes that could affect the association of tau filaments with each other which may be of biological relevance.

Association of filaments with each other is thought to be a fundamental process for formation of macroscopic pathological tau aggregates, such as neurofibrillary tangles. Here we observed that the unstructured N-terminal projection domain could be a driving factor behind such "tangle-like" interactions. It can also be speculated that the electrolytic perturbances associated with aging and pathology (182) could be playing a role in the process. Moreover, it is important to note that such changes would have a differential effect on the N-terminal variants of tau. In addition to the effect of electrolytes and ions, we observed a phenomenon of tau filament clustering at low pH values. It is tempting to speculate that the low lysosomal pH could be implicated in affecting the properties of tau filaments and potentially altering tau filament-filament association.

Biological consequences of this charge driven association of tau filaments will need to be tested in future studies, nonetheless, the current study has immediate consequences in modeling of ARA induced aggregation of tau isoforms *in vitro*. We were able to overcome the clustering behavior of tau filaments by elevating the ionic strength in our tau polymerization protocol (Figure 10). This update in the current protocol of ARA-induced tau aggregation of isoforms could help devise future studies of various aspects of tau polymerization that may have isoform-specific effects, like tau mutations, post-translational modifications, tau seeding and looking at the effect of previously identified tau aggregation inhibitors (183) on various tau isoforms.

| pH | 2N4R | 1N4R | 0N4R |
|---|---|---|---|
| 4.00 | + 31.5 | + 31.0 | + 32.2 |
| 4.50 | + 21.3 | + 22.1 | + 25.6 |
| 5.00 | + 12.1 | + 14.1 | + 19.5 |
| 5.50 | + 6.7 | + 9.4 | + 15.9 |
| **6.00** | **+ 3.3** | **+ 6.4** | **+ 13.2** |
| 6.50 | - 0.2 | + 3.2 | + 10.2 |
| 7.00 | - 3.4 | + 0.4 | + 7.4 |
| 7.50 | - 5.3 | - 1.4 | + 5.6 |
| **7.64** | **- 5.6** | **- 1.7** | **+ 5.3** |
| 8.00 | - 6.4 | - 2.4 | + 4.6 |
| 8.50 | - 7.3 | - 3.3 | + 3.7 |
| 9.00 | - 8.9 | - 4.8 | + 2.3 |
| 9.50 | - 12.3 | - 8.0 | - 0.8 |
| **10.00** | **- 18.1** | **- 13.6** | **- 6.1** |

**Table 1:** Theoretical net charge carried by the projection domain (amino acids 1-243, along with the histidine purification tag) of various 4R tau N-terminal variants over a pH range. Experimentally studied pH values are indicated in bold. The cells colored in dark gray represent pH values at which the projection domain of each isoform is predicted to carry an overall positive charge. Light gray cells represent the pH values at which the projection domain of each isoform is predicted to carry an overall negative charge.

| | | Net Charge (Projection domain) | |
|---|---|---|---|
| **Protein** | **pH** | **Wild-type** | **7-phos** |
| **2N4R** | High (7.64) | - 5.6 | - 10.6 |
| | Intermediate (6.1) | + 2.6 | - 2.3 |
| | Low (5) | + 12.1 | + 8.1 |
| **1N4R** | High (10) | - 13.6 | - 18.6 |
| | Intermediate (6.8) | + 1.4 | - 3.6 |
| | Low (6) | + 6.4 | + 1.5 |
| **0N4R** | High (10) | - 6.1 | - 11.1 |
| | Intermediate (8.7) | + 3.3 | - 1.7 |
| | Low (6) | + 13.2 | + 8.3 |

**Table 2:** Theoretical net charge carried by the projection domain (amino acids 1-243, along with the histidine purification tag) of various 4R tau wild-type and pseudo-phosphorylation (7-phos) N-terminal variants at three distict pH values (high, intermediate, low) chosen on an isoform-specific basis. The cells colored in dark gray represent pH values at which the projection domain of each isoform is predicted to carry an overall positive charge. Light gray cells represent the pH values at which the projection domain of each isoform is predicted to carry an overall negative charge.

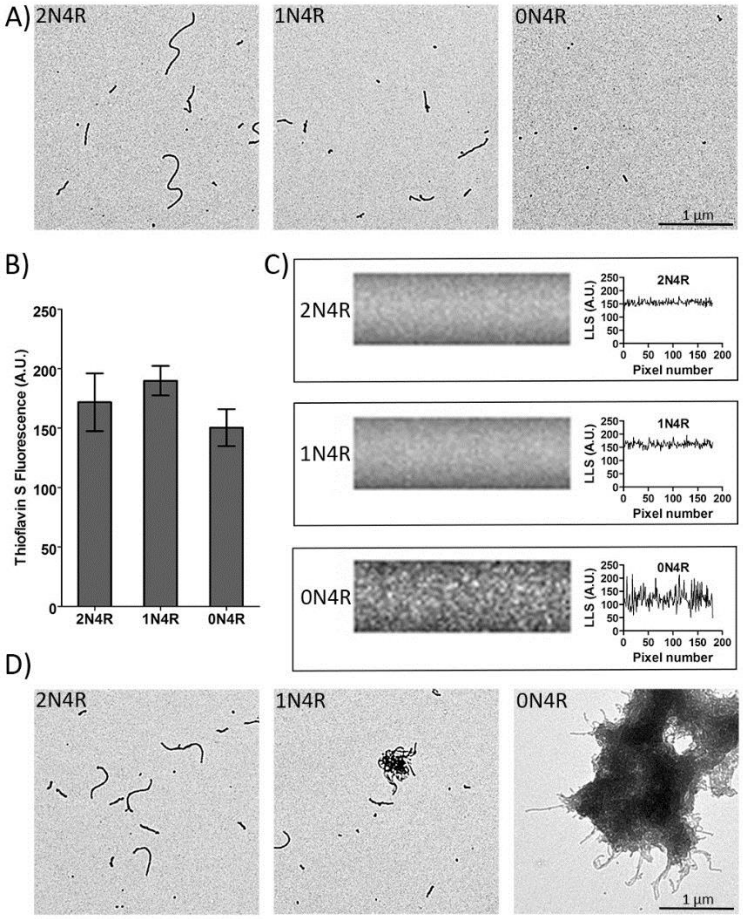


**Figure 6:** Discrepancies in ARA induced polymerization of 4R tau N-terminal variants. 2 µM protein was polymerized using 75 µM ARA overnight at 25° C under standard salt and pH conditions. A) electron micrographs of polymerized proteins obtained via a random selection criterion; B) extent of polymerization measured using ThioS fluorescence. Each bar represents data from 3 independent experiments ± SD; C) right-angle laser light scattering images (left) and the corresponding intensity of pixels across the width (right) for various 4R tau filaments; D) Electron micrographs obtained via searching the grids to obtain images of filament clusters, which are not evenly distributed. Scale bar is 1 µm and is applicable to each image.

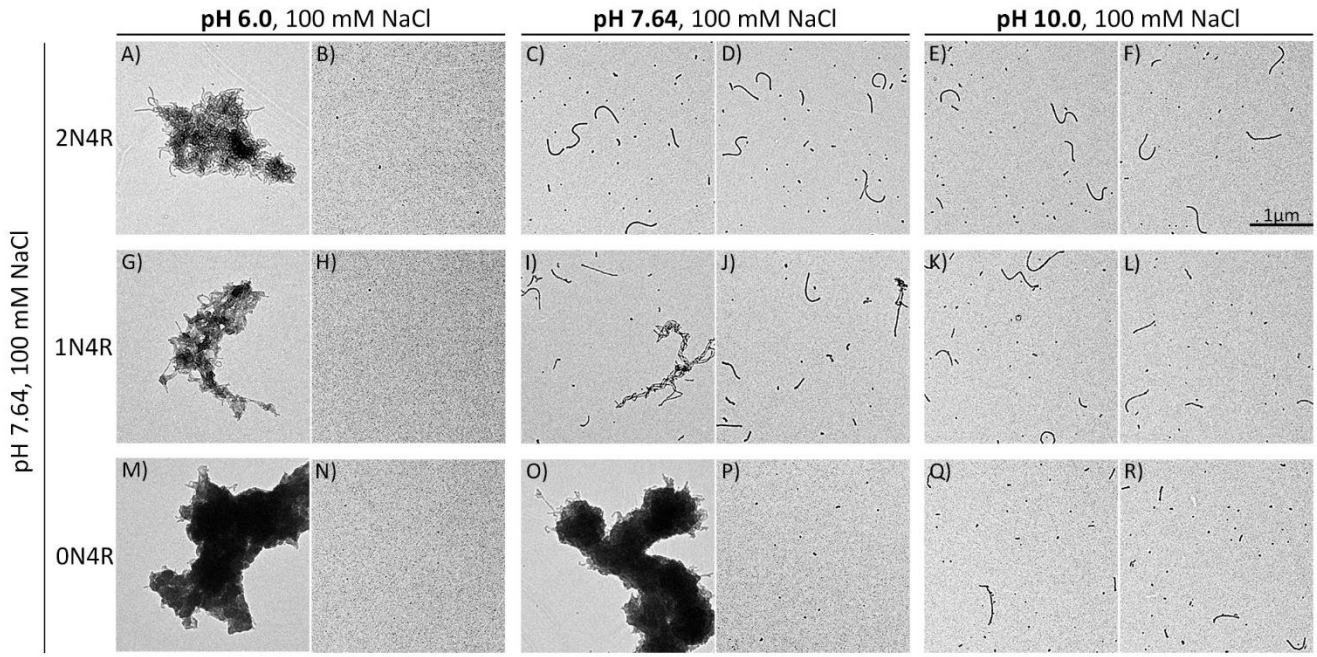


**Figure 7:** Effect of pH on filament clustering. Electron micrographs of 4R proteins polymerized using 2 µM protein and 75 µM ARA under the standard conditions of 100 mM NaCl at pH 7.64 (verticle axis), with filament fixaton conditions represented on the horizontal axis. Two images for each working condition are presented. Images on the right side for each panel (Image B, D, F, H, J, L, N, P, R) were obtained using a random selection to minimize bias, and images on the left side for each panel (Image A, C, E, G, I, K, M, O, Q) were obtained after extensive searching to locate clusters of filaments. Scale bar in image (F) represents 1 µm and is applicable to all images.

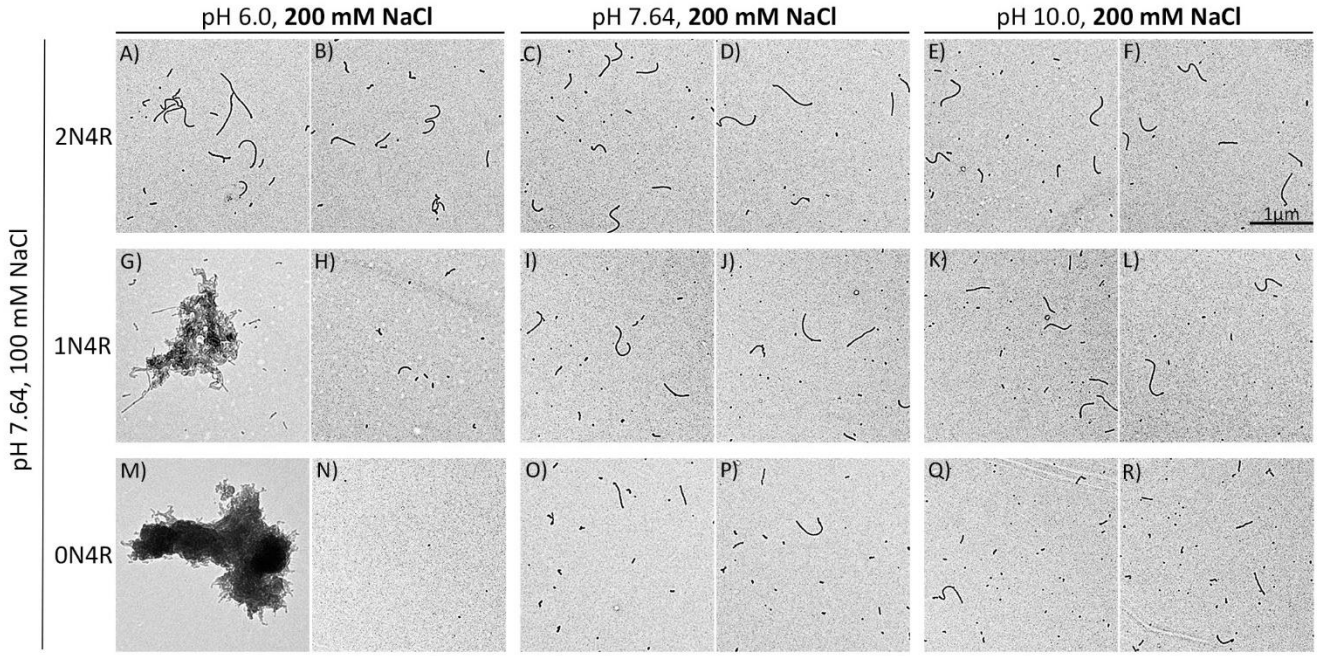


**Figure 8:** Countering the effect of pH by increasing ionic strength. Electron micrographs of 4R proteins polymerized using 2 µM protein and 75 µM ARA under the standard conditions of 100 mM NaCl at pH 7.64 (verticle axis), with filament fixation conditions represented on the horizontal axis. Two images for each working condition are presented. Images on the right side for each panel (Image B, D, F, H, J, L, N, P, R) were obtained using a random selection to minimize bias, and images on the left side for each panel (Image A, C, E, G, I, K, M, O, Q) were obtained after extensive searching to locate clusters of filaments. Scale bar in image (F) represents 1 µm and is applicable to all images.

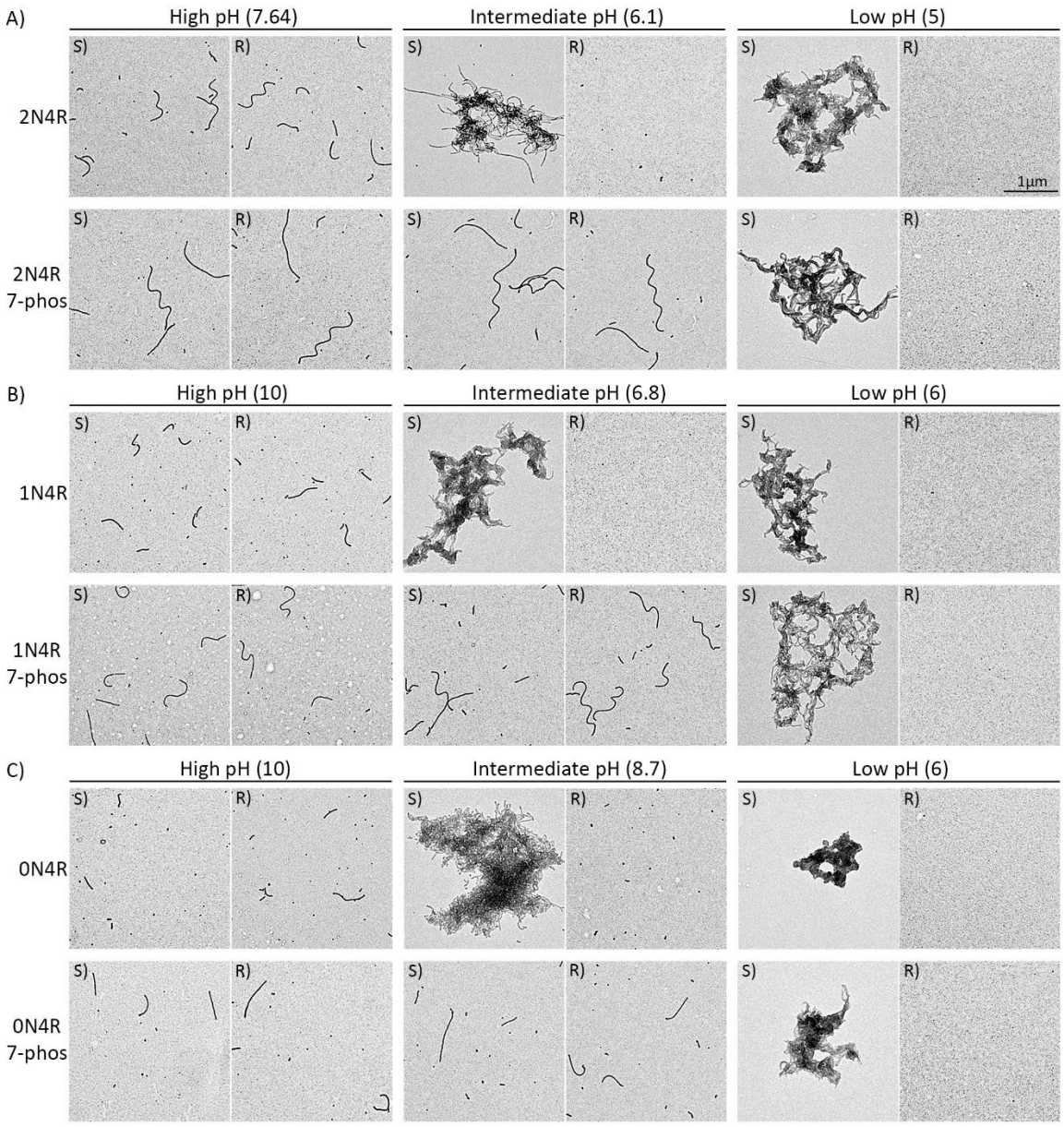


**Figure 9:** Enhanced acidity of projection domain by pseudo-phosphorylation reduces sensitivity to clustering. Electron micrographs of A) 2N4R, B) 1N4R, C) 0N4R) proteins (wild-type and 7-phos variants) polymerized using 2 µM protein and 75 µM ARA under the standard conditions of 100 mM NaCl at pH 7.64. Fixation buffer contained 100 mM NaCl at all the indicated pH vaulues. Two images for each working condition are presented. Images on the right side of each panel (designated as R) were obtained using a random selection to minimize bias, images on the left side of each panel (designated as S) were obtained after extensive searching to locate clusters of filaments. Scale bar in upper right panel represents 1 µm and is applicable to all images.

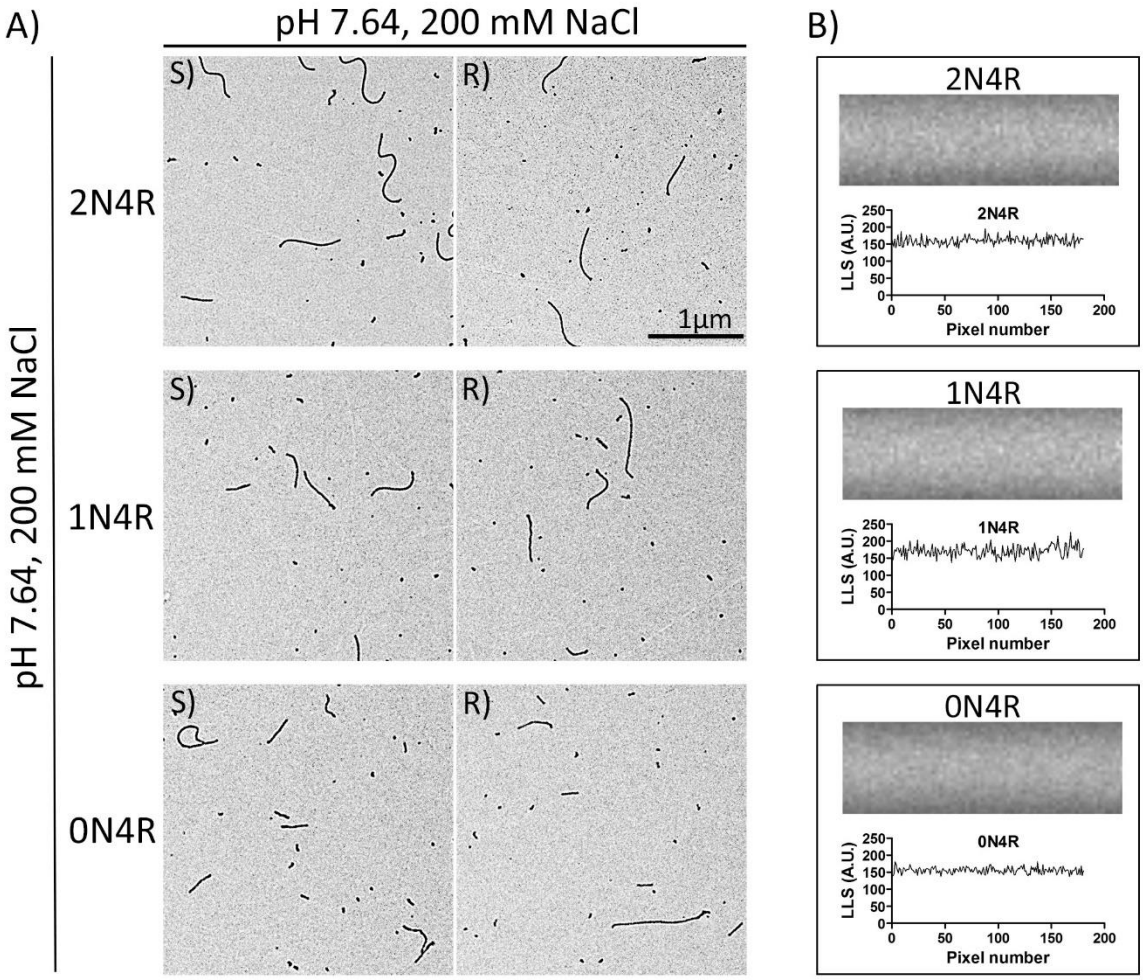


**Figure 10:** Polymerization at 200 mM NaCl eliminates clustering of filaments for all 4R tau isoforms and anomalous light scattering for 0N4R isoform. 4R proteins polymerized using 2 µM protein and 75 µM ARA. A) Electron micrographs of tau isoforms polymerized and fixed using a buffer containing 200 mM NaCl at pH 7.64. Two images for each working condition are presented. Images on the right side of each panel (designated as R) were obtained using a random selection to minimize bias, images on the left side of each panel (designated as S) were obtained after extensive searching to locate clusters of filaments. B) Right-angle laser light scattering images (top) and the corresponding intensity of pixels across the width (bottom) for polymerized 4R tau isoforms.

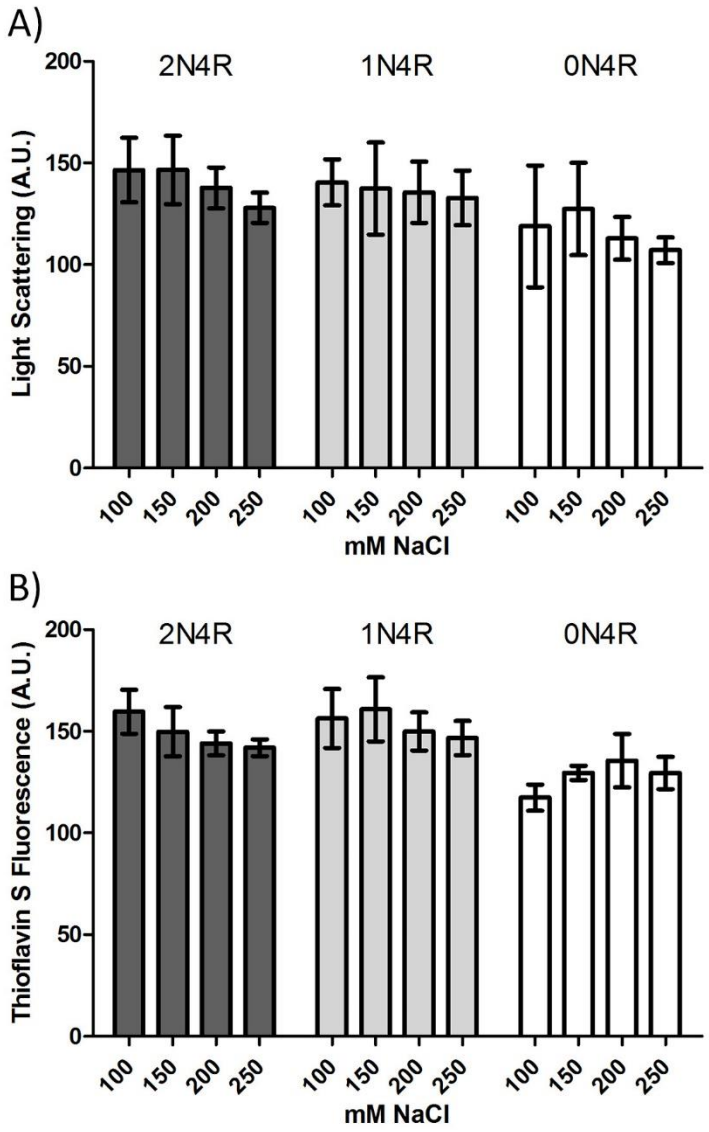


**Figure 11:** Polymerization of 4R tau proteins at varying amounts of salt. 2 µM 4R proteins polymerized using 75 µM ARA in HEPES buffer pH 7.64 containing salt concentations ranging from 100 mM to 250 mM overnight at 25° C. The final extent of polymerization was measured by A) ThioS fluorescence and B) right-angle laser light scattering (LLS). Each bar represents data from 3 independent experiments ± SD. One-way ANOVA analysis with Turkey's multiple comparison test was used to determine the statistical significance of data obtained for each isoform at different salt concentrations for each of the techniques employed, LLS and ThioS fluorescence.

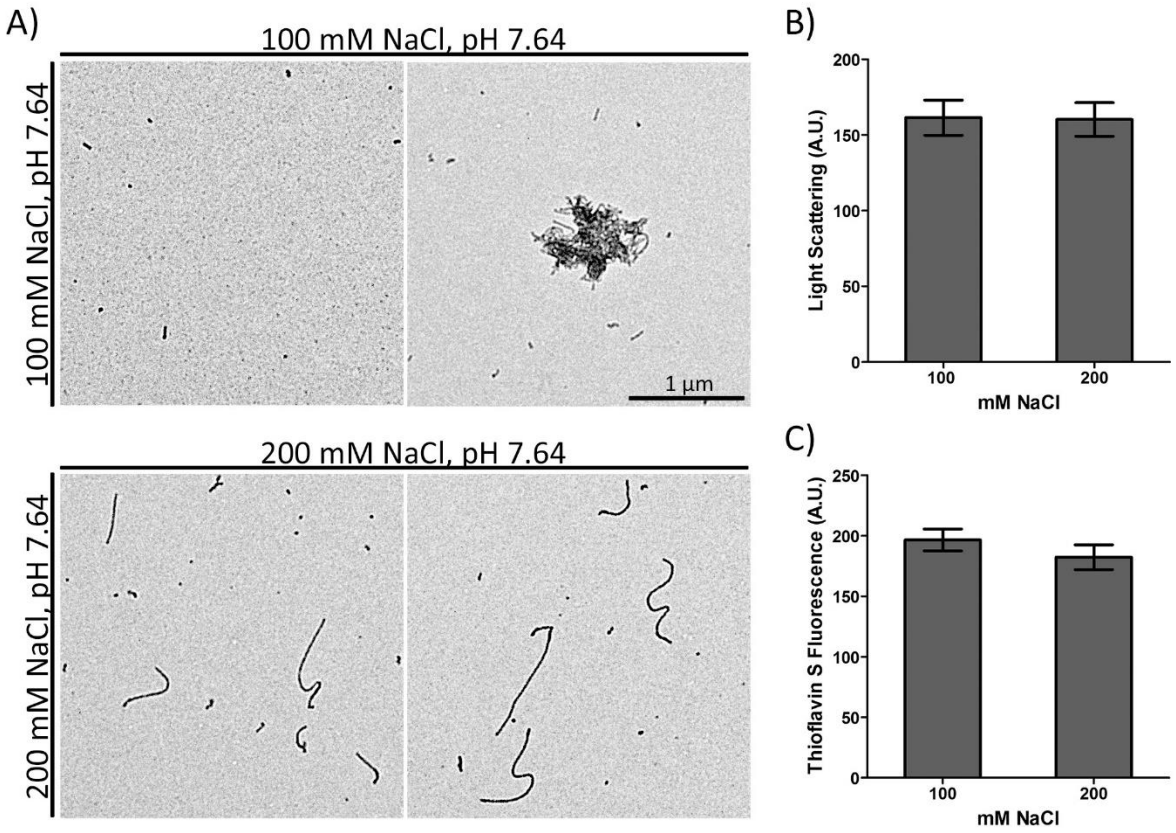


**Figure 12:** Aggregation of mixture of 4R tau isoforms. 4R proteins at a molar ratio of 2N:1N:0N, 9:54:37 polymerized using 2 µM total protein and 75 µM ARA at the salt and pH conditions indicated on the vertical axis, with filament fixaton conditions represented on the horizontal axis. Two images are presented to represent the uneven distribution of tau filaments resulting from clustering of tau filaments at 100 mM NaCl; Extent of polymerization measured using laser light scattering (B) and ThioS fluorescence (C). Each bar represents data from 3 independent experiments ± SD. Student's unpaired two-tailed t-test was performed to estimate the level of significance.

# CHAPTER 3: Effects of FTDP-17 mutants on aggregation and microtubule stabilization properties of 4R isoforms of tau

# Chapter 3: Effects of FTDP-17 mutants on aggregation and microtubule stabilization properties of 4R isoforms of tau

## 3.1 Introduction

Tauopathies are a group of about thirty different clinically and biochemically heterogeneous neurodegenerative disorders together accounting for a large proportion of senile dementias. Although the precise nature of pathology and clinical presentation of these diseases varies on individual basis, symptoms include progressive cognitive decline, memory deficits, behavioral alterations and motor dysfunction among others. A unifying and prominent feature of these diseases is the deposition of filamentous aggregates of the microtubule-stabilizing protein tau in neurons and glia.

In a normal adult human brain, tau exists in six distinct isoforms generated by alternate mRNA splicing of exons 2, 3 and 10 (10). Exon 10 encodes for one of the carboxy-terminal tandem repeats responsible for tau's interaction with microtubules (11,12). Alternate splicing of this exon generates tau with either three microtubule-stabilizing repeats (3R-tau) or four microtubule-stabilizing repeats (4R-tau). Further, inclusion or exclusion of amino-terminal acidic inserts encoded by exon 2 and 3 give rise to 0N, 1N or 2N tau within the 3R and 4R categories.

Both familial and sporadic forms of tauopathies have been demonstrated to have a characteristic pattern of tau isoform deposition in the brain and this pattern has often been used as one of the defining features to classify a tauopathy (reviewed in (115)). Across the spectrum of these tauopathies, the mutations associated with the familial form of tauopathies also known as the FTDP-17 (Fronto Temporal Dementia and Parkinsonism linked to chromosome 17) have been of interest to understand the biochemical nature of tau and its aggregation. To date more than 50 different exonic and intronic mutations in tau gene have been associated with FTDP-17

(130,184,185). A great majority of these mutations have been shown to either enhance tau's aggregation propensity, alter tau's interaction with microtubules or affect the splicing pattern of tau (77,114,186-190).

FTDP-17 mutations have often been used as a tool to study tau aggregation and toxicity in a wide range of *in vivo* model systems (133,191-193). However, there has been a lack of consensus about the resulting effect of these mutations and the toxic species of tau in these models (194-201). While epigenetic differences could explain this lack of consensus to some extent, it has been previously suggested that the heterogeneity seen in the patient's phenotype and *in vivo* model systems could be a consequence of the observation that the FTDP-17 mutations are not just biochemically different from the wild-type but also differ markedly from each other (77).

Further, isoforms of tau are known to be different from each other in terms of their ability to stabilize microtubules (155,202), their interaction with chaperone and other cellular proteins (203,204) and their subcellular localization (205). Thus, there could be minor conformational and functional differences between the tau isoforms in cells. Subsequently, it is also conceivable that if FTDP-17 mutations affect tau isoforms disproportionately, there would be differences in the observed phenotype based on the isoform most affected. Therefore, there is a need for a comparative study of FTDP-17 mutations in various tau isoforms to examine their effect on tau's ability to aggregate as well as tau's ability to stabilize microtubules.

Here, in this study, we chose to examine the effect of three different FTDP-17 mutations on aggregation propensity and microtubule stabilizing ability of tau *in vitro*. To understand whether the location of the mutant within the primary sequence of tau could alter the degree of such possible effects, mutations from three separate regions of tau were selected. R5L and R406W

were selected as they occur in the distal N-terminal and C-terminal regions of tau respectively. For the MTBR mutation, we chose to examine the effect of P301L as this is one of the most commonly occurring FTDP-17 mutation and has also been widely employed to model tau aggregation in various *in vivo* model systems (191,195,206-208). P301L occurs in exon 10 of tau and thus only exists in the 4R isoforms. Therefore, we chose to examine the impact of all three FTDP-17 mutations in 4R isoforms of tau.

We observed that the effect of a FTDP-17 mutation not only depends on the location of the mutation in tau's primary sequence but the precise effect can be influenced by the number of N-terminal inserts. We found subtle but significant differences in the effect of all three FTDP-17 mutations on aggregation as well as microtubule stabilizing propensity of various 4R tau isoforms.

## 3.2 Experimental Procedures

### 3.2.1. Protein purification

All three wild-type tau isoforms were cloned into the pT7c vector with an N-terminal poly-histidine tag. QuickChange II site-directed mutagenesis kit was used to generate the R5L, P301L and R406W mutants in all three isoforms (Agilent Technologies). Proteins were expressed in *E. coli* and purified as described previously. Protein amounts were quantitated using the Pierce™ BCA protein assay kit (Thermo Scientific).

### 3.2.2. Aggregation induction using Arachidonic acid:

Wild-type and mutant proteins, at a concentration of 2 µM, were incubated with Arachidonic Acid (Millipore) to a final concentration of 75 µM in the polymerization buffer containing 200 mM NaCl, 10 mM Hepes (pH 7.64), 0.1 mM EDTA, 5 mM DTT and 3.75% ethanol. Reactions were kept at a constant temperature of 25 °C over-night before proceeding to assays for quantifying the extent of polymerization.

### 3.2.3. Thioflavin S fluorescence assay

Thioflavin S (ThS) (Sigma) stock solution was prepared at a concentration of 0.224 mg/ml in MilliQ water and filtered through a 0.22 micron filter before use. 150 µL of each aggregated tau reaction solution was transferred to a separate well of a flat bottom, 96 well, white plate. 6 µL of ThS stock solution was added to each sample. The plate was shaken for 30 seconds and then incubated in dark for 20 minutes. The resulting fluorescence shift was measured at an excitation wavelength of 440 nm and an emission wavelength of 520 nm using a Cary Eclipse fluorescence spectrophotometer (Varian Analytical Instruments, Walnut Creek, CA). The PMT detector voltage was set at 650 V. Control reactions were set up in absence of ARA and used to measure background florescence readings which were then subtracted from each polymerization sample.

### 3.2.4. Right angle laser light scattering assay

180 µL of polymerized sample was transferred to a 5 mm X 5 mm optical glass fluorometer cuvettes (Starna Cells, Atascadero, CA). A 12 mW solid state laser, with a wavelength of 532 nm and operating at 7.6 mW (B&W Tek, Inc., Newark, DE) was used to illuminate the polymerized protein sample. An image of the amount of light scattered was collected at the angle perpendicular to the angle of the laser beam using a SONY XC-ST270 digital camera at varying apertures from f4-f11. The images at aperture f5.6-8 were analyzed using the histogram function

of Adobe Photoshop CS5 Version 12.0 x32 to obtain a mean intensity corresponding to the amount of scattered light.

### 3.2.5. Kinetics of ARA induced polymerization

Right angle laser light scattering was used to monitor arachidonic acid induced kinetics of tau polymerization. Ratio of proteins and arachidonic acid were kept the same as previously described. Proteins diluted in the polymerization buffer were added to a 5 mm X 5 mm optical glass fluorometer cuvette. Arachidonic acid was added to the cuvette at time zero and images of the scattered light were captured through the time course of aggregation at an aperture setting of f5.6-8 until the polymerization reactions had reached a steady state. Images were again analyzed using the histogram function of Adobe Photoshop CS5 Version 12.0 x32. Data were fit to the Gompertz equation

$$y = ae^{-e^{-(t-t_i)/b}}$$

Here, *a* represents the maximum amount of polymerization. The lag time (the time between initiating the reaction till the time when polymerization was detectable is calculated at $t_i$-*b*. The rate of polymerization, $k_{app,}$ is found to be proportional to the inverse of *b*. Three individual data sets were fit to this equation to extract information about various parameters describing maximum polymerization, lag time and rate of polymerization.

### 3.2.6. Transmission Electron Microscopy

Polymerization reactions were diluted 1:10 in polymerization buffer with the same concentration of NaCl, EDTA and Hepes as the polymerization buffer, and the fixative glutaraldehyde to a final concentration of 2%. Samples are allowed to fix for 5 minutes and subsequently deposited

on a 300 mesh formvar coated copper grid and stained with uranyl acetate according to a previously published protocol (209). Briefly, the copper grid was placed on top of a drop of the fixed sample solution for 1 minute, followed by blotting on filter paper. The grid was then placed on top of a drop of water, botted dry, then placed on top of 2% uranyl acetate solution, blotted dry. For final staining with 2% uranyl acetate, the grid was left on top of the uranyl acetate solution for 1 minute. The grid was then blotted dry a final time before storing at room temperature. When ready to collect images, grids were loaded on a FEI TECNAI F20 XT field electron microscope (Hillsboro, OR). Images were collected at a magnification of 3600x using a Gatan Digital Micrograph system.

### 3.2.7. Tubulin Polymerization assay

A fluorescence based tubulin polymerization assay kit (Cytoskeleton Inc, Denver, CO) was utilized according to the manufacturer's protocol to examine the effect of various test proteins on *in vitro* tubulin polymerization. All test proteins were used a final concentration of 1 μM. Tubulin at a concentration of 2 mg/ml in a buffer containing 80 mM PIPES pH 6.9, 2 mM $MgCl_2$, 0.5 mM EGTA and 1 mM GTP was mixed with the test protein in a black, flat bottom, 96 well plate. The final concentration of tubulin was 3.64 μM. A sample well containing 3 μM paclitaxel was used as a positive control. The fluorescence measurements were made with a FlexStation II Fluorometer (Molecular Devices Corporation, Sunnyvale , CA) using an excitation wavelength of 355 nm and an emission wavelength of 455 nm at a constant temperature of 37 °C. The data were collected every 1 minute for a total of 60 minutes. A buffer and tubulin only sample was used to obtain the baseline fluorescence readings to be subtracted from each of the test condition. The resulting data were fit to the Gompertz growth curve to obtain various

parameters describing the growth curves of tubulin in a similar manner as kinetics of tau aggregation mentioned above.

## 3.3 Results

### 3.3.1. Total amount of aggregation

Previously identified in vitro aggregation conditions using 2 μM protein and 75 μM arachidonic acid in the presence of 200 mM NaCl were utilized to determine the extent of aggregation of the 3 selected FTDP-17 mutations in various 4R tau isoforms (209). Followed by an overnight incubation of proteins with the inducer, two orthogonal techniques, ThioflavinS (ThS) fluorescence assay (Figure 13A, 13C and 13E) and Laser light scattering (LLS) assay (Figure 13B, 13D and 13F) were employed to assess the level of polymerized tau.

The N-terminal mutation R5L affected the aggregation of tau in an isoform dependent manner (Figure 13A and 13B). 2N4R R5L tau polymerized to the same extent as the wild-type protein. A small decrease in the ThS fluorescence signal was observed for the R5L 1N isoform compared to the wild-type but the data did not reach significance for the LLS assay. R5L lead to a decrease in the total amount of polymerized tau for 0N isoform measured by both ThS fluorescence and LLS.

The microtubule-stabilizing mutation P301L affected the level of polymerization irrespective of the isoform (Figure 13C and 13D). P301L tau polymerized to a higher extent compared to the corresponding wild-type protein in all three 4R isoforms. The C-terminal mutation R406W had no significant impact on the extent of aggregation for any of the isoforms under study (Figure 13E and 13F).

Overall, the extent of aggregation of the N-terminal mutation R5L was found to be dependent on the number of N-terminal inserts present. The effects of the microtubule-stabilizing region mutation P301L and the C-terminal mutation R406W were less impacted by the number of N-terminal inserts where all three isoforms were affected in the same manner.

### 3.3.2. Kinetics of Aggregation

Because tau mutations could conceptually change not only the overall amounts of aggregation, but also the rate of aggregation, we sought to determine whether the mutations had differential effects on the kinetics of polymerization in the backbones of the three tau isoforms. Polymerization for R5L, P301L, and R406W and their corresponding wild-type 0N4R, 1N4R, and 2N4R isoforms were monitored by LLS over time after the addition of ARA inducer.

R5L did not have a significant effect on the kinetics of polymerization of the 2N4R or 1N4R isoforms (Figure 14A and 14B). However, there was a significant reduction in the maximum amount of polymerization of the 0N4R isoform (Figure 14C and 14D). Fits of the data to a Gompertz growth curve also indicated that the lag time before polymerization was significantly lower for 0N4R R5L compared to the 0N4R WT (Figure 14E), although there was no significant difference in the apparent rate of polymerization for any of the R5L isoforms compared to their wild-type counterparts (Figure 14F).

The P301L mutation significantly influenced the kinetics of polymerization for each of the three 4R isoforms (Figure 15). All three P301L isoform variants had increased levels of polymerization (Figures 15A-D). An increase in the lag time before polymerization was observed for all the 4R isoforms with P301L mutation compared to the WT (Figures 15A-C,

15E). Only the 2N4R P301L variant had a significant impact on the apparent rate of polymerization, causing a small decrease in $k_{app}$ (Figure 15F).

The R406W mutation did not have a significant impact on the overall amount of polymerization for any of the 4R isoforms (Figure 16 A-D). With 2N and 0N isoforms, a decrease in the lag time before polymerization was observed (Figure 16E), while only 1N4R isoform had a significant change in the apparent rate of polymerization with the R406W mutation (Figure 16F).

Therefore, all three mutants in the study showed subtle differences in their effect on various parameters of polymerization kinetics. R5L primarily only had significant effects on the 0N4R isoform, P301L had significant effects on all three isoforms in terms of overall amount and lag time of polymerization along with a slight decrease in the apparent rate of 2N polymerization, and R406W only affected the lag time of polymerization in the 2N and 0N isoforms while the rate of polymerization was only influenced for the 1N4R isoform with R406W.

### 3.3.3. Morphology of Aggregates

Samples of polymerization reactions were prepared for viewing by electron microscope to determine whether the FTDP-17 mutations had any effects on the morphology of the filaments formed and whether any observed effects were different in the backbones of the 2N, 1N, and 0N isoforms. All isoforms and FTDP-17 variants formed filaments reminiscent of straight filaments from AD, which is characteristic of ARA-induced tau filaments (Figure 17). Upon quantitative analysis of the images, some differences between the FTDP-17 mutations in the isoforms become apparent. While quantitative electron microscopy is a useful tool in assessing filament morphology, care should be taken in reaching conclusions due to several important caveats: we are limited by only being able to view those filaments that adhered to the EM grid; there is

uncertainty whether the isoforms and/or FTDP-17 variants might adhere to the grid differently; adherence to the grid might potentially affect filament lengths (through breakage); the stain used for contrast might potentially distort actual filament lengths and might also be different for the variants; and the number of filaments analyzed per condition (~ 400-900 filaments) is small compared to the total filament population. Keeping these caveats in mind, an analysis of the frequency distribution of filament lengths reveals that all tau variants in 2N, 1N, and 0N isoforms have relatively exponential frequency distributions (Figure 18 A-C). It is also clear that the P301L isoform has a different distribution of filament lengths with fewer filaments <50 nm and proportionately more filaments longer than 50 nm for all three isoforms. This is consistent with the observation that P301L has a greater impact on the kinetics of polymerization than R5L or R406W in all three isoforms (Figure 14, 15, 16). When the total amount of polymerization, the number of filaments formed, and the average length of filaments is considered, only P301L has a significant effect on the 2N4R isoform, with significantly fewer, but significantly longer filaments (Figure 19 A-C). This is consistent with the observation of an increased lag time of polymerization kinetics for P301L in 2N4R (Figure 15E), while R5L and R406W did not significantly alter the kinetics of 2N4R polymerization (Figure 14, 16). For 1N4R variants, P301L did have a significant increase in the total amount of polymerization (Figure 19D), and significant decrease in the number of filaments (Figure 19E), and a significant increase in the length of filaments (Figure 19F). R5L did not significantly alter 1N4R filament morphology, while R406W had a significant increase in the number of filaments formed (Figure 19E). These observations are consistent with the kinetics data of 1N4R polymerization that showed significant alterations to 1N4R polymerization by P301L and R406W, but not R5L (Figure 14, 15, 16). All three variants altered the kinetics of 0N4R polymerization and all three variants also

affected the resulting filament morphologies. R5L had a significant reduction in total polymerization while P301L had a significant increase in total 0N4R polymerization (Figure 19G). P301L had a significant decrease in the number of 0N4R filaments formed (Figure 19H). R5L and R406W resulted in significantly shorter 0N4R filaments, while P301L resulted in significantly longer 0N4R filaments (Figure 19I). Taken together, these results are broadly consistent with the kinetic analysis of tau aggregation in that only P301L had significant effects on filament numbers and length distribution in the 2N4R isoform; P301L and R406W, but not R5L, had significant effects of filament morphology in the 1N4R isoform; and all three variants significantly affected filament morphology in the 0N4R backbone.

### 3.3.4. MT Assembly

We further sought to determine if the effect of mutations on the normal functioning of tau could also depend on the isoform backbone. A fluorescence based MT assembly assay was utilized to monitor tubulin polymerization in the presence of tau mutant and wild-type proteins. The resulting data was fit to the Gompertz curve to understand and compare the possible defects in MT stabilization.

Both R5L 2N4R and R5L 1N4R had no significant impact on the tubulin polymerization. R5L 2N4R and R5L 1N4R induced polymerization of tubulin to the same extent, at the similar rate and lag times as the corresponding wild-types (Figure 20 A, B, D, E, F). In contrast, R5L 0N4R showed compromised microtubule assembly. For R5L 0N4R, overall tubulin polymerization extent was lowered, polymerization occurred at a lower rate and the lag time observed before the initiation of tubulin polymerization was longer (Figure 20 C, D, E, F).

P301L led to a decrease in the maximum tubulin polymerization and a reduced rate of polymerization in both 2N4R and 1N4R backbones (Figure 21 A, B, D, E). However, in the 0N4R backbone, P301L only affected the rate of tubulin polymerization to a significant level (Figure 21 C, E). P301L did not significantly affect the lag time before initiation of polymerization in any of the 4R isoform backbones (Figure 21 F).

R406W 2N4R induced tubulin polymerization at a lower rate than the wild-type (Figure 22 A, E), with no significant no impact on the maximum level of polymerization or the lag time before polymerization (Figure 22 D, F). R406W 1N4R lead to a reduction in maximum tubulin polymerization and it also induced the polymerization at a much lower rate than the wild-type 1N4R protein (Figure 22 B, E). R406W 1N4R had no significant impact on the lag time before initiation of polymerization (Figure 22 F). R406W 0N4R increased the lag time before initiation of polymerization as well lowered the extent of tubulin polymerization without affecting the rate of tubulin polymerization (Figure 22 C, D, E, F).

Overall, the effect of mutations on tubulin polymerization seemed to be significantly dependent on the isoform. R5L only affected the 0N4R isoform to a significant level. P301L affected all three isoforms but the extent of affect seems to correlate with the number of N-terminal inserts. For P301L, the isoform with both N-terminal inserts (2N4R) was affected the most and the isoform lacking any N-terminal inserts (0N4R) was affected the least. R406W also altered the induction of tubulin polymerization of all three isoforms to varying degrees with the precise parameters affected being dependent on the isoform backbone.

## 3.4 Discussion

Tauopathies are a diverse group of neurodegenerative disorders characterized by dysfunction and aggregation of protein tau. Although the involvement of tau in pathology of these diseases has been unequivocally demonstrated, the underlying cause of heterogeneity among these disorders is poorly understood. In theory, this heterogeneity could arise from a disproportionate effect of disease and aging related mechanisms on the various isoforms of tau. Here, we examined whether known missense mutations in tau gene could differentially affect the properties related to both the aggregation and normal function of tau isoforms *in vitro*.

A great majority of tau mutations linked to neurodegenerative diseases are missense point mutations, centered around the microtubule stabilizing region, but mutations have been reported in the far N-terminal and C-terminal regions of tau as well (70,139).To further examine whether the observed effects on tau isoforms would be influenced by the location of the mutation in tau primary sequence, mutations were selected from the N-terminal region (R5L), the microtubule stabilizing region (P301L) and the C-terminal region (R406W).

Upon examining the effects of these mutations on *in vitro* aggregation of 4R isoforms of tau, we found that there are subtle but significant differences in how each mutation affected the aggregation of a particular tau isoform. While there were disproportionate effects on the overall extent of aggregation, the effects on the kinetics of aggregation were more striking. An interesting pattern emerged when comparing the rate of aggregation of single mutant in different N-terminal variants of tau. The rate of aggregation of the 0N isoform was found to be higher than the rate of aggregation for the 2N and 1N isoforms for all three mutants (Figure 23). Thus, the removal of N-terminal inserts caused all three mutants to aggregate at an increased rate. In

addition, the rate of P301L aggregation was increased in the 1N isoform as compared to the 2N isoform. Similar trends can also be seen in both the lag phase and the rate of polymerization of the 0N compared to the 2N and 1N wild-type proteins, although the differences are minor and not statistically significant under the conditions of the study. Overall, mutants exacerbated these possible differences between isoforms. In addition, it can be seen from this comparison that the effect of removal of the second N-terminal insert (exon 2) is bigger than the effect of removal of the first N-terminal insert (exon 3) on the parameters of kinetics with kinetics of aggregation of 2N isoform more similar to the 1N isoform and different from the 0N isoform. Overall, the observed effects of mutants on 4R tau isoforms seem to be disproportionately more in the 0N4R backbone. All three mutants tested in this study consistently had a greater impact on the *in vitro* aggregation properties of the 0N4R isoform as compared to the 1N or 2N isoforms.

The effect on MT assembly by these mutants were also isoform specific. R5L mutation affected the MT assembly induction of 0N4R isoform but did not influence the MT assembly induction by the 1N and 2N tau isoforms (Figure 20). P301L and R406W affected all three isoforms but the effect was again found to be disproportionate. For example, P301L reduced both the maximum amount of MT polymerization and rate of MT polymerization for the 2N and 1N isoform but it only affected the maximum amount of MT polymerization for the 0N isoform compared to the respective wild-type proteins (Figure 21). In a similar manner, microtubules polymerized at a lower rate with the total extent and the nucleation rate (lag phase) of MT polymerization remaining unchanged in presence R406W in 2N isoform in comparison to the WT 2N isoform (Figure 22). However, R406W only affected the nucleation phase of MT polymerization without affecting the total amount or the rate of MT polymerization in presence of 0N isoform with R406W mutation compared to the WT.

Although for MT stabilization, there is no discernable pattern observed here for R5L and R406W, the defect in MT assembly caused by P301L seems to diminish with removal of each N-terminal exons. The rate of MT polymerization improves as the N-terminal exons are removed in the 4R tau isoforms with P301L mutation. This observation points towards a role of N-terminal region of tau in MT stabilization. This region of tau is classically not thought to be involved in tau's interaction with microtubules. A possible explanation of the P301L MT assembly data can come from the acidic nature of the residues in exon 2 and exon 3 and a possible conformational change introduced by the P301L mutation into the global hairpin structure of tau. In the global hairpin structure of tau, long-range interactions can exist between the N-terminal region of tau and the MT stabilizing region. Also, in such a structure, the C-terminus is also thought to fold over to make long range contact with both the N-terminus as well as the MT stabilizing region. P301L could alter these interactions such that the N-terminal is brought closer to the MT stabilizing region for all three 4R isoforms. In this case, when both exon 2 and 3 are present, the negatively charged residues in exon 2 and 3 could interact with the positively charged residues in the MT assembly region. Thus, making the MTBR less available to interact with the acidic surface of microtubules. In such situation, the more acidic the N-terminal region is, the more favorable would be its interaction with the MT stabilizing region rich in positively charged residues, and more would be the MT stabilization defects. Consequently, the 0N isoform without the acidic N-terminal residues would have a better MT stabilizing ability than the 1N and 2N isoforms as was observed with the 4R tau isoforms with the P301L mutation. In agreement with this model, a small difference between the MT stabilizing ability of WT 4R isoforms of tau can also be detected under the conditions of this study (Figure 24). The rate of MT polymerization was found to be slightly better and the lag phase was shorter in presence of the 0N4R wild-type

isoform compared to 1N and 2N4R wild-type proteins. Another supporting argument comes from the recently published data where the N-terminally truncated forms of tau display stronger interactions with the microtubules (59). Further, this pulling down of the N-terminal region closer to the MT stabilizing region (tightening of the hairpin) is also thought to be favorable for aggregation and in line with this, P301L increases the amount of aggregation of all three 4R isoforms. Similar pattern was also detected for two other MT stabilizing region mutations, S320F and S352L (data not shown). For both these mutations, the MT assembly was found to be better in presence of the 0N4R isoforms compared to the 1N and 2N4R tau isoforms. Although this model fits our data the best, without any structural evidence, other possibilities cannot be excluded and future studies would help deduce more concrete answers.

Overall, through this study, we found out that the FTDP-17 mutants can have disproportionate effects on both the aggregation propensity as well as the microtubule stabilizing properties of tau isoforms. Some of the observed affects are rather subtle but still statistically significant. Whether or not these differences can elicit phenotypic differences *in vivo*, would need to be tested. Nonetheless, our data favors the idea that vulnerability of tau isoforms to the disease related mechanisms might be disproportionate and may not follow a predictable pattern.

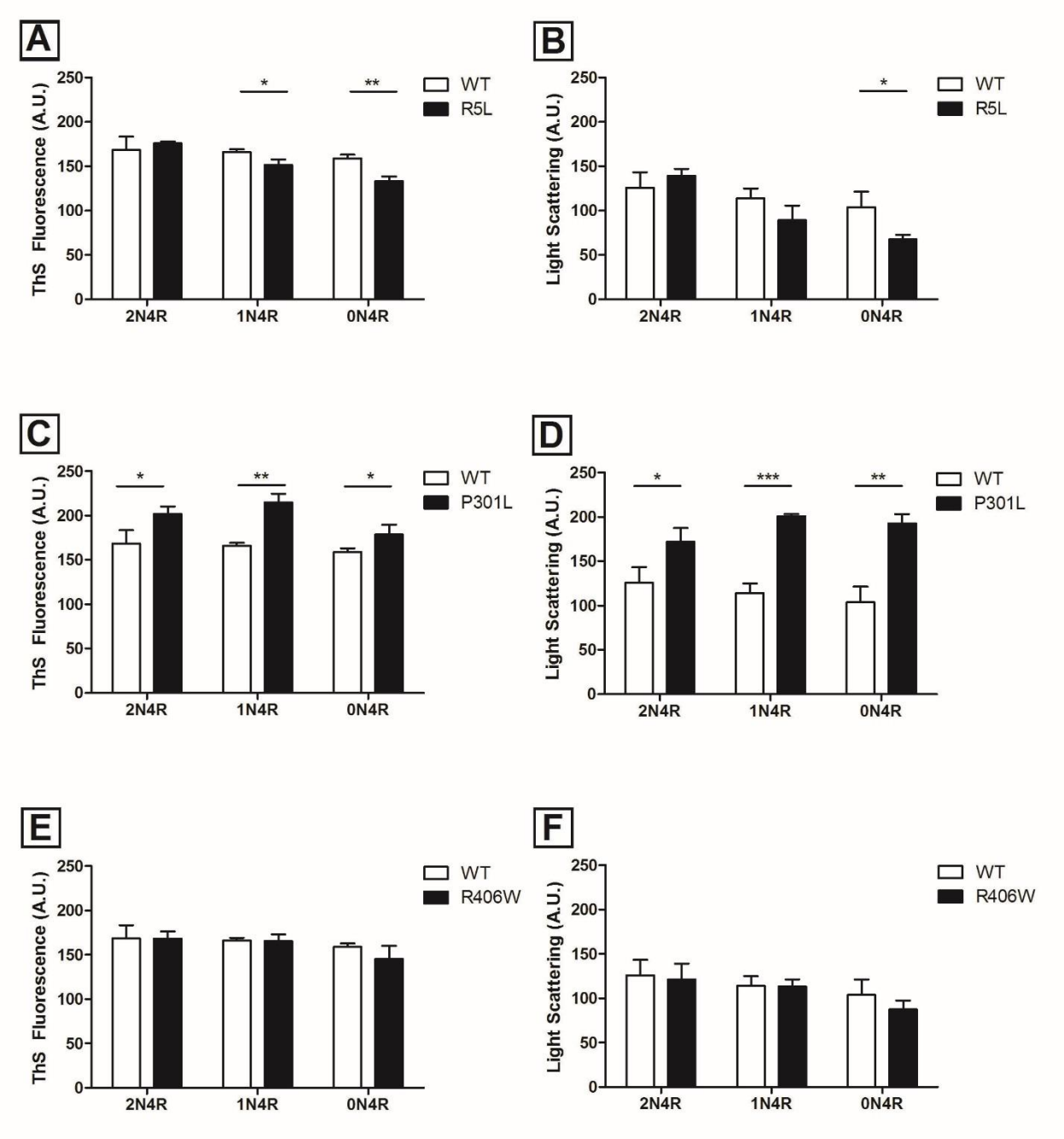


**Figure 13:** Polymerization of wild-type and FTDP-17 mutants in 4R isoforms of tau measured by Thioflavin S fluorescence and laser light scattering: 2 µM protein was incubated with 75 µM ARA at 25 °C over-night. The final extent of polymerization was measured using Thioflavin S fluorescence (A, C, E) and right-angle laser light scattering (B, D, F). Each bar represents the averaged data from three independent experiments ± SD. Stars represent the level of significance calculated using Student's unpaired t-tests, comparing each mutant to the respective wild-type isoform. (*), $p < 0.05$; (**), $p < 0.01$; (***), $p < 0.001$.

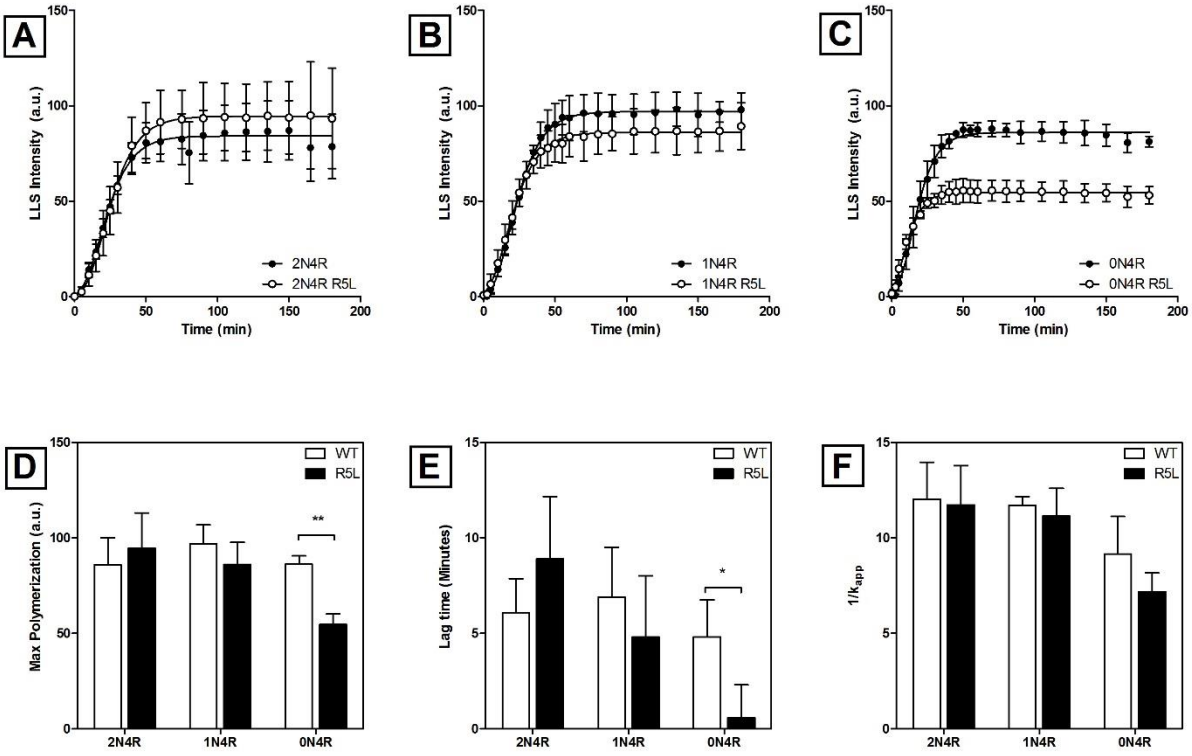


**Figure 14:** Polymerization kinetics of WT and R5L tau in 4R isoforms: A), B), C) Polymerization of 2 µM protein was initiated using 75 µM ARA at time zero and monitored using right-angle laser light scattering at specific intervals until a steady-state was reached. The error bars represent SD from three independent trials. Each trace represents the average fit of three trials to the Gompertz equation further used to calculate D) maximum polymerization, E) Lag time before polymerization and F) rate of polymerization ($k_{app}$). Stars represent the level of significance calculated using Student's unpaired t-tests, comparing parameters for the mutant to the respective wild-type isoform. (*), $p < 0.05$; (**), $p < 0.01$; (***), $p < 0.001$.

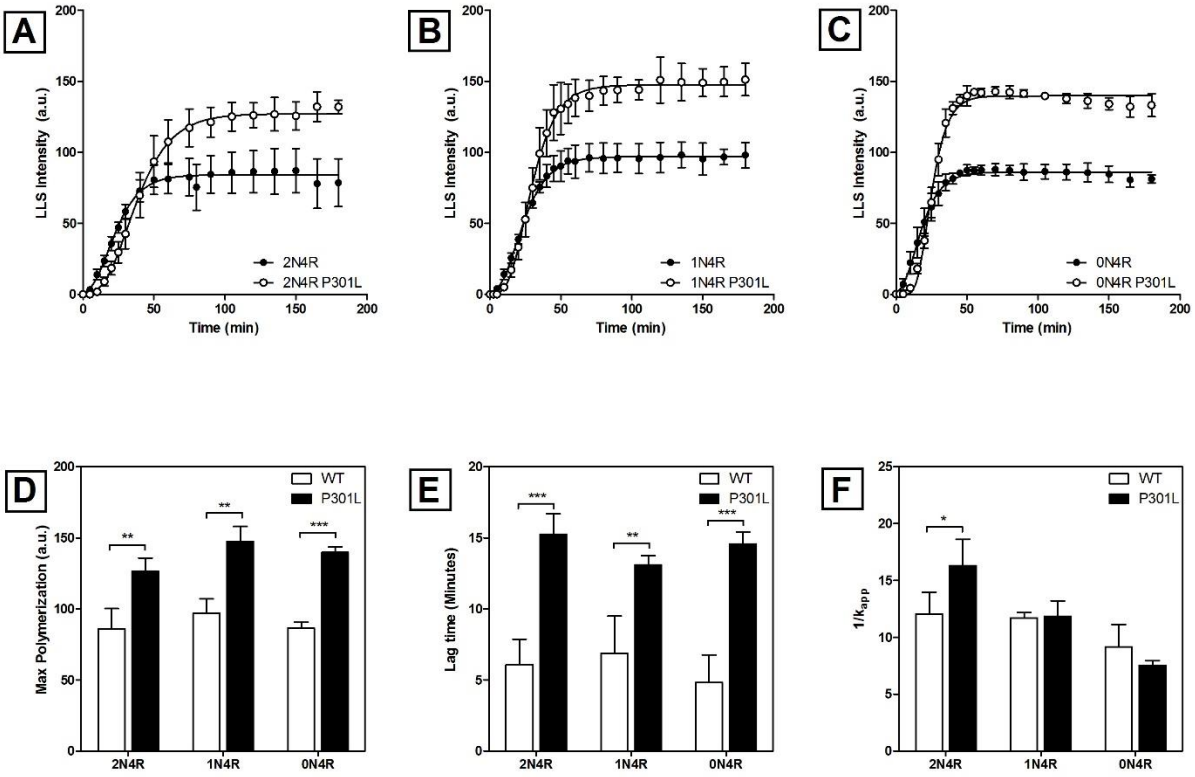


**Figure 15:** Polymerization kinetics of WT and P301L tau in 4R isoforms: A), B), C) Polymerization of 2 µM protein was initiated using 75 µM ARA at time zero and monitored using right-angle laser light scattering at specific intervals until a steady-state was reached. The error bars represent SD from three independent trials. Each trace represents the average fit of three trials to the Gompertz equation further used to calculate D) maximum polymerization, E) Lag time before polymerization and F) rate of polymerization ($k_{app}$). Stars represent the level of significance calculated using Student's unpaired t-tests, comparing parameters for the mutant to the respective wild-type isoform. (*), $p < 0.05$; (**), $p < 0.01$; (***), $p < 0.001$.

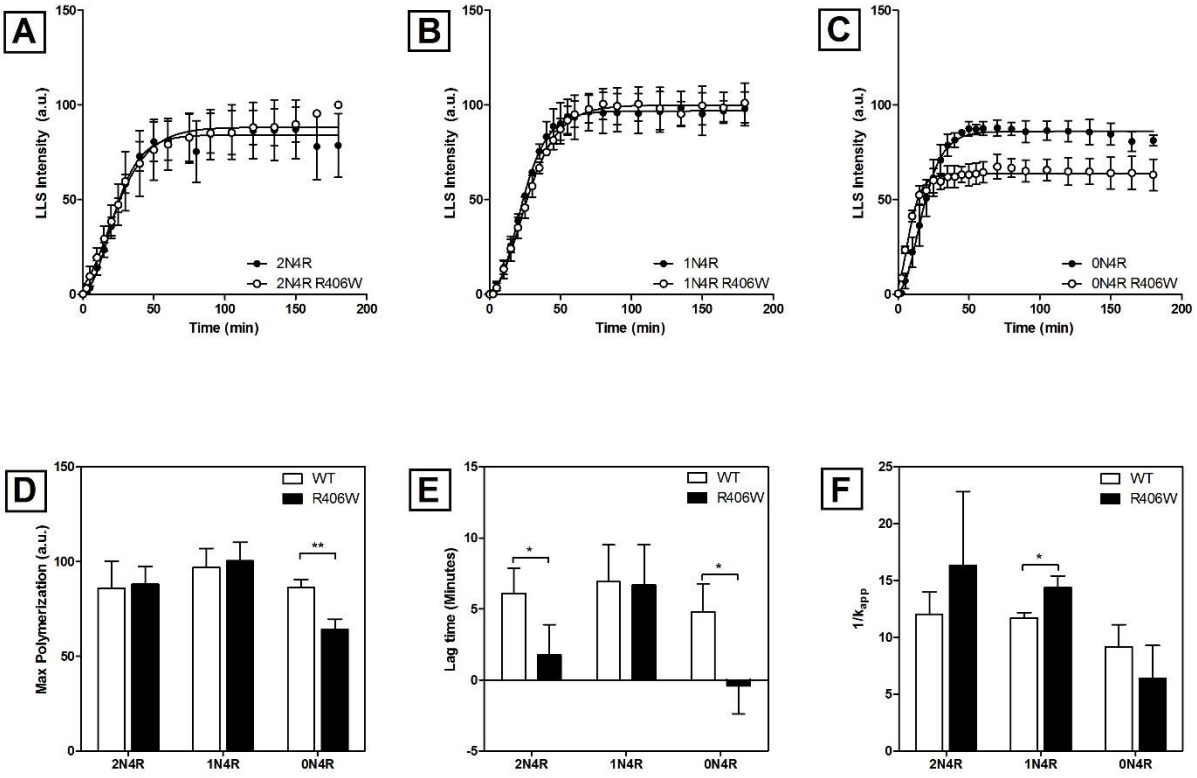


**Figure 16:** Polymerization kinetics of WT and R406W tau in 4R isoforms: A), B), C) Polymerization of 2 µM protein was initiated using 75 µM ARA at time zero and monitored using right-angle laser light scattering at specific intervals until a steady-state was reached. The error bars represent SD from three independent trials. Each trace represents the average fit of three trials to the Gompertz equation further used to calculate D) maximum polymerization, E) Lag time before polymerization and F) rate of polymerization ($k_{app}$). Stars represent the level of significance calculated using Student's unpaired t-tests, comparing parameters for the mutant to the respective wild-type isoform. (*), $p < 0.05$; (**), $p < 0.01$; (***), $p < 0.001$.

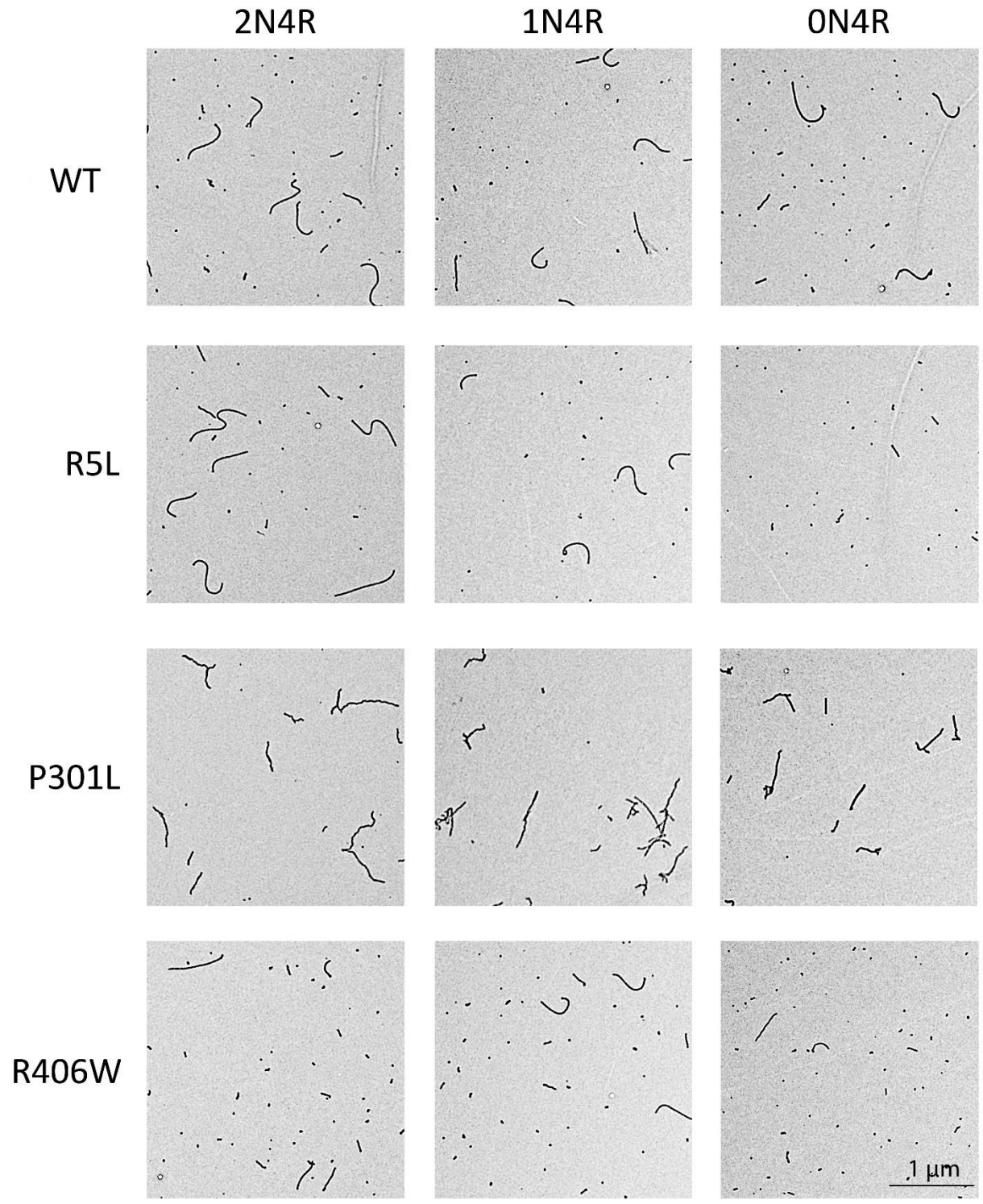


**Figure 17**: Electron micrographs of WT and mutant tau in 4R isoforms. 2 µM protein was polymerized using 75 µM ARA overnight at 25 °C and deposited on copper grids. Images were collected at 3600x magnification. Scale bar represents 1 µm.

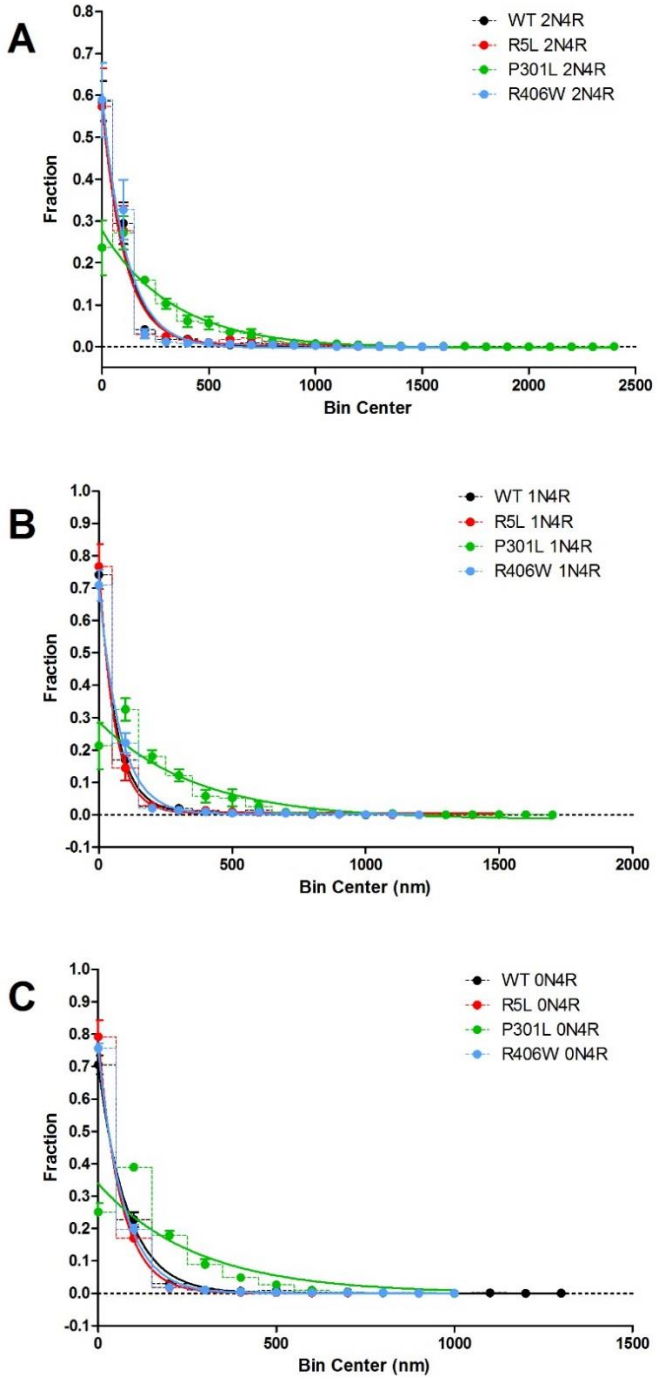


**Figure 18**: Quantitation of tau polymerization from electron micrographs (Frequency distribution of tau filaments for WT and FTDP-17 mutants in 4R isoforms of tau). Filament lengths were measured and placed into bins at 100 nm intervals. Length within each bin was summed and plotted as a fraction of the total length from all bins (y-axis) against the bin center value (x-axis). Error bars represent data from three independent trials. For each trial, quantified data from 5 separate images were pooled together and counted as one data point.

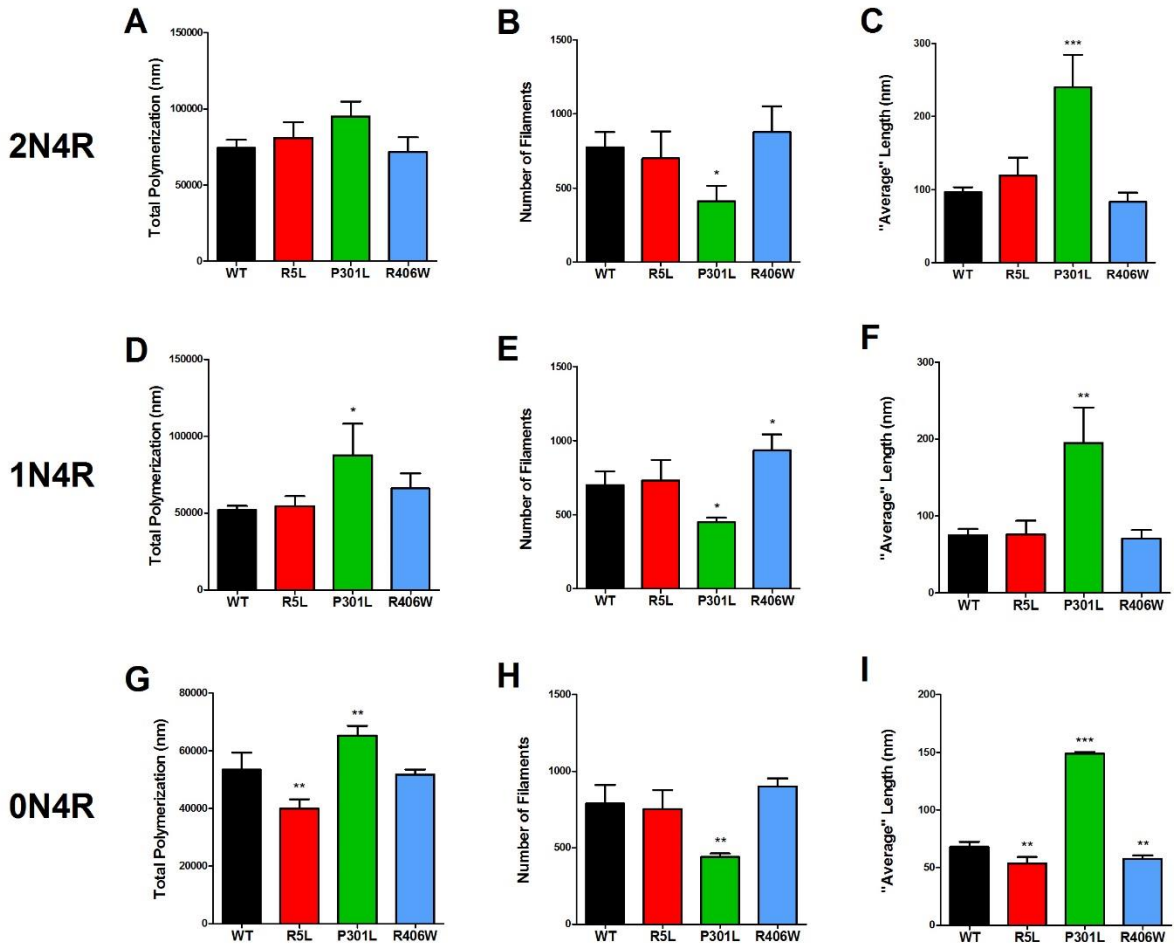


**Figure 19**: Quantitation of tau polymerization from electron micrographs. Error bars represent data from three independent trials. For each trial, quantified data from 5 separate images were pooled together to obtain one data point. One way ANOVA with Newman-Keuls Multiple Comparison Test was used to determine the statistical significance of data. Stars represent the level of significance of difference between WT and the FTDP-17 mutant. (*), $p < 0.05$; (**), $p < 0.01$; (***), $p < 0.001$.

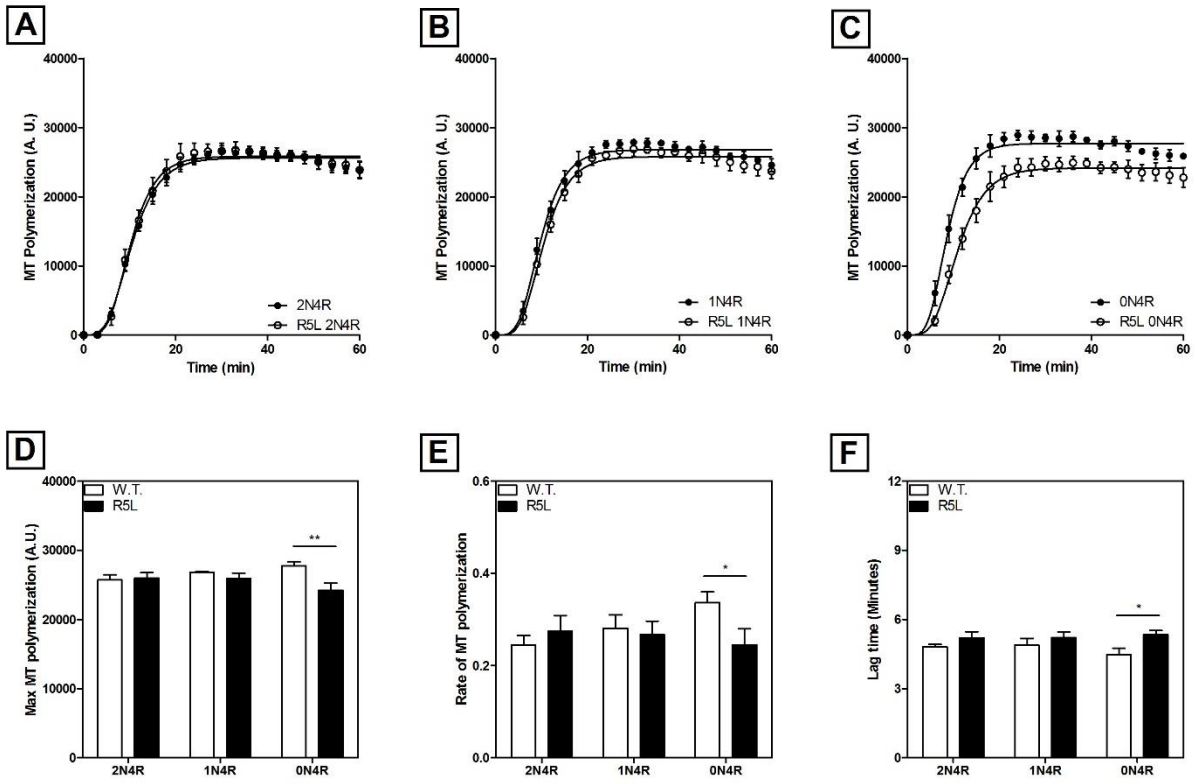


**Figure 20**: Microtubule assembly stabilization by WT and R5L tau protein. WT and R5L tau in (A) 2N4R, (B) 1N4R and (C) 0N4R isoforms were incubated with tubulin. Polymerization of tubulin was measured using a fluorescence assay as described in experimental procedures. Data were plotted as fluorescence (arbitrary units, y-axis) vs. time (minutes, x-axis) and fit to the Gompertz equation to obtain the parameters describing these curves such as D) Maximum amount of tubulin polymerization detected, E) the rate of microtubule polymerization and F) the lag time before microtubule polymerization is detectable. The data presented here is the obtained by three independent trials and presented as ± SD. Stars represent the level of significance calculated using Student's unpaired t-tests, comparing parameters for the mutant to the respective wild-type isoform. (*), $p < 0.05$; (**), $p < 0.01$; (***), $p < 0.001$.

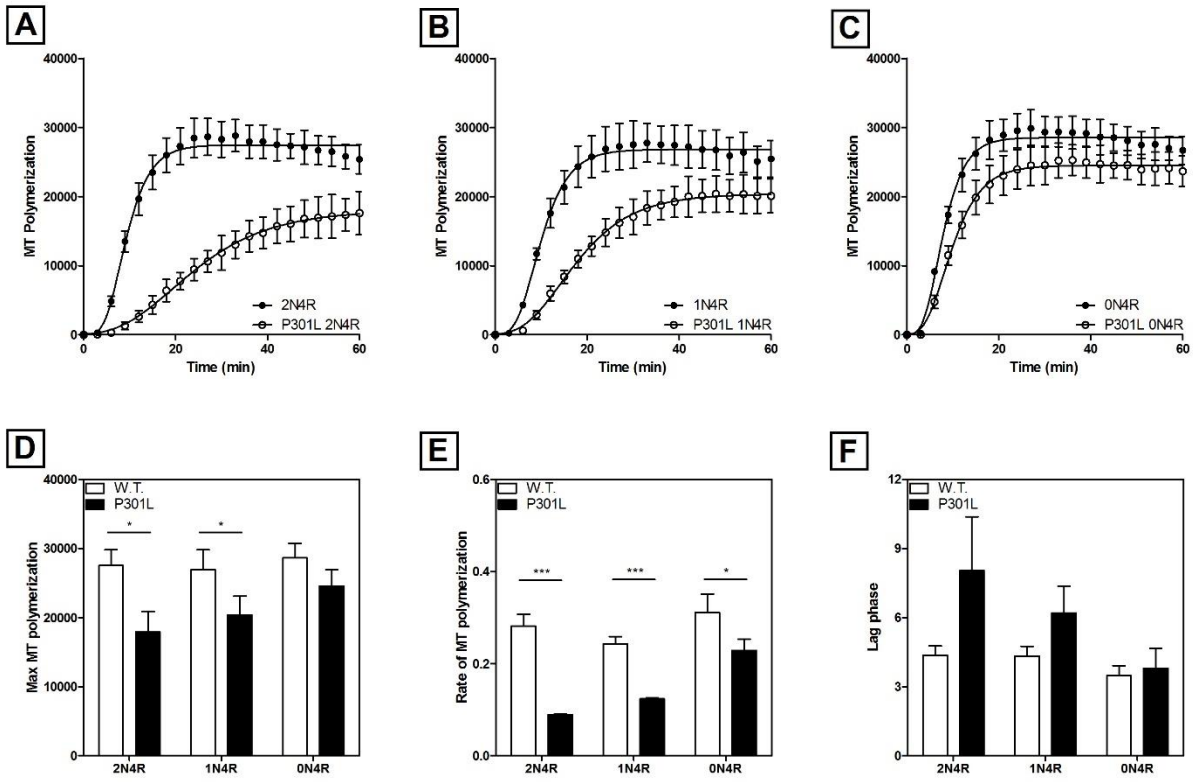


**Figure 21**: Microtubule assembly stabilization by WT and P301L tau protein. WT and P301L tau in (A) 2N4R, (B) 1N4R and (C) 0N4R isoforms were incubated with tubulin. Polymerization of tubulin was measured using a fluorescence assay as described in experimental procedures. Data were plotted as fluorescence (arbitrary units, y-axis) vs. time (minutes, x-axis) and fit to the Gompertz equation to obtain the parameters describing these curves such as D) Maximum amount of tubulin polymerization detected, E) the rate of microtubule polymerization and F) the lag time before microtubule polymerization is detectable. The data presented here is the obtained by three independent trials and presented as ± SD. Stars represent the level of significance calculated using Student's unpaired t-tests, comparing parameters for the mutant to the respective wild-type isoform. (*), $p < 0.05$; (**), $p < 0.01$; (***), $p < 0.001$.

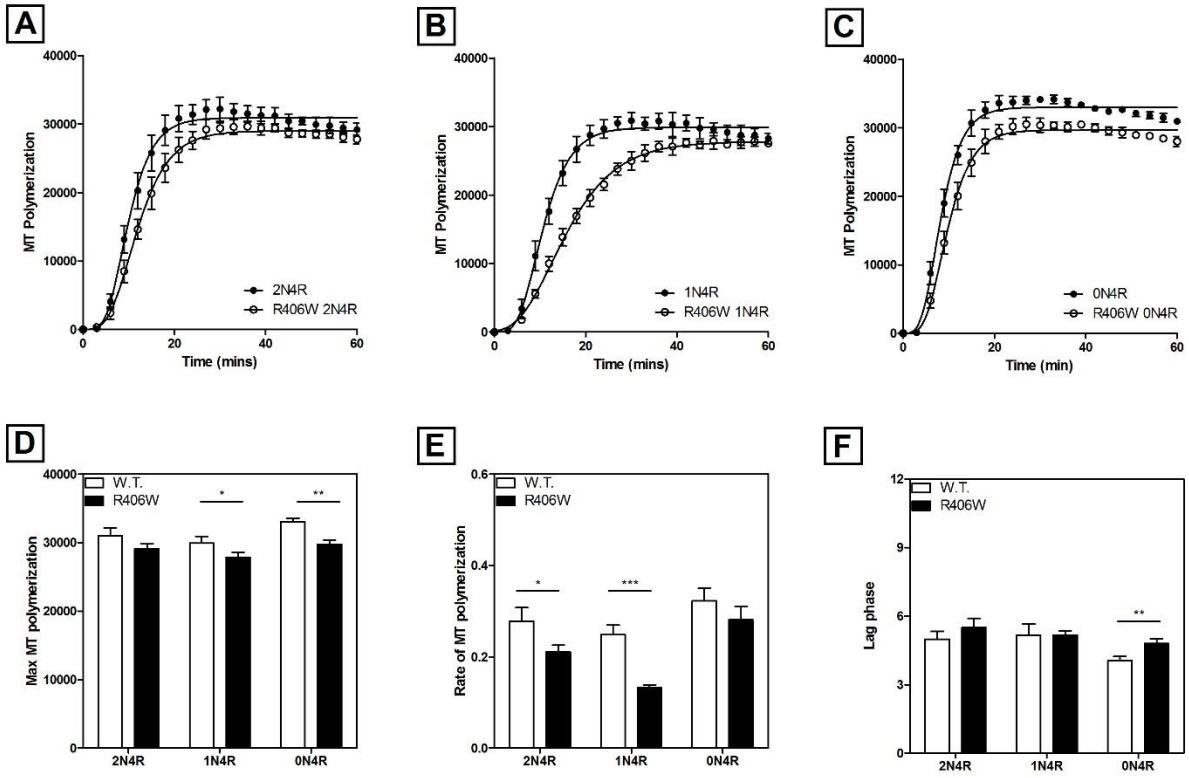


**Figure 22**: Microtubule assembly stabilization by WT and R406W tau protein. WT and R406W tau in (A) 2N4R, (B) 1N4R and (C) 0N4R isoforms were incubated with tubulin. Polymerization of tubulin was measured using a fluorescence assay as described in experimental procedures. Data were plotted as fluorescence (arbitrary units, y-axis) vs. time (minutes, x-axis) and fit to the Gompertz equation to obtain the parameters describing these curves such as D) Maximum amount of tubulin polymerization detected, E) the rate of microtubule polymerization and F) the lag time before microtubule polymerization is detectable. The data presented here is the obtained by three independent trials and presented as ± SD. Stars represent the level of significance calculated using Student's unpaired t-tests, comparing parameters for the mutant to the respective wild-type isoform. (*), $p < 0.05$; (**), $p < 0.01$; (***), $p < 0.001$.

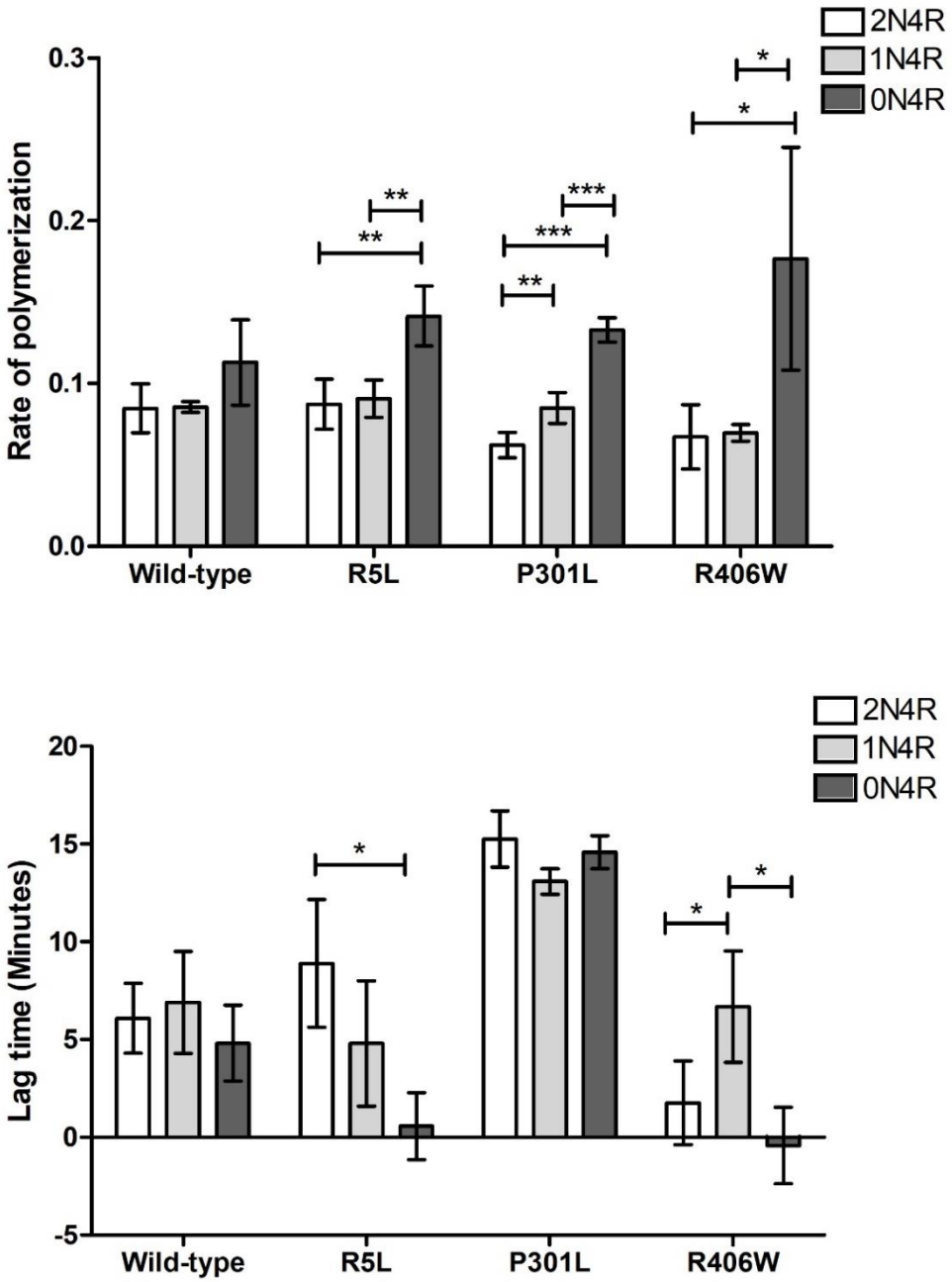


**Figure 23:** Comparison of kinetics between isoforms. One way ANOVA with Newman-Keuls Multiple Comparison Test was used to determine the statistical significance of data. Stars represent the level of significance of difference between various 4R isoforms wild-types or FTDP-17 mutants. (*), $p < 0.05$; (**), $p < 0.01$; (***), $p < 0.001$.

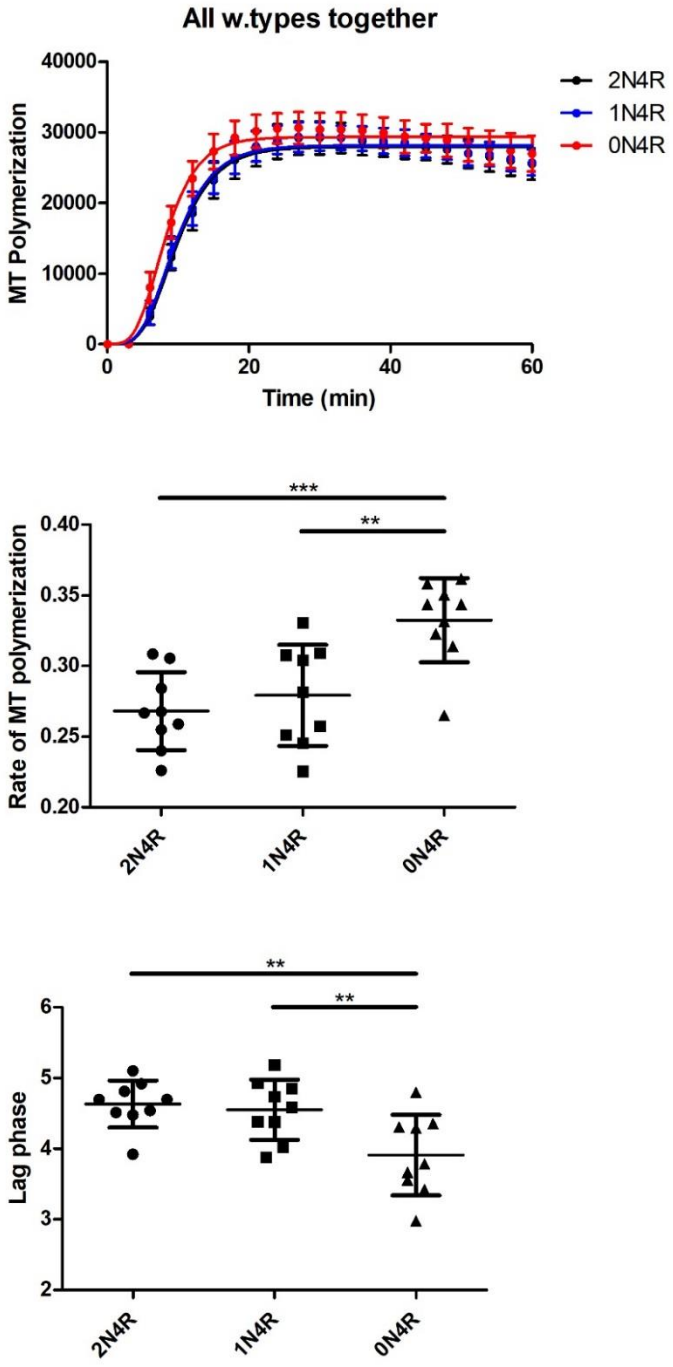


**Figure 24:** MT assembly wild-type 4R tau isoforms. Data from nine replicates for wild-type proteins is pooled together. One way ANOVA with Newman-Keuls Multiple Comparison Test was used to determine the statistical significance of data. Stars represent the level of significance of difference between various 4R isoforms wild-types or FTDP-17 mutants. (*), $p < 0.05$; (**), $p < 0.01$; (***), $p < 0.001$.

# Chapter 4: Conclusions and future directions

## Chapter 4: Conclusions and future directions

Tauopathies, including Alzheimer's disease, are progressive neurodegenerative disorders characterized by symptoms such as cognitive deficits, decline in memory, behavioral alterations and language difficulties. These disorders pose a huge health challenge for the aging population and are predicted to become more prevalent as the average human life-span increases. Currently, there are no known therapies that can slow the progression of these disorders. Although the underlying causative mechanisms still need to be elucidated, prevalence of intracellular neurofibrillary pathology composed by misfolded and aggregated tau is a major pathological hallmark for these diseases. Before effective therapies can be developed to prevent the aggregation and potential toxicity of tau aggregation, a better mechanistic understanding of factors influencing this process is warranted. One of the factors complicating our understanding of tau biology is the existence of six different isoforms of tau. The expression of these tau isoforms is tightly regulated in the brain, although the functional relevance of this tightly controlled expression ratio is not understood. Also, a lack of existence of any tertiary structure of tau has prevented researchers from understanding any possible conformational differences between these tau isoforms. Due to these reasons, understanding the differences between these isoforms has not been of priority. Often, any possible differences between these isoforms have been ignored and these isoforms of tau have been considered equivalent and interchangeable for the design of many studies. Contrary to this, there is evidence that points towards the differences between these isoforms of tau. For example, an imbalance of their expression ratio in the brain has been implicated for several tauopathies. In certain FTDP-17 cases, only specific isoforms of tau were found to be deposited as aggregates suggesting that these mutants may affect certain tau isoforms disproportionately. Therefore, there is a need for studies aimed towards understanding

the differences between tau isoforms and how any disease related mechanisms might affect them in comparison to each other. One of the ways employed to learn about tau aggregation is by inducing the aggregation of recombinant tau using inducer molecules such as arachidonic acid. Using this technique, one can determine if certain conditions can alter the extent or rate of tau aggregation. Further, it can also be determined if a certain condition can change the physical properties of tau filaments like their appearance, length or number. All these indicators together can help decipher the possible modulators of tau's conformation and aggregation which can further be tested in *in vivo* model systems. This methodology has been previously employed to study the aggregation of the 2N4R isoform of tau successfully. However, attempts to employ this technique to study the aggregation of other isoforms of tau has been difficult as these isoforms have failed to aggregate in a reliable and reproducible manner (discussed in chapter 2). This has prevented us from reliably deducing factors that can modulate the aggregation of these isoforms of tau in an effort to gain a mechanistic understanding of this process. It has also made it difficult to test any small molecule inhibitors of tau aggregation as a part of the long-term goal of finding effective therapies against tauopathies.

The first part of this dissertation is focused on identifying the challenges associated with aggregation of tau isoforms, understanding the underlying cause of it and using that knowledge for optimizing the aggregation protocol in order to obtain a more robust method for *in vitro* aggregation of various tau isoforms. We discovered that the highly acidic nature of exon 2 and 3 causes major behavioral changes in tau isoforms. Thus, the asymmetric distribution of charges could be widening the differences between the tau isoforms as removal of the N-terminal exons specifically would lead to loss of acidic residues. For the purposes of *in vitro* aggregation, these differences can largely be overcome by using higher ionic strength conditions and we were

successfully able to optimize the protocol to be able to polymerize all the 4R tau isoforms into filamentous aggregates.

This enabled the further study of the effects of FTDP-17 mutants on various 4R isoforms of tau. Looking at the effects of mutants on both the aggregation and microtubule stabilization properties of tau isoforms, we found out that mutations were not equivalent in different isoform backbones. Some mutants either preferentially affected a certain tau isoform or the level of the effect differed between the isoforms. This study reinforces the notion that the choice of isoform can have significant implications on the experimental results obtained in a study. Further, our data also indicates that the P301L mutation might cause tau to adopt a conformation that favors its aggregation. A conformational change could have effects beyond aggregation and microtubule stabilization properties of tau. Tau is known to have several binding partners and is involved in numerous signaling pathways. It can be speculated that the largely disordered nature of tau and an ability to alter its conformation could be working in its favor to be able to have several different binding partners and perform different cellular functions. A mutation that can favor one conformation or can possibly lock tau in one conformation would also have a large impact on several cellular pathways independent of protein aggregation. A conformational change can also further alter the post-translational modification pattern of tau. Future studies such as using FRET can be designed to measure the distances between various regions of tau to test the possibility that some FTDP-17 mutants could be in a conformationally different state than the wild-type.

The presented studies have helped us understand the differences between tau and how some disease related changes can possibly affect tau isoforms differentially. We also need to follow up these studies by investigating additional FTDP-17 mutants as well as other changes in tau like

phosphorylation, truncations, or other post-translational modifications in various isoforms of tau. It will also be important to investigate the differences in cultured cells or animal models. Overall, the ability to reliably conduct the *in vitro* studies with isoforms of tau has opened a new area of investigation that will help us to understand the roles of tau isoforms in disease.

## Bibliography


1. Weingarten, M. D., Lockwood, A. H., Hwo, S. Y., and Kirschner, M. W. (1975) A protein factor essential for microtubule assembly. *Proceedings of the National Academy of Sciences of the United States of America* **72**, 1858-1862
2. LoPresti, P., Szuchet, S., Papasozomenos, S. C., Zinkowski, R. P., and Binder, L. I. (1995) Functional implications for the microtubule-associated protein tau: localization in oligodendrocytes. *Proceedings of the National Academy of Sciences of the United States of America* **92**, 10369-10373
3. Cleveland, D. W., Hwo, S. Y., and Kirschner, M. W. (1977) Physical and chemical properties of purified tau factor and the role of tau in microtubule assembly. *J Mol Biol* **116**, 227-247
4. Grundke-Iqbal, I., Iqbal, K., Quinlan, M., Tung, Y. C., Zaidi, M. S., and Wisniewski, H. M. (1986) Microtubule-associated protein tau. A component of Alzheimer paired helical filaments. *The Journal of biological chemistry* **261**, 6084-6089
5. Kosik, K. S., Joachim, C. L., and Selkoe, D. J. (1986) Microtubule-associated protein tau (tau) is a major antigenic component of paired helical filaments in Alzheimer disease. *Proceedings of the National Academy of Sciences of the United States of America* **83**, 4044-4048
6. Nukina, N., and Ihara, Y. (1986) One of the antigenic determinants of paired helical filaments is related to tau protein. *J Biochem* **99**, 1541-1544
7. Wischik, C. M., Novak, M., Thogersen, H. C., Edwards, P. C., Runswick, M. J., Jakes, R., Walker, J. E., Milstein, C., Roth, M., and Klug, A. (1988) Isolation of a fragment of tau derived from the core of the paired helical filament of Alzheimer disease. *Proceedings of the National Academy of Sciences of the United States of America* **85**, 4506-4510
8. Kovacs, G. G. (2015) Invited review: Neuropathology of tauopathies: principles and practice. *Neuropathol Appl Neurobiol* **41**, 3-23
9. Andreadis, A., Brown, W. M., and Kosik, K. S. (1992) Structure and novel exons of the human tau gene. *Biochemistry* **31**, 10626-10633
10. Andreadis, A., Broderick, J. A., and Kosik, K. S. (1995) Relative exon affinities and suboptimal splice site signals lead to non-equivalence of two cassette exons. *Nucleic Acids Res* **23**, 3585-3593
11. Goode, B. L., and Feinstein, S. C. (1994) Identification of a novel microtubule binding and assembly domain in the developmentally regulated inter-repeat region of tau. *J Cell Biol* **124**, 769-782
12. Lee, G., Neve, R. L., and Kosik, K. S. (1989) The microtubule binding domain of tau protein. *Neuron* **2**, 1615-1624
13. Goedert, M., and Jakes, R. (1990) Expression of separate isoforms of human tau protein: correlation with the tau pattern in brain and effects on tubulin polymerization. *EMBO J* **9**, 4225-4230
14. Spillantini, M. G., Murrell, J. R., Goedert, M., Farlow, M. R., Klug, A., and Ghetti, B. (1998) Mutation in the tau gene in familial multiple system tauopathy with presenile dementia. *Proceedings of the National Academy of Sciences of the United States of America* **95**, 7737-7741

15. Hong, M., Zhukareva, V., Vogelsberg-Ragaglia, V., Wszolek, Z., Reed, L., Miller, B. I., Geschwind, D. H., Bird, T. D., McKeel, D., Goate, A., Morris, J. C., Wilhelmsen, K. C., Schellenberg, G. D., Trojanowski, J. Q., and Lee, V. M. (1998) Mutation-specific functional impairments in distinct tau isoforms of hereditary FTDP-17. *Science* **282**, 1914-1917
16. Kosik, K. S., Orecchio, L. D., Bakalis, S., and Neve, R. L. (1989) Developmentally regulated expression of specific tau sequences. *Neuron* **2**, 1389-1397
17. Goedert, M., Spillantini, M. G., Potier, M. C., Ulrich, J., and Crowther, R. A. (1989) Cloning and sequencing of the cDNA encoding an isoform of microtubule-associated protein tau containing four tandem repeats: differential expression of tau protein mRNAs in human brain. *Embo J* **8**, 393-399
18. Boutajangout, A., Authelet, M., Blanchard, V., Touchet, N., Tremp, G., Pradier, L., and Brion, J. P. (2004) Characterisation of cytoskeletal abnormalities in mice transgenic for wild-type human tau and familial Alzheimer's disease mutants of APP and presenilin-1. *Neurobiol Dis* **15**, 47-60
19. McMillan, P., Korvatska, E., Poorkaj, P., Evstafjeva, Z., Robinson, L., Greenup, L., Leverenz, J., Schellenberg, G. D., and D'Souza, I. (2008) Tau isoform regulation is region- and cell-specific in mouse brain. *J Comp Neurol* **511**, 788-803
20. Drubin, D. G., and Kirschner, M. W. (1986) Tau protein function in living cells. *J Cell Biol* **103**, 2739-2746
21. Bre, M. H., and Karsenti, E. (1990) Effects of brain microtubule-associated proteins on microtubule dynamics and the nucleating activity of centrosomes. *Cell Motil Cytoskeleton* **15**, 88-98
22. Panda, D., Goode, B. L., Feinstein, S. C., and Wilson, L. (1995) Kinetic stabilization of microtubule dynamics at steady state by tau and microtubule-binding domains of tau. *Biochemistry* **34**, 11117-11127
23. Stamer, K., Vogel, R., Thies, E., Mandelkow, E., and Mandelkow, E. M. (2002) Tau blocks traffic of organelles, neurofilaments, and APP vesicles in neurons and enhances oxidative stress. *J Cell Biol* **156**, 1051-1063
24. Caceres, A., and Kosik, K. S. (1990) Inhibition of neurite polarity by tau antisense oligonucleotides in primary cerebellar neurons. *Nature* **343**, 461-463
25. Knops, J., Kosik, K. S., Lee, G., Pardee, J. D., Cohen-Gould, L., and McConlogue, L. (1991) Overexpression of tau in a nonneuronal cell induces long cellular processes. *J Cell Biol* **114**, 725-733
26. Drubin, D. G., Feinstein, S. C., Shooter, E. M., and Kirschner, M. W. (1985) Nerve growth factor-induced neurite outgrowth in PC12 cells involves the coordinate induction of microtubule assembly and assembly-promoting factors. *J Cell Biol* **101**, 1799-1807
27. Esmaeli-Azad, B., McCarty, J. H., and Feinstein, S. C. (1994) Sense and antisense transfection analysis of tau function: tau influences net microtubule assembly, neurite outgrowth and neuritic stability. *J Cell Sci* **107**, 869-879
28. Harada, A., Oguchi, K., Okabe, S., Kuno, J., Terada, S., Ohshima, T., Sato-Yoshitake, R., Takei, Y., Noda, T., and Hirokawa, N. (1994) Altered microtubule organization in small-calibre axons of mice lacking tau protein. *Nature* **369**, 488-491
29. Chen, J., Kanai, Y., Cowan, N. J., and Hirokawa, N. (1992) Projection domains of MAP2 and tau determine spacings between microtubules in dendrites and axons. *Nature* **360**, 674-677

30. Selden, S. C., and Pollard, T. D. (1983) Phosphorylation of microtubule-associated proteins regulates their interaction with actin filaments. *J Biol Chem* **258**, 7064-7071
31. Moraga, D. M., Nunez, P., Garrido, J., and Maccioni, R. B. (1993) A tau fragment containing a repetitive sequence induces bundling of actin filaments. *J Neurochem* **61**, 979-986
32. Farias, G. A., Munoz, J. P., Garrido, J., and Maccioni, R. B. (2002) Tubulin, actin, and tau protein interactions and the study of their macromolecular assemblies. *J Cell Biochem* **85**, 315-324
33. Carlier, M. F., Simon, C., Cassoly, R., and Pradel, L. A. (1984) Interaction between microtubule-associated protein tau and spectrin. *Biochimie* **66**, 305-311
34. Brandt, R., Leger, J., and Lee, G. (1995) Interaction of tau with the neural plasma membrane mediated by tau's amino-terminal projection domain. *J Cell Biol* **131**, 1327-1340
35. Rendon, A., Jung, D., and Jancsik, V. (1990) Interaction of microtubules and microtubule-associated proteins (MAPs) with rat brain mitochondria. *Biochem J* **269**, 555-556
36. Lee, G., Newman, S. T., Gard, D. L., Band, H., and Panchamoorthy, G. (1998) Tau interacts with src-family non-receptor tyrosine kinases. *J Cell Sci* **111**, 3167-3177
37. Ittner, L. M., Ke, Y. D., Delerue, F., Bi, M., Gladbach, A., van Eersel, J., Wolfing, H., Chieng, B. C., Christie, M. J., Napier, I. A., Eckert, A., Staufenbiel, M., Hardeman, E., and Gotz, J. (2010) Dendritic function of tau mediates amyloid-beta toxicity in Alzheimer's disease mouse models. *Cell* **142**, 387-397
38. Hwang, S. C., Jhon, D. Y., Bae, Y. S., Kim, J. H., and Rhee, S. G. (1996) Activation of phospholipase C-gamma by the concerted action of tau proteins and arachidonic acid. *The Journal of biological chemistry* **271**, 18342-18349
39. Jenkins, S. M., and Johnson, G. V. (1998) Tau complexes with phospholipase C-gamma in situ. *Neuroreport* **9**, 67-71
40. Flanagan, L. A., Cunningham, C. C., Chen, J., Prestwich, G. D., Kosik, K. S., and Janmey, P. A. (1997) The structure of divalent cation-induced aggregates of PIP2 and their alteration by gelsolin and tau. *Biophys J* **73**, 1440-1447
41. DeVos, S. L., Goncharoff, D. K., Chen, G., Kebodeaux, C. S., Yamada, K., Stewart, F. R., Schuler, D. R., Maloney, S. E., Wozniak, D. F., Rigo, F., Bennett, C. F., Cirrito, J. R., Holtzman, D. M., and Miller, T. M. (2013) Antisense reduction of tau in adult mice protects against seizures. *J Neurosci* **33**, 12887-12897
42. Hong, X. P., Peng, C. X., Wei, W., Tian, Q., Liu, Y. H., Yao, X. Q., Zhang, Y., Cao, F. Y., Wang, Q., and Wang, J. Z. (2010) Essential role of tau phosphorylation in adult hippocampal neurogenesis. *Hippocampus* **20**, 1339-1349
43. Kimura, T., Whitcomb, D. J., Jo, J., Regan, P., Piers, T., Heo, S., Brown, C., Hashikawa, T., Murayama, M., Seok, H., Sotiropoulos, I., Kim, E., Collingridge, G. L., Takashima, A., and Cho, K. (2014) Microtubule-associated protein tau is essential for long-term depression in the hippocampus. *Philos Trans R Soc Lond B Biol Sci* **369**, 20130144
44. Ahmed, T., Van der Jeugd, A., Blum, D., Galas, M. C., D'Hooge, R., Buee, L., and Balschun, D. (2014) Cognition and hippocampal synaptic plasticity in mice with a homozygous tau deletion. *Neurobiol Aging* **35**, 2474-2478
45. Violet, M., Delattre, L., Tardivel, M., Sultan, A., Chauderlier, A., Caillierez, R., Talahari, S., Nesslany, F., Lefebvre, B., Bonnefoy, E., Buee, L., and Galas, M. C. (2014) A major

role for Tau in neuronal DNA and RNA protection in vivo under physiological and hyperthermic conditions. *Front Cell Neurosci* **8**, 84
46. Sultan, A., Nesslany, F., Violet, M., Begard, S., Loyens, A., Talahari, S., Mansuroglu, Z., Marzin, D., Sergeant, N., Humez, S., Colin, M., Bonnefoy, E., Buee, L., and Galas, M. C. (2011) Nuclear tau, a key player in neuronal DNA protection. *J Biol Chem* **286**, 4566-4575
47. Schweers, O., Schonbrunn-Hanebeck, E., Marx, A., and Mandelkow, E. (1994) Structural studies of tau protein and Alzheimer paired helical filaments show no evidence for beta-structure. *The Journal of biological chemistry* **269**, 24290-24297
48. Mukrasch, M. D., Bibow, S., Korukottu, J., Jeganathan, S., Biernat, J., Griesinger, C., Mandelkow, E., and Zweckstetter, M. (2009) Structural polymorphism of 441-residue tau at single residue resolution. *PLoS Biol* **7**, e34
49. Fellous, A., Francon, J., Lennon, A. M., and Nunez, J. (1977) Microtubule assembly in vitro. Purification of assembly-promoting factors. *Eur J Biochem* **78**, 167-174
50. Neve, R. L., Harris, P., Kosik, K. S., Kurnit, D. M., and Donlon, T. A. (1986) Identification of cDNA clones for the human microtubule-associated protein tau and chromosomal localization of the genes for tau and microtubule-associated protein 2. *Brain Res* **387**, 271-280
51. Wang, J. Z., Grundke-Iqbal, I., and Iqbal, K. (1996) Glycosylation of microtubule-associated protein tau: an abnormal posttranslational modification in Alzheimer's disease. *Nat Med* **2**, 871-875
52. Brandt, R., and Lee, G. (1994) Orientation, assembly, and stability of microtubule bundles induced by a fragment of tau protein. *Cell Motil Cytoskeleton* **28**, 143-154
53. Littauer, U. Z., Giveon, D., Thierauf, M., Ginzburg, I., and Ponstingl, H. (1986) Common and distinct tubulin binding sites for microtubule-associated proteins. *Proc Natl Acad Sci U S A* **83**, 7162-7166
54. Kadavath, H., Hofele, R. V., Biernat, J., Kumar, S., Tepper, K., Urlaub, H., Mandelkow, E., and Zweckstetter, M. (2015) Tau stabilizes microtubules by binding at the interface between tubulin heterodimers. *Proc Natl Acad Sci U S A* **112**, 7501-7506
55. Drewes, G., Trinczek, B., Illenberger, S., Biernat, J., Schmitt-Ulms, G., Meyer, H. E., Mandelkow, E. M., and Mandelkow, E. (1995) Microtubule-associated protein/microtubule affinity-regulating kinase (p110mark). A novel protein kinase that regulates tau-microtubule interactions and dynamic instability by phosphorylation at the Alzheimer-specific site serine 262. *The Journal of biological chemistry* **270**, 7679-7688
56. Sengupta, A., Kabat, J., Novak, M., Wu, Q., Grundke-Iqbal, I., and Iqbal, K. (1998) Phosphorylation of tau at both Thr 231 and Ser 262 is required for maximal inhibition of its binding to microtubules. *Arch Biochem Biophys* **357**, 299-309
57. Ksiezak-Reding, H., Pyo, H. K., Feinstein, B., and Pasinetti, G. M. (2003) Akt/PKB kinase phosphorylates separately Thr212 and Ser214 of tau protein in vitro. *Biochim Biophys Acta* **1639**, 159-168
58. Georgieff, I. S., Liem, R. K., Couchie, D., Mavilia, C., Nunez, J., and Shelanski, M. L. (1993) Expression of high molecular weight tau in the central and peripheral nervous systems. *J Cell Sci* **105 ( Pt 3)**, 729-737
59. Derisbourg, M., Leghay, C., Chiappetta, G., Fernandez-Gomez, F. J., Laurent, C., Demeyer, D., Carrier, S., Buee-Scherrer, V., Blum, D., Vinh, J., Sergeant, N., Verdier,

Y., Buee, L., and Hamdane, M. (2015) Role of the Tau N-terminal region in microtubule stabilization revealed by new endogenous truncated forms. *Sci Rep* **5**, 9659
60. Kanaan, N. M., Morfini, G. A., LaPointe, N. E., Pigino, G. F., Patterson, K. R., Song, Y., Andreadis, A., Fu, Y., Brady, S. T., and Binder, L. I. (2011) Pathogenic forms of tau inhibit kinesin-dependent axonal transport through a mechanism involving activation of axonal phosphotransferases. *The Journal of neuroscience : the official journal of the Society for Neuroscience* **31**, 9858-9868
61. Sillen, A., Barbier, P., Landrieu, I., Lefebvre, S., Wieruszeski, J. M., Leroy, A., Peyrot, V., and Lippens, G. (2007) NMR investigation of the interaction between the neuronal protein tau and the microtubules. *Biochemistry* **46**, 3055-3064
62. Jeganathan, S., von Bergen, M., Brutlach, H., Steinhoff, H. J., and Mandelkow, E. (2006) Global hairpin folding of tau in solution. *Biochemistry* **45**, 2283-2293
63. Rapoport, M., Dawson, H. N., Binder, L. I., Vitek, M. P., and Ferreira, A. (2002) Tau is essential to beta -amyloid-induced neurotoxicity. *Proceedings of the National Academy of Sciences of the United States of America* **99**, 6364-6369
64. Leroy, K., Boutajangout, A., Authelet, M., Woodgett, J. R., Anderton, B. H., and Brion, J. P. (2002) The active form of glycogen synthase kinase-3beta is associated with granulovacuolar degeneration in neurons in Alzheimer's disease. *Acta Neuropathol* **103**, 91-99
65. Patterson, K. R., Remmers, C., Fu, Y., Brooker, S., Kanaan, N. M., Vana, L., Ward, S., Reyes, J. F., Philibert, K., Glucksman, M. J., and Binder, L. I. (2011) Characterization of prefibrillar Tau oligomers in vitro and in Alzheimer disease. *J Biol Chem* **286**, 23063-23076
66. Lei, P., Ayton, S., Moon, S., Zhang, Q., Volitakis, I., Finkelstein, D. I., and Bush, A. I. (2014) Motor and cognitive deficits in aged tau knockout mice in two background strains. *Mol Neurodegener* **9**, 29
67. Arriagada, P. V., Growdon, J. H., Hedley-Whyte, E. T., and Hyman, B. T. (1992) Neurofibrillary tangles but not senile plaques parallel duration and severity of Alzheimer's disease. *Neurology* **42**, 631-639
68. Schonheit, B., Zarski, R., and Ohm, T. G. (2004) Spatial and temporal relationships between plaques and tangles in Alzheimer-pathology. *Neurobiol Aging* **25**, 697-711
69. Ishihara, T., Hong, M., Zhang, B., Nakagawa, Y., Lee, M. K., Trojanowski, J. Q., and Lee, V. M. (1999) Age-dependent emergence and progression of a tauopathy in transgenic mice overexpressing the shortest human tau isoform. *Neuron* **24**, 751-762
70. Hutton, M., Lendon, C. L., Rizzu, P., Baker, M., Froelich, S., Houlden, H., Pickering-Brown, S., Chakraverty, S., Isaacs, A., Grover, A., Hackett, J., Adamson, J., Lincoln, S., Dickson, D., Davies, P., Petersen, R. C., Stevens, M., de Graaff, E., Wauters, E., van Baren, J., Hillebrand, M., Joosse, M., Kwon, J. M., Nowotny, P., Che, L. K., Norton, J., Morris, J. C., Reed, L. A., Trojanowski, J., Basun, H., Lannfelt, L., Neystat, M., Fahn, S., Dark, F., Tannenberg, T., Dodd, P. R., Hayward, N., Kwok, J. B., Schofield, P. R., Andreadis, A., Snowden, J., Craufurd, D., Neary, D., Owen, F., Oostra, B. A., Hardy, J., Goate, A., van Swieten, J., Mann, D., Lynch, T., and Heutink, P. (1998) Association of missense and 5'-splice-site mutations in tau with the inherited dementia FTDP-17. *Nature* **393**, 702-705

71. Poorkaj, P., Bird, T. D., Wijsman, E., Nemens, E., Garruto, R. M., Anderson, L., Andreadis, A., Wiederholt, W. C., Raskind, M., and Schellenberg, G. D. (1998) Tau is a candidate gene for chromosome 17 frontotemporal dementia. *Ann Neurol* **43**, 815-825
72. Giannetti, A. M., Lindwall, G., Chau, M. F., Radeke, M. J., Feinstein, S. C., and Kohlstaedt, L. A. (2000) Fibers of tau fragments, but not full length tau, exhibit a cross beta-structure: implications for the formation of paired helical filaments. *Protein Sci* **9**, 2427-2435
73. Li, L., von Bergen, M., Mandelkow, E. M., and Mandelkow, E. (2002) Structure, stability, and aggregation of paired helical filaments from tau protein and FTDP-17 mutants probed by tryptophan scanning mutagenesis. *The Journal of biological chemistry* **277**, 41390-41400
74. Perez, M., Valpuesta, J. M., Medina, M., Montejo de Garcini, E., and Avila, J. (1996) Polymerization of tau into filaments in the presence of heparin: the minimal sequence required for tau-tau interaction. *J Neurochem* **67**, 1183-1190
75. von Bergen, M., Friedhoff, P., Biernat, J., Heberle, J., Mandelkow, E. M., and Mandelkow, E. (2000) Assembly of tau protein into Alzheimer paired helical filaments depends on a local sequence motif ((306)VQIVYK(311)) forming beta structure. *Proceedings of the National Academy of Sciences of the United States of America* **97**, 5129-5134
76. Iliev, A. I., Ganesan, S., Bunt, G., and Wouters, F. S. (2006) Removal of pattern-breaking sequences in microtubule binding repeats produces instantaneous tau aggregation and toxicity. *J Biol Chem* **281**, 37195-37204
77. Combs, B., and Gamblin, T. C. (2012) FTDP-17 tau mutations induce distinct effects on aggregation and microtubule interactions. *Biochemistry* **51**, 8597-8607
78. Chang, E., Kim, S., Yin, H., Nagaraja, H. N., and Kuret, J. (2008) Pathogenic missense MAPT mutations differentially modulate tau aggregation propensity at nucleation and extension steps. *J Neurochem* **107**, 1113-1123
79. Khlistunova, I., Biernat, J., Wang, Y., Pickhardt, M., von Bergen, M., Gazova, Z., Mandelkow, E., and Mandelkow, E. M. (2006) Inducible expression of Tau repeat domain in cell models of tauopathy: aggregation is toxic to cells but can be reversed by inhibitor drugs. *The Journal of biological chemistry* **281**, 1205-1214
80. Friedhoff, P., von Bergen, M., Mandelkow, E. M., Davies, P., and Mandelkow, E. (1998) A nucleated assembly mechanism of Alzheimer paired helical filaments. *Proceedings of the National Academy of Sciences of the United States of America* **95**, 15712-15717
81. Sillen, A., Leroy, A., Wieruszeski, J. M., Loyens, A., Beauvillain, J. C., Buee, L., Landrieu, I., and Lippens, G. (2005) Regions of tau implicated in the paired helical fragment core as defined by NMR. *Chembiochem* **6**, 1849-1856
82. Wischik, C. M., Novak, M., Edwards, P. C., Klug, A., Tichelaar, W., and Crowther, R. A. (1988) Structural characterization of the core of the paired helical filament of Alzheimer disease. *Proceedings of the National Academy of Sciences of the United States of America* **85**, 4884-4888
83. Delacourte, A., and Defossez, A. (1986) Alzheimer's disease: Tau proteins, the promoting factors of microtubule assembly, are major components of paired helical filaments. *J Neurol Sci* **76**, 173-186

84. Crowther, R. A. (1991) Straight and paired helical filaments in Alzheimer disease have a common structural unit. *Proceedings of the National Academy of Sciences of the United States of America* **88**, 2288-2292
85. Eschmann, N. A., Georgieva, E. R., Ganguly, P., Borbat, P. P., Rappaport, M. D., Akdogan, Y., Freed, J. H., Shea, J. E., and Han, S. (2017) Signature of an aggregation-prone conformation of tau. *Sci Rep* **7**, 44739
86. Hernandez, F., Cuadros, R., and Avila, J. (2004) Zeta 14-3-3 protein favours the formation of human tau fibrillar polymers. *Neurosci Lett* **357**, 143-146
87. Ishiguro, K., Takamatsu, M., Tomizawa, K., Omori, A., Takahashi, M., Arioka, M., Uchida, T., and Imahori, K. (1992) Tau protein kinase I converts normal tau protein into A68-like component of paired helical filaments. *The Journal of biological chemistry* **267**, 10897-10901
88. Ishiguro, K., Shiratsuchi, A., Sato, S., Omori, A., Arioka, M., Kobayashi, S., Uchida, T., and Imahori, K. (1993) Glycogen synthase kinase 3 beta is identical to tau protein kinase I generating several epitopes of paired helical filaments. *FEBS Lett* **325**, 167-172
89. Imahori, K., and Uchida, T. (1997) Physiology and pathology of tau protein kinases in relation to Alzheimer's disease. *J Biochem (Tokyo)* **121**, 179-188
90. Liao, H., Li, Y., Brautigan, D. L., and Gundersen, G. G. (1998) Protein phosphatase 1 is targeted to microtubules by the microtubule-associated protein Tau. *The Journal of biological chemistry* **273**, 21901-21908
91. Sontag, E., Nunbhakdi-Craig, V., Lee, G., Brandt, R., Kamibayashi, C., Kuret, J., White, C. L., 3rd, Mumby, M. C., and Bloom, G. S. (1999) Molecular interactions among protein phosphatase 2A, tau, and microtubules. Implications for the regulation of tau phosphorylation and the development of tauopathies. *The Journal of biological chemistry* **274**, 25490-25498
92. Kopke, E., Tung, Y. C., Shaikh, S., Alonso, A. C., Iqbal, K., and Grundke-Iqbal, I. (1993) Microtubule-associated protein tau. Abnormal phosphorylation of a non-paired helical filament pool in Alzheimer disease. *The Journal of biological chemistry* **268**, 24374-24384
93. Martin, L., Latypova, X., and Terro, F. (2011) Post-translational modifications of tau protein: implications for Alzheimer's disease. *Neurochem Int* **58**, 458-471
94. Braak, E., Braak, H., and Mandelkow, E. M. (1994) A sequence of cytoskeleton changes related to the formation of neurofibrillary tangles and neuropil threads. *Acta Neuropathol (Berl)* **87**, 554-567
95. Combs, B., Voss, K., and Gamblin, T. C. (2011) Pseudohyperphosphorylation has differential effects on polymerization and function of tau isoforms. *Biochemistry* **50**, 9446-9456
96. Gorsky, M. K., Burnouf, S., Dols, J., Mandelkow, E., and Partridge, L. (2016) Acetylation mimic of lysine 280 exacerbates human Tau neurotoxicity in vivo. *Sci Rep* **6**, 22685
97. Tracy, T. E., Sohn, P. D., Minami, S. S., Wang, C., Min, S. W., Li, Y., Zhou, Y., Le, D., Lo, I., Ponnusamy, R., Cong, X., Schilling, B., Ellerby, L. M., Huganir, R. L., and Gan, L. (2016) Acetylated Tau Obstructs KIBRA-Mediated Signaling in Synaptic Plasticity and Promotes Tauopathy-Related Memory Loss. *Neuron* **90**, 245-260
98. Reyes, J. F., Geula, C., Vana, L., and Binder, L. I. (2012) Selective tau tyrosine nitration in non-AD tauopathies. *Acta Neuropathol* **123**, 119-132

99. Liu, F., Zaidi, T., Iqbal, K., Grundke-Iqbal, I., and Gong, C. X. (2002) Aberrant glycosylation modulates phosphorylation of tau by protein kinase A and dephosphorylation of tau by protein phosphatase 2A and 5. *Neuroscience* **115**, 829-837
100. Schweers, O., Mandelkow, E. M., Biernat, J., and Mandelkow, E. (1995) Oxidation of cysteine-322 in the repeat domain of microtubule-associated protein tau controls the in vitro assembly of paired helical filaments. *Proceedings of the National Academy of Sciences of the United States of America* **92**, 8463-8467
101. Braak, H., and Braak, E. (1991) Neuropathological stageing of Alzheimer-related changes. *Acta Neuropathol* **82**, 239-259
102. Kidd, M. (1963) Paired helical filaments in electron microscopy of Alzheimer's disease. *Nature* **197**, 192-193
103. Goedert, M., Spillantini, M. G., Cairns, N. J., and Crowther, R. A. (1992) Tau proteins of Alzheimer paired helical filaments: abnormal phosphorylation of all six brain isoforms. *Neuron* **8**, 159-168
104. Bancher, C., Brunner, C., Lassmann, H., Budka, H., Jellinger, K., Seitelberger, F., Grundke-Iqbal, I., Iqbal, K., and Wisniewski, H. M. (1989) Tau and ubiquitin immunoreactivity at different stages of formation of Alzheimer neurofibrillary tangles. *Prog Clin Biol Res* **317**, 837-848
105. Ginsberg, S. D., Crino, P. B., Lee, V. M., Eberwine, J. H., and Trojanowski, J. Q. (1997) Sequestration of RNA in Alzheimer's disease neurofibrillary tangles and senile plaques. *Ann Neurol* **41**, 200-209
106. Leroy, K., Yilmaz, Z., and Brion, J. P. (2007) Increased level of active GSK-3beta in Alzheimer's disease and accumulation in argyrophilic grains and in neurones at different stages of neurofibrillary degeneration. *Neuropathology and applied neurobiology* **33**, 43-55
107. Marui, W., Iseki, E., Ueda, K., and Kosaka, K. (2000) Occurrence of human alpha-synuclein immunoreactive neurons with neurofibrillary tangle formation in the limbic areas of patients with Alzheimer's disease. *J Neurol Sci* **174**, 81-84
108. Huang, Y., Liu, X. Q., Wyss-Coray, T., Brecht, W. J., Sanan, D. A., and Mahley, R. W. (2001) Apolipoprotein E fragments present in Alzheimer's disease brains induce neurofibrillary tangle-like intracellular inclusions in neurons. *Proceedings of the National Academy of Sciences of the United States of America* **98**, 8838-8843.
109. Waring, S. C., and Rosenberg, R. N. (2008) Genome-wide association studies in Alzheimer disease. *Arch. Neurol.* **65**, 329-334
110. Delacourte, A., David, J. P., Sergeant, N., Buee, L., Wattez, A., Vermersch, P., Ghozali, F., Fallet-Bianco, C., Pasquier, F., Lebert, F., Petit, H., and Di Menza, C. (1999) The biochemical pathway of neurofibrillary degeneration in aging and Alzheimer's disease. *Neurology* **52**, 1158-1165
111. Shipton, O. A., Leitz, J. R., Dworzak, J., Acton, C. E., Tunbridge, E. M., Denk, F., Dawson, H. N., Vitek, M. P., Wade-Martins, R., Paulsen, O., and Vargas-Caballero, M. (2011) Tau protein is required for amyloid {beta}-induced impairment of hippocampal long-term potentiation. *J. Neurosci.* **31**, 1688-1692
112. Andorfer, C., Acker, C. M., Kress, Y., Hof, P. R., Duff, K., and Davies, P. (2005) Cell-cycle reentry and cell death in transgenic mice expressing nonmutant human tau isoforms. *J. Neurosci.* **25**, 5446-5454

113. Bandyopadhyay, B., Li, G., Yin, H., and Kuret, J. (2007) Tau aggregation and toxicity in a cell culture model of tauopathy. *The Journal of biological chemistry* **282**, 16454-16464
114. D'Souza, I., Poorkaj, P., Hong, M., Nochlin, D., Lee, V. M., Bird, T. D., and Schellenberg, G. D. (1999) Missense and silent tau gene mutations cause frontotemporal dementia with parkinsonism-chromosome 17 type, by affecting multiple alternative RNA splicing regulatory elements. *Proceedings of the National Academy of Sciences of the United States of America* **96**, 5598-5603
115. Sergeant, N., Delacourte, A., and Buee, L. (2005) Tau protein as a differential biomarker of tauopathies. *Biochim Biophys Acta* **1739**, 179-197
116. Hauw, J. J., Daniel, S. E., Dickson, D., Horoupian, D. S., Jellinger, K., Lantos, P. L., McKee, A., Tabaton, M., and Litvan, I. (1994) Preliminary NINDS neuropathologic criteria for Steele-Richardson-Olszewski syndrome (progressive supranuclear palsy). *Neurology* **44**, 2015-2019
117. Litvan, I., and Hutton, M. (1998) Clinical and genetic aspects of progressive supranuclear palsy. *J Geriatr Psychiatry Neurol* **11**, 107-114
118. Steele, J. C., Richardson, J. C., and Olszewski, J. (1964) Progressive Supranuclear Palsy. A Heterogeneous Degeneration Involving the Brain Stem, Basal Ganglia and Cerebellum with Vertical Gaze and Pseudobulbar Palsy, Nuchal Dystonia and Dementia. *Arch. Neurol.* **10**, 333-359
119. Pollock, N. J., Mirra, S. S., Binder, L. I., Hansen, L. A., and Wood, J. G. (1986) Filamentous aggregates in Pick's disease, progressive supranuclear palsy, and Alzheimer's disease share antigenic determinants with microtubule-associated protein, tau. *Lancet* **2**, 1211
120. Tellez-Nagel, I., and Wisniewski, H. M. (1973) Ultrastructure of neurofibrillary tangles in Steele-Richardson-Olszewski syndrome. *Arch Neurol* **29**, 324-327
121. Williams, D. R., de Silva, R., Paviour, D. C., Pittman, A., Watt, H. C., Kilford, L., Holton, J. L., Revesz, T., and Lees, A. J. (2005) Characteristics of two distinct clinical phenotypes in pathologically proven progressive supranuclear palsy: Richardson's syndrome and PSP-parkinsonism. *Brain* **128**, 1247-1258
122. Chambers, C. B., Lee, J. M., Troncoso, J. C., Reich, S., and Muma, N. A. (1999) Overexpression of four-repeat tau mRNA isoforms in progressive supranuclear palsy but not in Alzheimer's disease. *Ann Neurol* **46**, 325-332
123. Feany, M. B., Mattiace, L. A., and Dickson, D. W. (1996) Neuropathologic overlap of progressive supranuclear palsy, Pick's disease and corticobasal degeneration. *J Neuropathol Exp Neurol* **55**, 53-67
124. Rebeiz, J. J., Kolodny, E. H., and Richardson, E. P., Jr. (1968) Corticodentatonigral degeneration with neuronal achromasia. *Arch Neurol* **18**, 20-33
125. Ksiezak-Reding, H., Morgan, K., Mattiace, L. A., Davies, P., Liu, W. K., Yen, S. H., Weidenheim, K., and Dickson, D. W. (1994) Ultrastructure and biochemical composition of paired helical filaments in corticobasal degeneration. *Am J Pathol* **145**, 1496-1508
126. Constantinidis, J., Richard, J., and Tissot, R. (1974) Pick's disease. Histological and clinical correlations. *Eur Neurol* **11**, 208-217
127. Munoz-Garcia, D., and Ludwin, S. K. (1984) Classic and generalized variants of Pick's disease: a clinicopathological, ultrastructural, and immunocytochemical comparative study. *Ann Neurol* **16**, 467-480

128. Hof, P. R., Bouras, C., Perl, D. P., and Morrison, J. H. (1994) Quantitative neuropathologic analysis of Pick's disease cases: cortical distribution of Pick bodies and coexistence with Alzheimer's disease. *Acta Neuropathol* **87**, 115-124
129. Wilhelmsen, K. C., Lynch, T., Pavlou, E., Higgins, M., and Nygaard, T. G. (1994) Localization of disinhibition-dementia-parkinsonism-amyotrophy complex to 17q21-22. *Am J Hum Genet* **55**, 1159-1165
130. Ghetti, B., Oblak, A. L., Boeve, B. F., Johnson, K. A., Dickerson, B. C., and Goedert, M. (2015) Invited review: Frontotemporal dementia caused by microtubule-associated protein tau gene (MAPT) mutations: a chameleon for neuropathology and neuroimaging. *Neuropathology and applied neurobiology* **41**, 24-46
131. von Bergen, M., Barghorn, S., Biernat, J., Mandelkow, E. M., and Mandelkow, E. (2005) Tau aggregation is driven by a transition from random coil to beta sheet structure. *Biochim Biophys Acta* **1739**, 158-166
132. Tanemura, K., Akagi, T., Murayama, M., Kikuchi, N., Murayama, O., Hashikawa, T., Yoshiike, Y., Park, J. M., Matsuda, K., Nakao, S., Sun, X., Sato, S., Yamaguchi, H., and Takashima, A. (2001) Formation of filamentous tau aggregations in transgenic mice expressing V337M human tau. *Neurobiol Dis* **8**, 1036-1045
133. Kraemer, B. C., Zhang, B., Leverenz, J. B., Thomas, J. H., Trojanowski, J. Q., and Schellenberg, G. D. (2003) Neurodegeneration and defective neurotransmission in a Caenorhabditis elegans model of tauopathy. *Proceedings of the National Academy of Sciences of the United States of America* **100**, 9980-9985
134. Lindquist, S. G., Holm, I. E., Schwartz, M., Law, I., Stokholm, J., Batbayli, M., Waldemar, G., and Nielsen, J. E. (2008) Alzheimer disease-like clinical phenotype in a family with FTDP-17 caused by a MAPT R406W mutation. *Eur J Neurol* **15**, 377-385
135. Rosso, S. M., van Herpen, E., Deelen, W., Kamphorst, W., Severijnen, L. A., Willemsen, R., Ravid, R., Niermeijer, M. F., Dooijes, D., Smith, M. J., Goedert, M., Heutink, P., and van Swieten, J. C. (2002) A novel tau mutation, S320F, causes a tauopathy with inclusions similar to those in Pick's disease. *Ann Neurol* **51**, 373-376
136. Bessi, V., Bagnoli, S., Nacmias, B., Tedde, A., Sorbi, S., and Bracco, L. (2010) Semantic dementia associated with mutation V363I in the tau gene. *J Neurol Sci* **296**, 112-114
137. van Herpen, E., Rosso, S. M., Serverijnen, L. A., Yoshida, H., Breedveld, G., van de Graaf, R., Kamphorst, W., Ravid, R., Willemsen, R., Dooijes, D., Majoor-Krakauer, D., Kros, J. M., Crowther, R. A., Goedert, M., Heutink, P., and van Swieten, J. C. (2003) Variable phenotypic expression and extensive tau pathology in two families with the novel tau mutation L315R. *Ann Neurol* **54**, 573-581
138. Cummings, J. L., and Altman, J. (2005) Genotype, proteotype, phenotype relationships in neurodegenerative diseases. Highlights from the 21st Ipsen Foundation Alzheimer's Disease Symposium, September 13, 2004, Paris, France. *Rev Neurol Dis* **2**, 80-84
139. Poorkaj, P., Muma, N. A., Zhukareva, V., Cochran, E. J., Shannon, K. M., Hurtig, H., Koller, W. C., Bird, T. D., Trojanowski, J. Q., Lee, V. M., and Schellenberg, G. D. (2002) An R5L tau mutation in a subject with a progressive supranuclear palsy phenotype. *Ann Neurol* **52**, 511-516
140. Murrell, J. R., Spillantini, M. G., Zolo, P., Guazzelli, M., Smith, M. J., Hasegawa, M., Redi, F., Crowther, R. A., Pietrini, P., Ghetti, B., and Goedert, M. (1999) Tau gene mutation G389R causes a tauopathy with abundant pick body-like inclusions and axonal deposits. *J Neuropathol Exp Neurol* **58**, 1207-1226

141. Lippa, C. F., Zhukareva, V., Kawarai, T., Uryu, K., Shafiq, M., Nee, L. E., Grafman, J., Liang, Y., St George-Hyslop, P. H., Trojanowski, J. Q., and Lee, V. M. (2000) Frontotemporal dementia with novel tau pathology and a Glu342Val tau mutation. *Ann Neurol* **48**, 850-858
142. Wilson, D. M., and Binder, L. I. (1997) Free fatty acids stimulate the polymerization of tau and amyloid beta peptides. In vitro evidence for a common effector of pathogenesis in Alzheimer's disease. *Am J Pathol* **150**, 2181-2195
143. Chang, E., Honson, N. S., Bandyopadhyay, B., Funk, K. E., Jensen, J. R., Kim, S., Naphade, S., and Kuret, J. (2009) Modulation and detection of tau aggregation with small-molecule ligands. *Curr Alzheimer Res* **6**, 409-414
144. Kampers, T., Friedhoff, P., Biernat, J., Mandelkow, E. M., and Mandelkow, E. (1996) RNA stimulates aggregation of microtubule-associated protein tau into Alzheimer-like paired helical filaments. *FEBS Lett* **399**, 344-349
145. King, M. E., Ahuja, V., Binder, L. I., and Kuret, J. (1999) Ligand-dependent tau filament formation: implications for Alzheimer's disease progression. *Biochemistry* **38**, 14851-14859
146. Wood, J. G., Mirra, S. S., Pollock, N. J., and Binder, L. I. (1986) Neurofibrillary tangles of Alzheimer disease share antigenic determinants with the axonal microtubule-associated protein tau (tau). *Proceedings of the National Academy of Sciences of the United States of America* **83**, 4040-4043
147. Goedert, M., Wischik, C. M., Crowther, R. A., Walker, J. E., and Klug, A. (1988) Cloning and sequencing of the cDNA encoding a core protein of the paired helical filament of Alzheimer disease: identification as the microtubule-associated protein tau. *Proceedings of the National Academy of Sciences of the United States of America* **85**, 4051-4055
148. Goedert, M., Spillantini, M. G., Jakes, R., Rutherford, D., and Crowther, R. A. (1989) Multiple isoforms of human microtubule-associated protein tau: sequences and localization in neurofibrillary tangles of Alzheimer's disease. *Neuron* **3**, 519-526
149. Himmler, A., Drechsel, D., Kirschner, M. W., and Martin, D. W., Jr. (1989) Tau consists of a set of proteins with repeated C-terminal microtubule-binding domains and variable N-terminal domains. *Molecular and cellular biology* **9**, 1381-1388
150. Trabzuni, D., Wray, S., Vandrovcova, J., Ramasamy, A., Walker, R., Smith, C., Luk, C., Gibbs, J. R., Dillman, A., Hernandez, D. G., Arepalli, S., Singleton, A. B., Cookson, M. R., Pittman, A. M., de Silva, R., Weale, M. E., Hardy, J., and Ryten, M. (2012) MAPT expression and splicing is differentially regulated by brain region: relation to genotype and implication for tauopathies. *Human molecular genetics* **21**, 4094-4103
151. Goedert, M., Spillantini, M. G., Crowther, R. A., Chen, S. G., Parchi, P., Tabaton, M., Lanska, D. J., Markesbery, W. R., Wilhelmsen, K. C., Dickson, D. W., Petersen, R. B., and Gambetti, P. (1999) Tau gene mutation in familial progressive subcortical gliosis. *Nat Med* **5**, 454-457
152. Conrad, C., Zhu, J., Conrad, C., Schoenfeld, D., Fang, Z., Ingelsson, M., Stamm, S., Church, G., and Hyman, B. T. (2007) Single molecule profiling of tau gene expression in Alzheimer's disease. *Journal of neurochemistry* **103**, 1228-1236
153. Yoshida, M. (2006) Cellular tau pathology and immunohistochemical study of tau isoforms in sporadic tauopathies. *Neuropathology : official journal of the Japanese Society of Neuropathology* **26**, 457-470

154. Schoch, K. M., DeVos, S. L., Miller, R. L., Chun, S. J., Norrbom, M., Wozniak, D. F., Dawson, H. N., Bennett, C. F., Rigo, F., and Miller, T. M. (2016) Increased 4R-Tau Induces Pathological Changes in a Human-Tau Mouse Model. *Neuron* **90**, 941-947
155. Panda, D., Samuel, J. C., Massie, M., Feinstein, S. C., and Wilson, L. (2003) Differential regulation of microtubule dynamics by three- and four-repeat tau: implications for the onset of neurodegenerative disease. *Proceedings of the National Academy of Sciences of the United States of America* **100**, 9548-9553
156. Levy, S. F., Leboeuf, A. C., Massie, M. R., Jordan, M. A., Wilson, L., and Feinstein, S. C. (2005) Three- and four-repeat tau regulate the dynamic instability of two distinct microtubule subpopulations in qualitatively different manners. Implications for neurodegeneration. *The Journal of biological chemistry* **280**, 13520-13528
157. Adams, S. J., DeTure, M. A., McBride, M., Dickson, D. W., and Petrucelli, L. (2010) Three repeat isoforms of tau inhibit assembly of four repeat tau filaments. *PloS one* **5**, e10810
158. Dinkel, P. D., Siddiqua, A., Huynh, H., Shah, M., and Margittai, M. (2011) Variations in filament conformation dictate seeding barrier between three- and four-repeat tau. *Biochemistry* **50**, 4330-4336
159. Lacovich, V., Espindola, S. L., Alloatti, M., Pozo Devoto, V., Cromberg, L., Carna, M., Forte, G., Gallo, J. M., Bruno, L., Stokin, G. B., Avale, M. E., and Falzone, T. L. (2016) Tau isoforms imbalance impairs the axonal transport of the amyloid precursor protein in human neurons. *The Journal of neuroscience : the official journal of the Society for Neuroscience*
160. Baker, M., Litvan, I., Houlden, H., Adamson, J., Dickson, D., Perez-Tur, J., Hardy, J., Lynch, T., Bigio, E., and Hutton, M. (1999) Association of an extended haplotype in the tau gene with progressive supranuclear palsy. *Hum Mol Genet* **8**, 711-715
161. Caffrey, T. M., Joachim, C., and Wade-Martins, R. (2008) Haplotype-specific expression of the N-terminal exons 2 and 3 at the human MAPT locus. *Neurobiology of aging* **29**, 1923-1929
162. Ghanem, D., Tran, H., Dhaenens, C. M., Schraen-Maschke, S., Sablonniere, B., Buee, L., Sergeant, N., and Caillet-Boudin, M. L. (2009) Altered splicing of Tau in DM1 is different from the foetal splicing process. *FEBS Lett* **583**, 675-679
163. Houlden, H., Baker, M., Morris, H. R., MacDonald, N., Pickering-Brown, S., Adamson, J., Lees, A. J., Rossor, M. N., Quinn, N. P., Kertesz, A., Khan, M. N., Hardy, J., Lantos, P. L., St George-Hyslop, P., Munoz, D. G., Mann, D., Lang, A. E., Bergeron, C., Bigio, E. H., Litvan, I., Bhatia, K. P., Dickson, D., Wood, N. W., and Hutton, M. (2001) Corticobasal degeneration and progressive supranuclear palsy share a common tau haplotype. *Neurology* **56**, 1702-1706
164. Allen, M., Kachadoorian, M., Quicksall, Z., Zou, F., Chai, H. S., Younkin, C., Crook, J. E., Pankratz, V. S., Carrasquillo, M. M., Krishnan, S., Nguyen, T., Ma, L., Malphrus, K., Lincoln, S., Bisceglio, G., Kolbert, C. P., Jen, J., Mukherjee, S., Kauwe, J. K., Crane, P. K., Haines, J. L., Mayeux, R., Pericak-Vance, M. A., Farrer, L. A., Schellenberg, G. D., Parisi, J. E., Petersen, R. C., Graff-Radford, N. R., Dickson, D. W., Younkin, S. G., and Ertekin-Taner, N. (2014) Association of MAPT haplotypes with Alzheimer's disease risk and MAPT brain gene expression levels. *Alzheimer's research & therapy* **6**, 39

165. Lagunes, T., Herrera-Rivero, M., Hernandez-Aguilar, M. E., and Aranda-Abreu, G. E. (2014) Abeta(1-42) induces abnormal alternative splicing of tau exons 2/3 in NGF-induced PC12 cells. *Anais da Academia Brasileira de Ciencias* **86**, 1927-1934
166. Gamblin, T. C., King, M. E., Kuret, J., Berry, R. W., and Binder, L. I. (2000) Oxidative regulation of fatty acid-induced tau polymerization. *Biochemistry* **39**, 14203-14210
167. Horowitz, P. M., LaPointe, N., Guillozet-Bongaarts, A. L., Berry, R. W., and Binder, L. I. (2006) N-terminal fragments of tau inhibit full-length tau polymerization in vitro. *Biochemistry* **45**, 12859-12866
168. von Bergen, M., Barghorn, S., Muller, S. A., Pickhardt, M., Biernat, J., Mandelkow, E. M., Davies, P., Aebi, U., and Mandelkow, E. (2006) The core of tau-paired helical filaments studied by scanning transmission electron microscopy and limited proteolysis. *Biochemistry* **45**, 6446-6457
169. Carlson, S. W., Branden, M., Voss, K., Sun, Q., Rankin, C. A., and Gamblin, T. C. (2007) A complex mechanism for inducer mediated tau polymerization. *Biochemistry* **46**, 8838-8849
170. Snowden, S. G., Ebshiana, A. A., Hye, A., An, Y., Pletnikova, O., O'Brien, R., Troncoso, J., Legido-Quigley, C., and Thambisetty, M. (2017) Association between fatty acid metabolism in the brain and Alzheimer disease neuropathology and cognitive performance: A nontargeted metabolomic study. *PLoS medicine* **14**, e1002266
171. Ong, W. Y., Farooqui, T., and Farooqui, A. A. (2010) Involvement of cytosolic phospholipase A(2), calcium independent phospholipase A(2) and plasmalogen selective phospholipase A(2) in neurodegenerative and neuropsychiatric conditions. *Current medicinal chemistry* **17**, 2746-2763
172. Bradley-Whitman, M. A., and Lovell, M. A. (2015) Biomarkers of lipid peroxidation in Alzheimer disease (AD): an update. *Archives of toxicology* **89**, 1035-1044
173. Sharon, R., Bar-Joseph, I., Mirick, G. E., Serhan, C. N., and Selkoe, D. J. (2003) Altered fatty acid composition of dopaminergic neurons expressing alpha-synuclein and human brains with alpha-synucleinopathies. *The Journal of biological chemistry* **278**, 49874-49881
174. Gray, E. G., Paula-Barbosa, M., and Roher, A. (1987) Alzheimer's disease: paired helical filaments and cytomembranes. *Neuropathology and applied neurobiology* **13**, 91-110
175. Voss, K., and Gamblin, T. C. (2009) GSK-3β phosphorylation of functionally distinct tau isoforms has differential, but mild effects. *Mol Neurodegener* **4**, 1-12
176. Abraha, A., Ghoshal, N., Gamblin, T. C., Cryns, V., Berry, R. W., Kuret, J., and Binder, L. I. (2000) C-terminal inhibition of tau assembly in vitro and in Alzheimer's disease. *J Cell Sci* **113 Pt 21**, 3737-3745
177. Reynolds, M. R., Berry, R. W., and Binder, L. I. (2005) Site-specific nitration differentially influences tau assembly in vitro. *Biochemistry* **44**, 13997-14009
178. King, M. E., Gamblin, T. C., Kuret, J., and Binder, L. I. (2000) Differential assembly of human tau isoforms in the presence of arachidonic acid. *J Neurochem* **74**, 1749-1757
179. Rankin, C. A., Sun, Q., and Gamblin, T. C. (2005) Pseudo-phosphorylation of tau at Ser202 and Thr205 affects tau filament formation. *Brain Res Mol Brain Res* **138**, 84-93
180. Novak, M., Jakes, R., Edwards, P. C., Milstein, C., and Wischik, C. M. (1991) Difference between the tau protein of Alzheimer paired helical filament core and normal tau revealed by epitope analysis of monoclonal antibodies 423 and 7.51. *Proceedings of the National Academy of Sciences of the United States of America* **88**, 5837-5841

181. Wegmann, S., Medalsy, I. D., Mandelkow, E., and Muller, D. J. (2013) The fuzzy coat of pathological human Tau fibrils is a two-layered polyelectrolyte brush. *Proceedings of the National Academy of Sciences of the United States of America* **110**, E313-321
182. Mattson, M. P., Mark, R. J., Furukawa, K., and Bruce, A. J. (1997) Disruption of brain cell ion homeostasis in Alzheimer's disease by oxy radicals, and signaling pathways that protect therefrom. *Chemical research in toxicology* **10**, 507-517
183. Paranjape, S. R., Riley, A. P., Somoza, A. D., Oakley, C. E., Wang, C. C., Prisinzano, T. E., Oakley, B. R., and Gamblin, T. C. (2015) Azaphilones Inhibit Tau Aggregation and Dissolve Tau Aggregates in Vitro. *ACS Chem Neurosci*
184. Iyer, A., Lapointe, N. E., Zielke, K., Berdynski, M., Guzman, E., Barczak, A., Chodakowska-Zebrowska, M., Barcikowska, M., Feinstein, S., and Zekanowski, C. (2013) A novel MAPT mutation, G55R, in a frontotemporal dementia patient leads to altered Tau function. *PLoS One* **8**, e76409
185. Cohn-Hokke, P. E., Wong, T. H., Rizzu, P., Breedveld, G., van der Flier, W. M., Scheltens, P., Baas, F., Heutink, P., Meijers-Heijboer, E. J., van Swieten, J. C., and Pijnenburg, Y. A. (2014) Mutation frequency of PRKAR1B and the major familial dementia genes in a Dutch early onset dementia cohort. *J Neurol* **261**, 2085-2092
186. Arrasate, M., Perez, M., Armas-Portela, R., and Avila, J. (1999) Polymerization of tau peptides into fibrillar structures. The effect of FTDP-17 mutations. *FEBS Lett* **446**, 199-202
187. Barghorn, S., Zheng-Fischhofer, Q., Ackmann, M., Biernat, J., von Bergen, M., Mandelkow, E. M., and Mandelkow, E. (2000) Structure, microtubule interactions, and paired helical filament aggregation by tau mutants of frontotemporal dementias. *Biochemistry* **39**, 11714-11721
188. Nacharaju, P., Lewis, J., Easson, C., Yen, S., Hackett, J., Hutton, M., and Yen, S. H. (1999) Accelerated filament formation from tau protein with specific FTDP-17 missense mutations. *FEBS Lett* **447**, 195-199
189. Hasegawa, M., Smith, M. J., and Goedert, M. (1998) Tau proteins with FTDP-17 mutations have a reduced ability to promote microtubule assembly. *FEBS Lett* **437**, 207-210
190. Clark, L. N., Poorkaj, P., Wszolek, Z., Geschwind, D. H., Nasreddine, Z. S., Miller, B., Li, D., Payami, H., Awert, F., Markopoulou, K., Andreadis, A., D'Souza, I., Lee, V. M., Reed, L., Trojanowski, J. Q., Zhukareva, V., Bird, T., Schellenberg, G., and Wilhelmsen, K. C. (1998) Pathogenic implications of mutations in the tau gene in pallido-ponto-nigral degeneration and related neurodegenerative disorders linked to chromosome 17. *Proceedings of the National Academy of Sciences of the United States of America* **95**, 13103-13107
191. Lewis, J., McGowan, E., Rockwood, J., Melrose, H., Nacharaju, P., Van Slegtenhorst, M., Gwinn-Hardy, K., Paul Murphy, M., Baker, M., Yu, X., Duff, K., Hardy, J., Corral, A., Lin, W. L., Yen, S. H., Dickson, D. W., Davies, P., and Hutton, M. (2000) Neurofibrillary tangles, amyotrophy and progressive motor disturbance in mice expressing mutant (P301L) tau protein. *Nat Genet* **25**, 402-405
192. Wittmann, C. W., Wszolek, M. F., Shulman, J. M., Salvaterra, P. M., Lewis, J., Hutton, M., and Feany, M. B. (2001) Tauopathy in Drosophila: neurodegeneration without neurofibrillary tangles. *Science* **293**, 711-714

193. Delobel, P., Flament, S., Hamdane, M., Jakes, R., Rousseau, A., Delacourte, A., Vilain, J. P., Goedert, M., and Buee, L. (2002) Functional characterization of FTDP-17 tau gene mutations through their effects on Xenopus oocyte maturation. *The Journal of biological chemistry* **277**, 9199-9205
194. Mocanu, M. M., Nissen, A., Eckermann, K., Khlistunova, I., Biernat, J., Drexler, D., Petrova, O., Schonig, K., Bujard, H., Mandelkow, E., Zhou, L., Rune, G., and Mandelkow, E. M. (2008) The potential for beta-structure in the repeat domain of tau protein determines aggregation, synaptic decay, neuronal loss, and coassembly with endogenous Tau in inducible mouse models of tauopathy. *The Journal of neuroscience : the official journal of the Society for Neuroscience* **28**, 737-748
195. Santacruz, K., Lewis, J., Spires, T., Paulson, J., Kotilinek, L., Ingelsson, M., Guimaraes, A., DeTure, M., Ramsden, M., McGowan, E., Forster, C., Yue, M., Orne, J., Janus, C., Mariash, A., Kuskowski, M., Hyman, B., Hutton, M., and Ashe, K. H. (2005) Tau suppression in a neurodegenerative mouse model improves memory function. *Science* **309**, 476-481
196. Eckermann, K., Mocanu, M. M., Khlistunova, I., Biernat, J., Nissen, A., Hofmann, A., Schonig, K., Bujard, H., Haemisch, A., Mandelkow, E., Zhou, L., Rune, G., and Mandelkow, E. M. (2007) The beta-propensity of Tau determines aggregation and synaptic loss in inducible mouse models of tauopathy. *The Journal of biological chemistry* **282**, 31755-31765
197. Spires, T. L., Orne, J. D., SantaCruz, K., Pitstick, R., Carlson, G. A., Ashe, K. H., and Hyman, B. T. (2006) Region-specific dissociation of neuronal loss and neurofibrillary pathology in a mouse model of tauopathy. *Am J Pathol* **168**, 1598-1607
198. Noble, W., Planel, E., Zehr, C., Olm, V., Meyerson, J., Suleman, F., Gaynor, K., Wang, L., LaFrancois, J., Feinstein, B., Burns, M., Krishnamurthy, P., Wen, Y., Bhat, R., Lewis, J., Dickson, D., and Duff, K. (2005) Inhibition of glycogen synthase kinase-3 by lithium correlates with reduced tauopathy and degeneration in vivo. *Proceedings of the National Academy of Sciences of the United States of America* **102**, 6990-6995
199. Povellato, G., Tuxworth, R. I., Hanger, D. P., and Tear, G. (2014) Modification of the Drosophila model of in vivo Tau toxicity reveals protective phosphorylation by GSK3beta. *Biol Open* **3**, 1-11
200. Chatterjee, S., Sang, T. K., Lawless, G. M., and Jackson, G. R. (2009) Dissociation of tau toxicity and phosphorylation: role of GSK-3beta, MARK and Cdk5 in a Drosophila model. *Hum Mol Genet* **18**, 164-177
201. Nishimura, I., Yang, Y., and Lu, B. (2004) PAR-1 kinase plays an initiator role in a temporally ordered phosphorylation process that confers tau toxicity in Drosophila. *Cell* **116**, 671-682
202. Scott, C. W., Blowers, D. P., Barth, P. T., Lo, M. M., Salama, A. I., and Caputo, C. B. (1991) Differences in the abilities of human tau isoforms to promote microtubule assembly. *J Neurosci Res* **30**, 154-162
203. Voss, K., Combs, B., Patterson, K. R., Binder, L. I., and Gamblin, T. C. (2012) Hsp70 alters tau function and aggregation in an isoform specific manner. *Biochemistry* **51**, 888-898
204. Liu, C., Song, X., Nisbet, R., and Gotz, J. (2016) Co-immunoprecipitation with Tau Isoform-specific Antibodies Reveals Distinct Protein Interactions and Highlights a Putative Role for 2N Tau in Disease. *J Biol Chem* **291**, 8173-8188

205. Liu, C., and Gotz, J. (2013) Profiling murine tau with 0N, 1N and 2N isoform-specific antibodies in brain and peripheral organs reveals distinct subcellular localization, with the 1N isoform being enriched in the nucleus. *PLoS One* **8**, e84849
206. Poorkaj, P., Grossman, M., Steinbart, E., Payami, H., Sadovnick, A., Nochlin, D., Tabira, T., Trojanowski, J. Q., Borson, S., Galasko, D., Reich, S., Quinn, B., Schellenberg, G., and Bird, T. D. (2001) Frequency of tau gene mutations in familial and sporadic cases of non-Alzheimer dementia. *Arch Neurol* **58**, 383-387
207. Terwel, D., Lasrado, R., Snauwaert, J., Vandeweert, E., Van Haesendonck, C., Borghgraef, P., and Van Leuven, F. (2005) Changed conformation of mutant Tau-P301L underlies the moribund tauopathy, absent in progressive, nonlethal axonopathy of Tau-4R/2N transgenic mice. *The Journal of biological chemistry* **280**, 3963-3973
208. Oddo, S., Caccamo, A., Shepherd, J. D., Murphy, M. P., Golde, T. E., Kayed, R., Metherate, R., Mattson, M. P., Akbari, Y., and LaFerla, F. M. (2003) Triple-transgenic model of Alzheimer's disease with plaques and tangles: intracellular Abeta and synaptic dysfunction. *Neuron* **39**, 409-421
209. Mutreja, Y., and Gamblin, T. C. (2017) Optimization of in vitro conditions to study the arachidonic acid induction of 4R isoforms of the microtubule-associated protein tau. *Methods in cell biology* **141**, 65-88